

Copyright Warning & Restrictions

The copyright law of the United States (Title 17, United States Code) governs the making of photocopies or other reproductions of copyrighted material.

Under certain conditions specified in the law, libraries and archives are authorized to furnish a photocopy or other reproduction. One of these specified conditions is that the photocopy or reproduction is not to be “used for any purpose other than private study, scholarship, or research.” If a user makes a request for, or later uses, a photocopy or reproduction for purposes in excess of “fair use” that user may be liable for copyright infringement,

This institution reserves the right to refuse to accept a copying order if, in its judgment, fulfillment of the order would involve violation of copyright law.

Please Note: The author retains the copyright while the New Jersey Institute of Technology reserves the right to distribute this thesis or dissertation

Printing note: If you do not wish to print this page, then select “Pages from: first page # to: last page #” on the print dialog screen

The Van Houten library has removed some of the personal information and all signatures from the approval page and biographical sketches of theses and dissertations in order to protect the identity of NJIT graduates and faculty.

ABSTRACT

CYCLOIDAL-DRIVE JOINT DESIGN FOR WEARABLE EXOSKELETONS

**by
Abhi J. Rawal**

This thesis's scope was to construct a highly back drivable and compact joint design that can be used for wearable exoskeletons specifically designed to assist with rehabilitation. A compact cycloidal gear transmission was designed to satisfy the compactness requirement while ensuring the minimum torque is required for backdriving the mechanism. The joint was designed based on the compact cycloidal drive specifications, and the backdrivability test was performed to measure the minimum torque required (1.20 Nm) to backdrive. The joint design incorporates various important features such as rotation lock feature to prevent hyperextension, a housing design that offers the benefit of using the joint for the left and right limb, a motor mount that securely holds a brushless DC motor, and a sensor bracket that securely positions a control sensor over the motor for controlling the motor position and speed. Successful evaluation of the 3D printed prototype validated the integrity of the design.

**CYCLOIDAL-DRIVE JOINT DESIGN
FOR WEARABLE EXOSKELETONS**

**by
Abhi J. Rawal**

**A Thesis
Submitted to the Faculty of
New Jersey Institute of Technology
in Partial Fulfillment of the Requirements for the Degree of
Master of Science in Mechanical Engineering**

Department of Mechanical and Industrial Engineering

December 2020

Blank Page

APPROVAL PAGE

**CYCLOIDAL-DRIVE JOINT DESIGN
FOR WEARABLE EXOSKELETONS**

Abhi J. Rawal

Dr. Lu Lu, Thesis Advisor Date
Assistant Professor of Mechanical and Industrial Engineering, NJIT

Dr. Xianlian Alex Zhou, Committee Member Date
Associate Professor of Biomedical Engineering, NJIT

Dr. Zhiming Ji, Committee Member Date
Professor of Mechanical and Industrial Engineering, NJIT

BIOGRAPHICAL SKETCH

Author: Abhi J. Rawal

Degree: Master of Science

Date: December 2020

Undergraduate and Graduate Education:

- Master of Science in Mechanical Engineering,
New Jersey Institute of Technology, Newark, New Jersey, 2020
- Bachelor of Science in Mechanical Engineering,
New Jersey Institute of Technology, Newark, New Jersey, 2017

Major: Mechanical Engineering

I dedicate this work to my guru H.D.H Hariprasad Swamiji Maharaj and my family.
A special feeling of gratitude to my guru for motivating me to pursue this graduate degree and gifting me the ability to complete it.

ACKNOWLEDGMENT

I would like to express my sincere gratitude to my thesis advisor, Dr. Lu Lu, for providing me this research opportunity and for his continuous support. Besides Dr. Lu, I would like to thank the rest of my thesis committee: Dr. Xianlian Alex Zhou and Dr. Zhiming Ji, for their insightful comments and guidance. My sincere thank also goes to my fellow lab mate: Neethan Ratnakumar, who has extensively helped me with prototyping.

TABLE OF CONTENTS

Chapter	Page
1 INTRODUCTION.....	1
1.1 Objective	1
1.2 Background Information	1
1.3 The Structure and Operating Principles of Cycloidal Drive.....	7
2 DESIGN OF THE CYCLOIDAL HOUSING AND ROLLERS.....	11
2.1 Transmission Ratio	11
2.2 Housing Circle Circumference and Roller Radius	11
2.3 Design of Rotating Arm.....	14
3 DESIGN OF THE CYCLOIDAL ROTOR AND THE ECCENTRIC SHAFT	16
3.1 Shaft Eccentricity.....	16
3.2 Parametric Equations Defining Cycloidal Rotor Profile	17
3.3 Pin-Hole Diameter (D_H).....	18
3.4 Eccentric Shaft	22
3.5 Motor Shaft	24
4 DESIGN OF THE FIXED ARM ASSEMBLY AND REPRESENTATION OF THE FINAL ASSEMBLY.....	25
4.1 Design of the Fixed Arm Side Plates.....	24
4.2 Design of the Motor Mount & Sensor Holding Bracket.....	26
4.3 Design of the Fixed Arm Assembly.....	27
4.4 Complete Assembly.....	29
4.5 Backdrivability Test.....	36

TABLE OF CONTENTS
(Continued)

Chapter	Page
5 CONCLUSION AND FUTURE WORK.....	39
5.1 Conclusion.....	39
5.2 Future Work.....	39
APPENDIX A MANUFACTURING DRAWINGS	42
APPENDIX B BASELINE PUSH-PULL FORCE GAUGE.....	72
REFERENCES	74

LIST OF FIGURES

Figure	Page
1.1 Rolling Joint: two-stage timing belt transmission system that provides a transmission ratio of 8.85:1 and requires 3.33 Nm torque to backdrive.....	3
1.2 Capstan drive system with a transmission ratio of 10:1 and the capstan wheel diameter of 120 mm.....	4
1.3 The two-stage planetary mechanism with timing belt offering the transmission ratio of 24:1 and required 3 Nm torque to backdrive the joint design.....	5
1.4 The exploded view of a harmonic drive assembly.....	6
1.5 The exploded view of a cycloidal drive assembly.....	7
1.6 Representation of the offset between the center axis of the roller gear and the center axis of the cycloidal disk.....	8
2.1 Representation of rollers arranged on the housing circle.....	12
2.2 Roller design.....	13
2.3 Rotating arm-side plate.....	14
2.4 Exploded view of the rotating arm assembly.....	15
3.1 Representation of eccentricity using cross section of the eccentric shaft.....	16
3.2 Modeling of the cycloidal rotor and rollers in Autodesk Fusion 360	18
3.3 Representation of the pin-holes and the mounting circle	19
3.4 Representation of the pin with 2 mm diameter	20
3.5 Interaction of rotor assembly with fixed pins.....	20
3.6 Representation of center axis of the rotating shaft driven by the motor and the center axis of the cycloidal rotor.....	22
3.7 Cross-section of the eccentric shaft.....	23

**LIST OF FIGURES
(Continued)**

Figure	Page
3.8 Representation of the motor shaft that will transfer torque from the motor to the eccentric shaft.....	24
4.1 Fixed arm side plates.....	25
4.2 Motor mount & sensor holding bracket assembly.....	26
4.3 Exploded view of the fixed arm assembly.....	27
4.4 Complete assembly.....	29
4.5 Internal mechanisms of the joint.....	30
4.6 Backdrivability test set up.....	36
4.7 Backdrivability test set up diagram.....	37
5.1 Sketch of the double rotor eccentric shaft.....	40
5.2 Increase in length required for the pointed components.....	41

LIST OF TABLES

Table		Page
2.1	List of Components Involved in the Rotating Arm Assembly.....	15
3.1	List of Components of the Cycloidal Rotor Assembly.....	21
4.1	List of Components Involved in the Fixed Arm Assembly.....	28
4.2	Step by Step Assembly Instructions.....	31

LIST OF SYMBOLS

i	Transmission Ratio
n	Number of Rotor teeth
N	Number of Rollers
R	Rotor Radius
R_r	Roller Radius
E	Eccentricity
\emptyset	Contact Angle
D_H	Pin-Hole Diameter
D_P	Pin Diameter
D_{Mount}	Mounting Circle Diameter

CHAPTER 1

INTRODUCTION

1.1 Objective

The scope of this thesis was to design and prototype a highly back drivable, stable, and compact joint design using the cycloidal mechanism that can be used for wearable exoskeletons designs specifically built for rehabilitation applications.

1.2 Background Information

Exoskeletons are wearable electro-mechanical device that allow human movements with expanded strength. Exoskeletons are mainly deployed to assist with military operations, rehabilitation applications, and to amplify the working capabilities of workers on factory floors. Specifically, for rehabilitation applications, many exoskeletons have been developed over the past decades by academic researchers and the U.S. government in conjunction with industry giants using various mechanisms to provide assistance with lower limb and upper limb.

In North America, Rehabilitation robotics first started in 1960 with the development of an externally powered exoskeleton at Case Institute of Technology, Ohio [10]. In 1985 the Clinical Robotics Laboratory was established as part of the joint U.S Department of Veterans Affairs and Stanford University Robotics program in the Spinal Cord Injury Center, VA for the development of a new generation of robots assisting people in Activities of Daily Living (ADLs) [10].

The overall goal of the Rehabilitation robotics is to support patients with disorders that affect movement and muscle tone so they can gain back the ability to perform activities

of daily living with ease and comfort. Therefore, any ideal wearable exoskeletons that are designed to assist patients with musculoskeletal disorders must be stable and must fluently respond to the user's movements. To achieve stability and user dominance, it is paramount to have joints that are easily backdrivable and have a higher transmission ratio to control the torque output. Also, it must be compact since it gets mounted on users' bodies.

User safety is the most crucial factor when it comes to wearable assistive exoskeletons. To ensure user safety, the exoskeleton must be designed to prevent hyperextension. Fluid backdrivability is the key to avert hyperextension; in other words, it allows users to quickly and smoothly apply torque from the driven side of the actuator in the opposite direction to overcome the opposite motion of the actuator caused by the driving mechanism.

In recent years, many wearable assistive exoskeletons have been developed using various mechanical joints such as Rolling joint [11], Rope (Capstan) drive [12], Two-stage planetary mechanism with timing belt [13], and Harmonic drive [15]. However, these mechanisms have several disadvantages that do not help in designing a stable, compact, and highly backdrivable exoskeleton actuator.

The Rolling joint (Figure 1.1) consists of a pair of sectional gears meshed, and the top sectional gear is connected to the actuator by an input pulley and a cable. As the actuator drives the first sectional gear, it causes the meshed gear to rotate in a specific rotational direction depending on the actuation direction. This joint design is inefficient when it comes to maintaining compactness while having a greater transmission ratio. Even with double stage reducer, the design uses two 64 mm diameter sectional gears and can only offer a transmission ratio of 8.85 to 1. This itself proves the joint cannot offer compactness if a user were to increase the transmission ratio for higher stability. It becomes

uncomfortable for users to wear a bulky joint. The joint also requires 3.33 Nm torque to backdrive; this doesn't support smooth backdrivability [11].

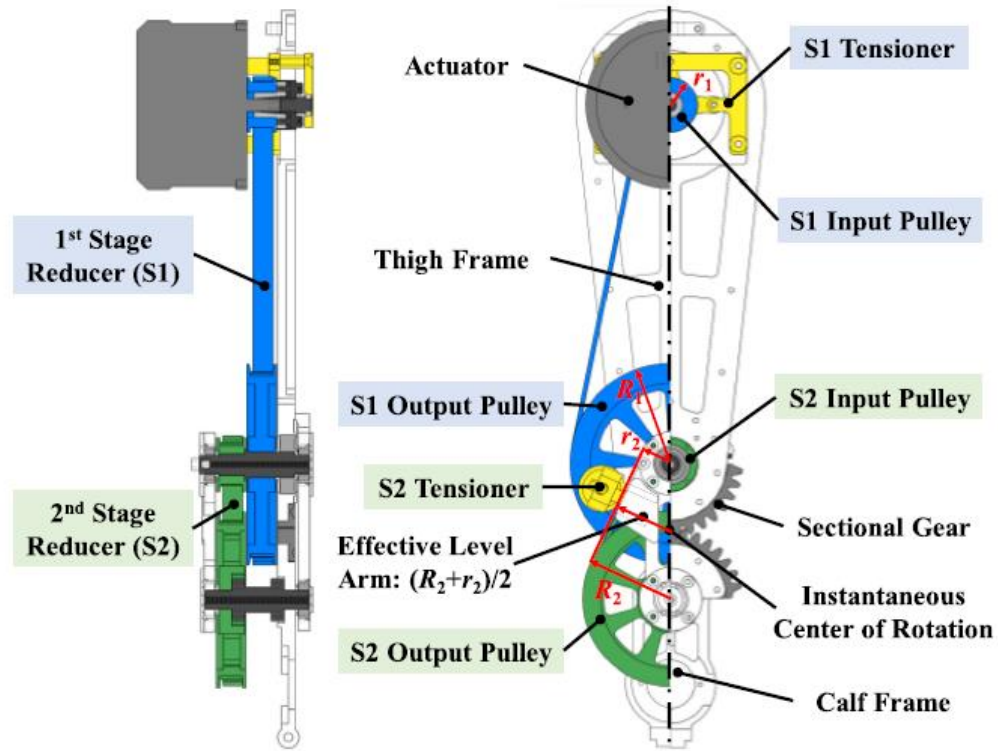


Figure 1.1 Rolling Joint: two-stage timing belt transmission system that provides a transmission ratio of 8.85:1 and requires 3.33 Nm torque to backdrive.

Source: Wang, J., Li, X., Huang, T.-H., Yu, S., Li, Y., Chen, T., Carriero, A., Oh-Park, M., & Su, H. (2018). Comfort-Centered Design of a Lightweight and Backdrivable Knee Exoskeleton. *IEEE Robotics and Automation Letters*, 3(4), 4265–4272. <https://doi.org/10.1109/lra.2018.2864352>

The Capstan (Rope) drive (Figure 1.2) consists of a capstan pulley and a capstan wheel. The capstan pulley is a small cylinder around which rope is wound and is directly connected to a motor shaft, and the capstan wheel is driven by the rope connected to the capstan pulley. The design offers a 10:1 transmission ratio with the Capstan wheel of 120 mm diameter [12]. A huge drawback with this mechanism is an increase in the transmission ratio will demand an increase in the size of the capstan wheel. As the capstan wheel increases in size, the center distance between the capstan wheel and the capstan pulley will

have to increase, ultimately compromising the compactness. The value of the current diameter of the capstan wheel is already not the desired value if the transmission ratio is to be set to 10:1.

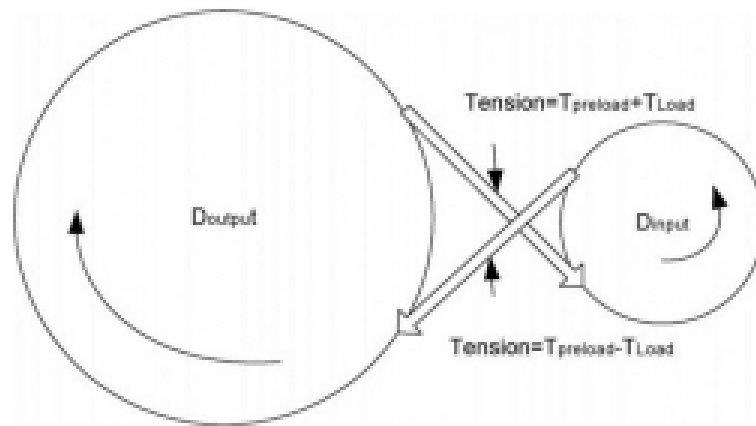


Figure 1.2 Capstan drive system with the transmission ratio of 10:1 and the capstan wheel diameter of 120 mm.

Source: Eib, Andrew (2018). Design of a Backdrivable Upper-Limb Exoskeleton for Use in Rehabilitation Therapy of Stroke Patients. Master's thesis, Texas A&M University.
From <http://hdl.handle.net/1969.1/173937>

The two-stage planetary mechanism with a timing belt (Figure 1.3) uses a planetary gears box in conjunction with a timing belt and sprocket connecting it with a motor. The design offers a 24:1 transmission ratio and required 3 Nm torque to backdrive [13]. Even though the design offers a great transmission ratio, it requires more than 1 Nm torque to backdrive the mechanism. Higher torque required to backdrive will increase the possibility of hyperextension if a user is unable to exert the required torque. Also, the design does not have any safety mechanisms placed to prevent hyperextension. Also, the design is not compact as multiple mechanisms are involved in amplifying the transmission ratio.

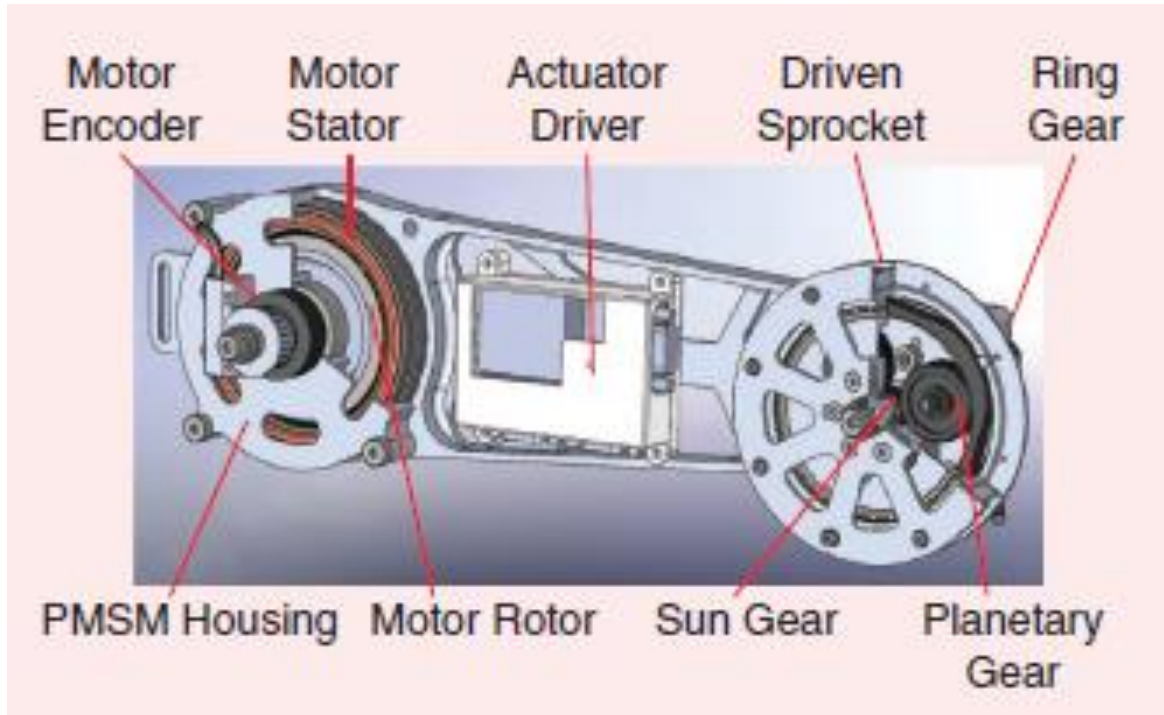


Figure 1.3 The two-stage planetary mechanism with timing belt offering the transmission ratio of 24:1 and required 3 Nm torque to backdrive the joint design.

Source: Lv, G., Zhu, H., & Gregg, R. D. (2018). On the Design and Control of Highly Backdrivable Lower-Limb Exoskeletons: A Discussion of Past and Ongoing Work. *IEEE Control Systems*, 38(6), 88–113. <https://doi.org/10.1109/mcs.2018.2866605>

Harmonic drive (Figure 1.4) is composed of three components: elliptical wave generator with roller bearing, circular spline, and flex-spline. The elliptical wave generator with a roller bearing is inserted into the flex-spline, the flex-spline adopts the elliptical shape of the elliptical wave generator, then gets assembled with the circular spline. The external teeth on the flex-spline mesh with the internal teeth of the circular spline. As the elliptical wave generator (input shaft) rotates, the flex-spline (output shaft) also rotates at a different velocity based on the transmission ratio [14]. The Harmonic drives are not easily backdrivable with a small amount of torque due to high stiction torque [15]. Its inability to easily backdrive with lower torque makes this mechanism not suitable for the rehabilitation robotics applications where backdrivability is a key feature.

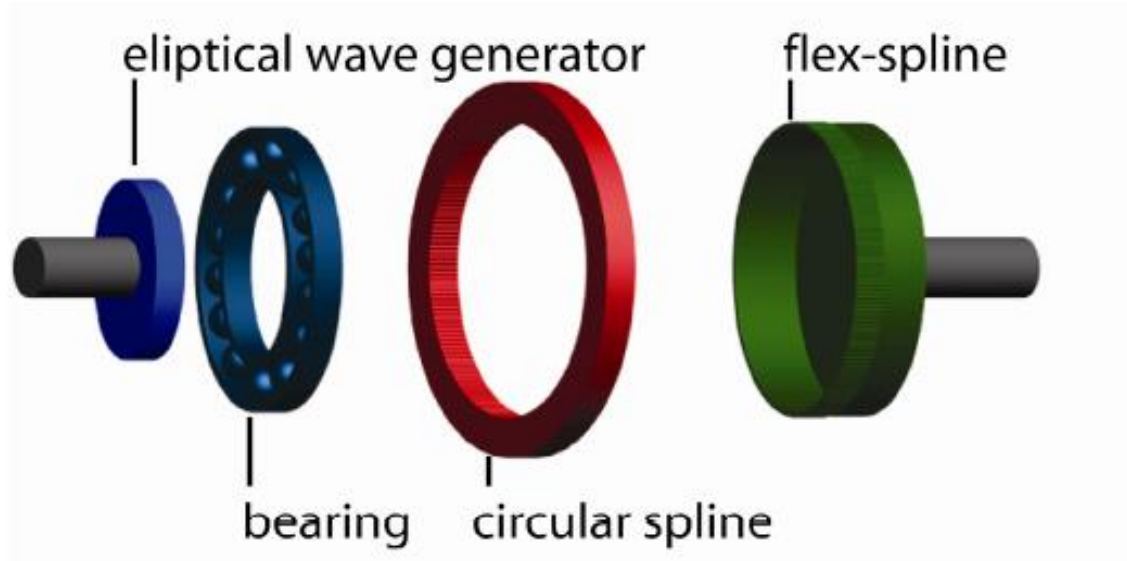


Figure 1.4 The exploded view of a harmonic drive assembly.

Source: J. W. Sensinger and J. H. Lipsey, Cycloid vs. harmonic drives for use in high ratio, single stage robotic transmissions, *2012 IEEE International Conference on Robotics and Automation*, Saint Paul, MN, 2012, pp. 4130-4135, doi: 10.1109/ICRA.2012.6224739

The cycloidal mechanism is an ideal solution that allows the design of a highly backdrivable joint that is stable and compact. This thesis focuses on the development of a joint design that utilizes a single-stage cycloidal drive to achieve a higher transmission ratio (10:1) while maintaining the design compactness and backdrivability.

1.3 The Structure and Operating Principles of Cycloidal Drive

Cycloidal drives can be classified into four categories [16]:

1. Rotating ring gear epicycloid drive
2. Stationary ring gear epicycloid drive
3. Rotating ring gear hypocycloid drive
4. Stationary ring gear hypocycloid drive

The rotating ring gear epicycloid drive is designed as a part of this thesis to provide a higher transmission ratio and design compactness while maintaining lower backdrivable torque for the proposed joint design.

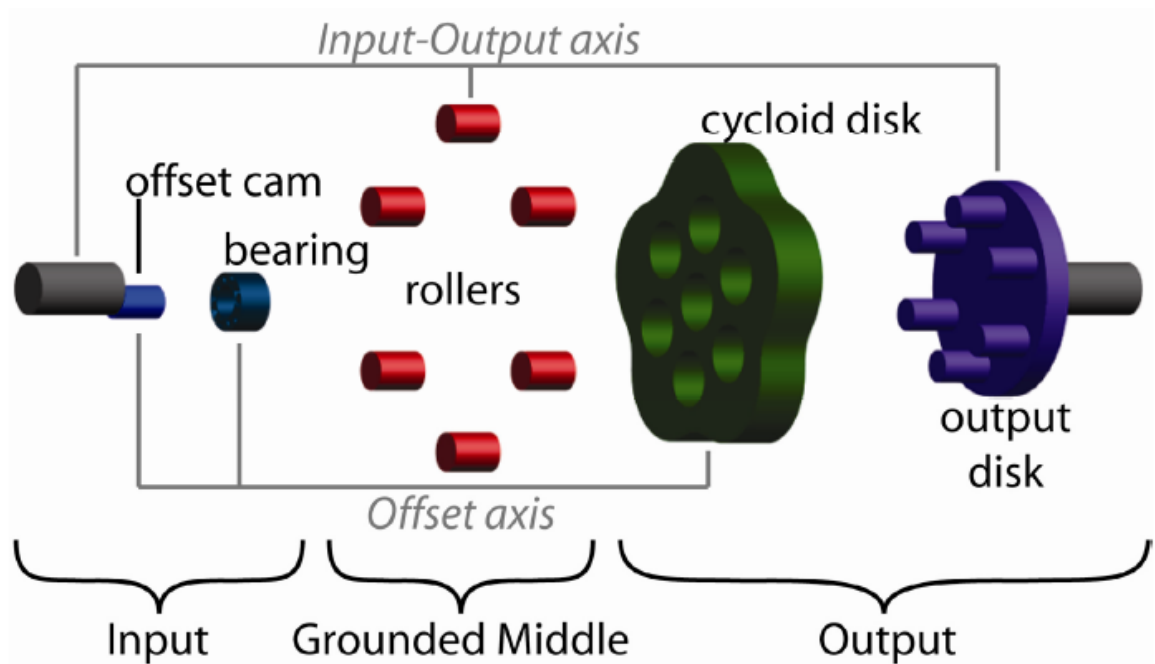


Figure 1.5 The exploded view of a cycloidal drive assembly.

Source: J. W. Sensinger and J. H. Lipsey, Cycloid vs. harmonic drives for use in high ratio, single stage robotic transmissions, *2012 IEEE International Conference on Robotics and Automation*, Saint Paul, MN, 2012, pp. 4130-4135, doi: 10.1109/ICRA.2012.6224739

The cycloidal drive is generally designed using the following components: an eccentric input shaft (offset cam), bearings, a cycloidal disk, rollers, and an output shaft, as shown in Figure 1.5.

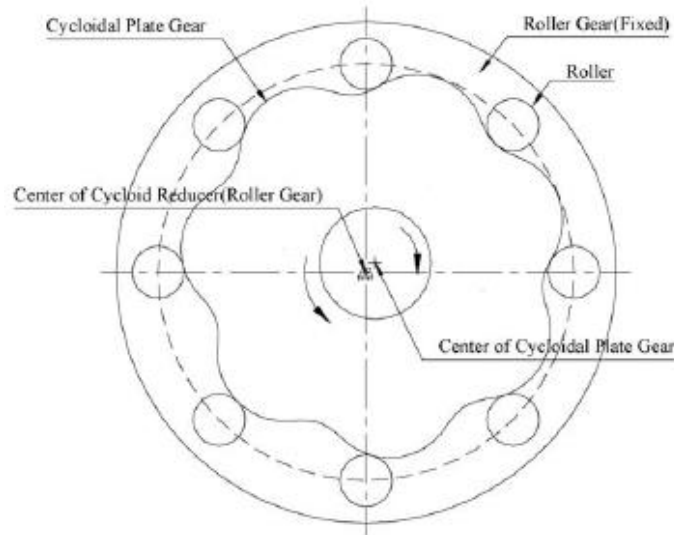


Figure 1.6 Representation of the offset between the center axis of the roller gear and the center axis of the cycloidal disk.

Source: Shin, J.-H., & Kwon, S.-M. (2006). On the lobe profile design in a cycloid reducer using instant velocity center. *Mechanism and Machine Theory*, 41(5), 596–616.
<https://doi.org/10.1016/j.mechmachtheory.2005.08.001>

The complete assembly consists of the cycloidal disk mounted on the eccentric input shaft with a bearing placed between to allow the cycloidal disk to rotate in eccentric motion without much friction in the opposite direction of the rotating input shaft. The word *Eccentricity* is defined as the offset between the center axis of the eccentric input shaft or the roller gear and the center axis of the cycloidal disk as it is mounted on the eccentric input shaft, as shown in Figure 1.6. Also, the output pins located on the output disk are inserted into the holes located on the cycloidal disk. As the eccentric input shaft rotates, it also forces the cycloidal disk to rotate in eccentric motion in the opposite direction, ultimately pushing the cycloidal disk against the fixed rollers. As the cycloidal disk is

rotating, it interacts with the fixed rollers and also the output pins of the output disk, ultimately transferring torque to the output disk and causing it to rotate in the opposite direction of the rotating eccentric input shaft.

The number of rollers is always one greater than the number of teeth on the cycloidal disk. This difference in the number of rollers and the number of teeth determines the transmission ratio of the mechanism. The higher transmission ratio will significantly reduce the rotating velocity of the output shaft, and according to the law of conservation of energy, it would amplify the output torque [17].

The main disadvantages of the earlier discussed mechanisms are their inability to maintain compactness and provide smooth backdrivability when a higher transmission ratio is required to obtain a higher output torque. The cycloidal drive is an ideal mechanism that can offer a high transmission ratio while maintaining a thinner profile and lower reflected inertia that allows torque less than 1 Nm to backdrive [15].

Despite offering a number of advantages over the earlier discussed mechanisms, the cycloidal drives in comparison to harmonic drives have significant backlash. In a recent comparison study [15], the cycloidal drives exhibited considerable backlash in comparison to harmonic drives. The research concluded that cycloidal drives exhibited 1.4 degrees of backlash with the transmission ratio set to 70:1, and as the ratio was increased the backlash gradually decreased. On the other hand, the harmonic drives exhibited no backlash with an even greater (100:1) transmission ratio. Regardless of the backlash, the fluid backdrivability provided by the cycloidal drive outweighs the benefit of no backlash provided by the harmonic drives. In robotics applications, backdrivability is paramount to ensure user safety by eliminating possibilities of hyperextension.

Chapter 2 to 4 represents the design methodology of the proposed cycloidal drive joint. Chapter 2 discusses the design of the moving arm assembly, including cycloidal housing and rollers. Chapter 3 discusses the design of the cycloidal rotor and the eccentric shaft. Chapter 4 discusses the design of the fixed arm assembly and the motor mount. Chapter 4 also discusses the static backdrivability test and summarizes the results.

CHAPTER 2

DESIGN OF THE CYCLOIDAL HOUSING AND ROLLERS

2.1 Transmission Ratio

The transmission ratio is the ratio between the rotational speeds of two meshing gears. In the case of a cycloidal gearbox design, the transmission ratio is defined by the number of rollers and the number of rotor teeth. Equation 2.1 [4] can be utilized to compute a transmission ratio of a cycloidal gearbox system.

$$\text{Transmission Ratio (i)} = \frac{n}{N - n} \quad (2.1)$$

n = Number of Rotor Teeth

N = Number of Rollers

Condition: $N = 1 + n$

For this specific design, the gear ratio is set to 10:1 based on stakeholder requirements. The number of Rotor Teeth (n) is set to 10, and the Number of Rollers (N) is set to 11.

2.2 Housing Circle Circumference and Roller Radius

Housing circle circumference defines the circular boundary on which rollers with radius R_r are fixed. To compute the Housing Circle Circumference, first, a designer must specify the radius R of the rotor. Rotor Radius (R) is set to 26 mm for this design based on stakeholder requirements.

$$\text{Housing Circle Circumference} = 2 * R * \pi \quad (2.2)$$

Housing Circle Circumference can be computed using equation 2.2 [2] after the Rotor Radius (R) is specified.

For the design, the Housing Circle Circumference is 56π mm. In other words, rollers will be placed on the boundary of a 56 mm diameter circle profile.

Roller Radius (R_r) can be computed using equation 2.3 [2] once the Housing Circle Circumference is computed.

$$\text{Roller Radius } (R_r) = \frac{\text{Housing Circle Circumference}}{4 * N} \quad (2.3)$$

For this design, the roller radius (R_r) is computed to be 4 mm based on the Housing Circle Circumference and the Number of Rollers (N).

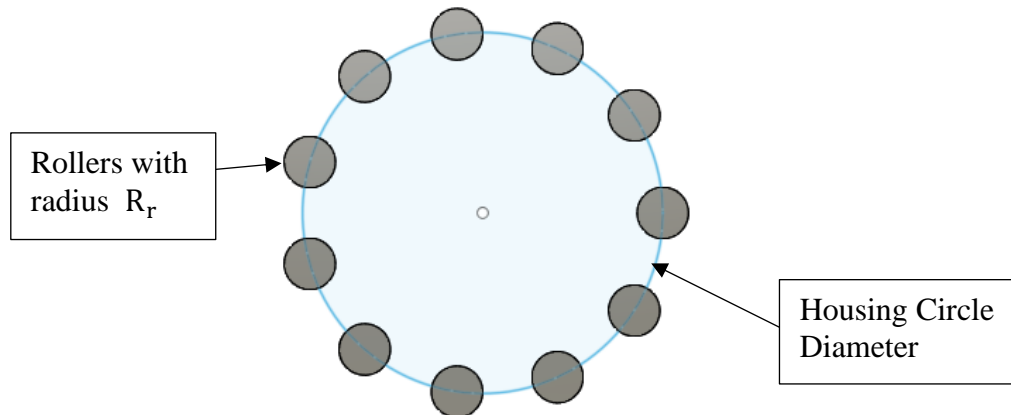


Figure 2.1 Representation of rollers arranged on the housing circle.

The height of the rollers can be defined according to the desired thickness of the cycloidal rotor. In this case, the thickness of the rotor is set to 3 mm, so the height of the rollers was chosen to be 10 mm. The selected roller height provides ample surface contact with circular slots (see figure 2.3) on the rotating arm side plate to ensure design robustness. Having ample surface contact between the rollers and the circular slots is vital since the rotor exerts high torque on the rollers when it is in motion.

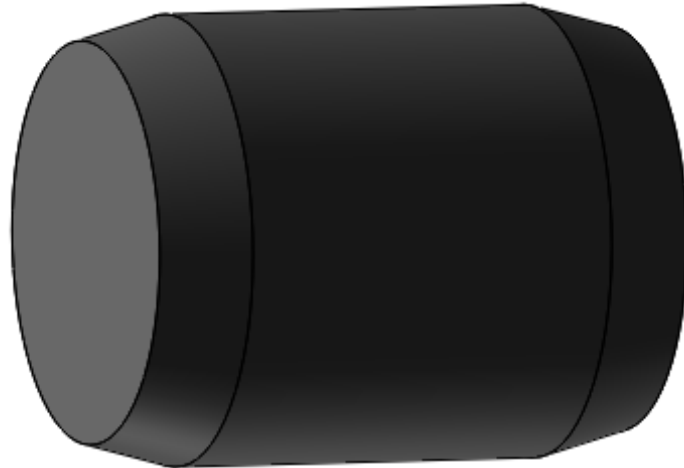


Figure 2.2 Roller design.

316 Stainless Steel Dowel Pin 8 mm Diameter, 10 mm Long. (2019). McMASTER-CARR.
<https://www.mcmaster.com/93600A762/>

2.3 Design of Rotating Arm

The rotating arm was designed based on the Housing Circle Diameter and the Roller Radius (R_r). The rotating arm is designed such that rollers can be easily mounted into the circular slots. In total, 11 circular slots have been created around the center axis to match the number of rollers.

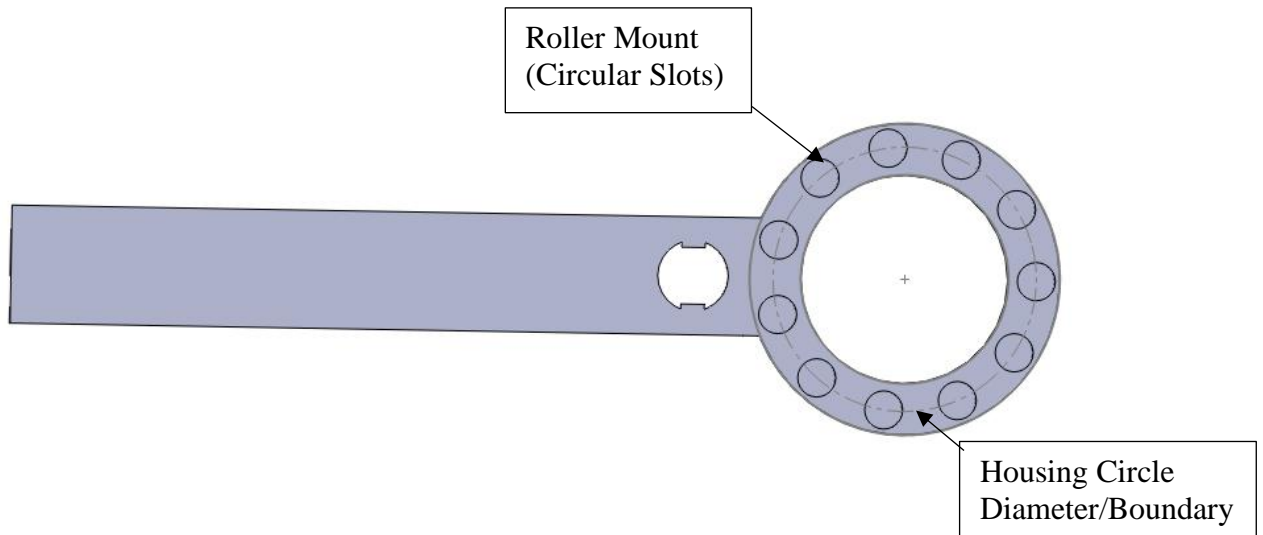


Figure 2.3 Rotating arm-side plate.

Rotating arm assembly consists of two side plates and eleven rollers. Rollers are simply inserted into circular slots and secured by two side plates. The side plates are secured by a pair of the M4 hex nut and M4 hex screw; it keeps the assembly intact. As mentioned in chapter 1, the design is based on the rotating ring gear epicycloid drive concept, where the ring gear rotates or serves as the output shaft. The rollers here can be viewed as the ring gear that is fixed with the side plates, ultimately rotating the assembly. Appendix A includes manufacturing drawings of the components involved in the rotating arm assembly.

Components involved in the rotating arm assembly:

Table 2.1 List of Components Involved in the Rotating Arm Assembly

	Components	Quantity
1	Rollers	11
2	Rotating Arm Side Plates	2
3	Rotating Arm Side Plates Connector	1
4	Washer 2	2
5	Hex Nut, M4 x 0.7 mm Thread	1
6	Hex Screw, M4 x 0.7 mm, 12 mm Long	1

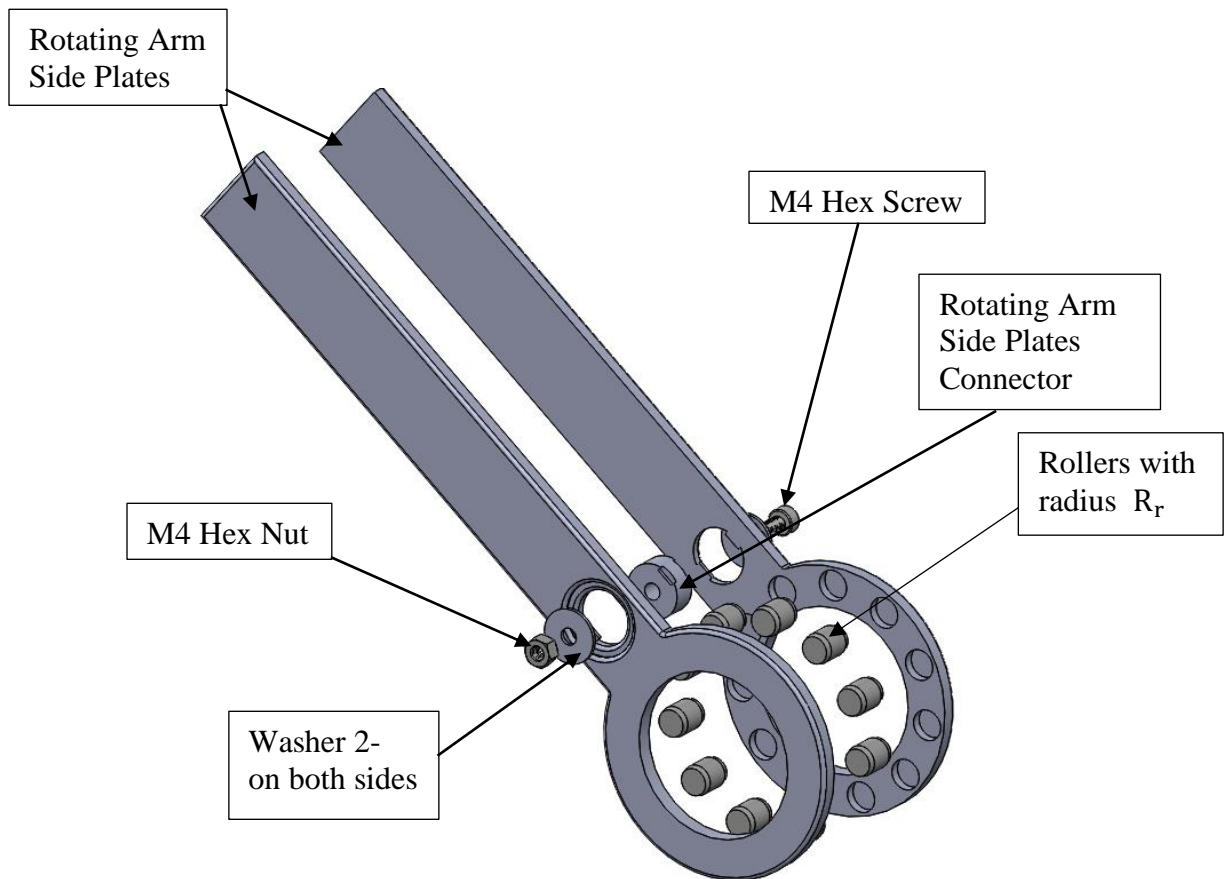


Figure 2.4 Exploded view of the rotating arm assembly.

CHAPTER 3

DESIGN OF THE CYCLOIDAL ROTOR AND THE ECCENTRIC SHAFT

3.1 Shaft Eccentricity

Shaft eccentricity is defined as an offset between the center axis of rotation and the axis of symmetry. For the cycloidal mechanism, the shaft eccentricity is the offset between the center axis of the rotating shaft and the center axis of the cycloidal rotor mounted onto the shaft at a specific offset. It is one of the requirements in defining the cycloidal rotor design. Shaft eccentricity can be computed using equation 3.1 [2].

$$\text{Eccentricity (E)} = 0.5 * R_r \quad (3.1)$$

For this design, the shaft eccentricity (E) is 2 mm based on the roller radius (R_r) computed in chapter 2. The design of the eccentric shaft is discussed in detail in section 3.4.

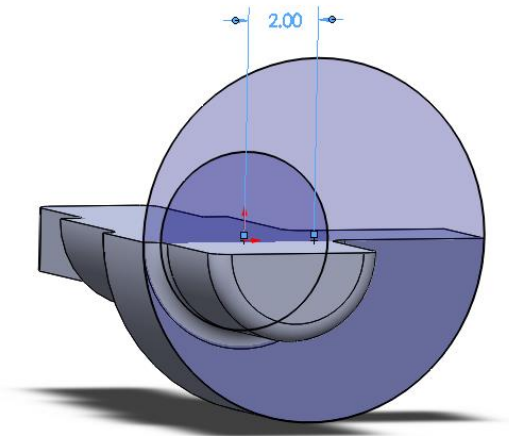


Figure 3.1 Representation of eccentricity using cross section of the eccentric shaft.

3.2 Parametric Equations Defining Cycloidal Rotor Profile

Once the Rotor Radius (R), Eccentricity (E), Roller Radius (R_r), and the Number of Rollers (N) is set, equations 3.2 [6], 3.3 [6], and 3.4 [6] can be used to generate cycloidal rotor profile.

$$\phi = -\tan^{-1} \left[\frac{\sin((1-N)\theta)}{\left(\frac{R}{EN}\right) - \cos((1-N)\theta)} \right], (0^\circ \leq \theta \leq 360^\circ) \quad (3.2)$$

$$X = R\cos\theta - R_r\cos(\theta - \phi) - E\cos(N\theta) \quad (3.3)$$

$$Y = -R\sin(\theta) + R_r\sin(\theta - \phi) + E\sin(N\theta) \quad (3.4)$$

ϕ is the contact angle between the cycloidal rotor teeth and the rollers. Equation 3.2 can be utilized to compute the contact angle using different θ values ranging from 0 to 360 degrees. The precision of the rotor profile depends on the step value of the angle θ . The smaller the step is, the corresponding shape is more precise. In other words, the meshing between rotor teeth and rollers will be precise, resulting in negligible backlash.

Equation 3.3 and Equation 3.4 provide the X-Y location (point) based on the contact angle ϕ , the corresponding angle θ , Rotor Radius (R), Eccentricity (E), Roller Radius (R_r), and Number of Rollers (N). Modeling of the cycloidal rotor was done using Autodesk Fusion 360. A python script [2] was utilized to generate the rotor geometry in Autodesk Fusion 360.

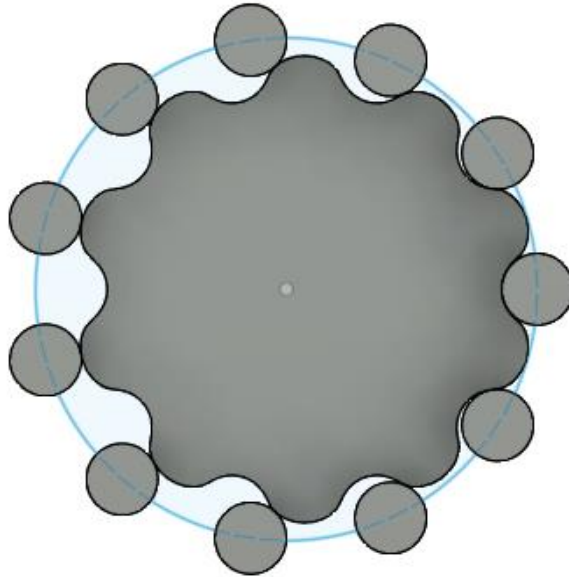


Figure 3.2 Modeling of the cycloidal rotor and rollers in Autodesk Fusion 360.

3.3 Pin-Hole Diameter (D_H)

To ensure a two-way motion transfer, from the motor shaft to the rotating arm assembly and from the rotating arm assembly to the motor shaft, it is necessary to create the Pin-Hole feature on the cycloidal rotor. Pins are mounted on the fixed arms and engage in these holes created on the cycloidal rotor. Due to the eccentric motion, the cycloidal rotor rotates around these pins and transfers gradual torque from the input shaft. Equation 3.5 [3][5] can be utilized to compute the Pin-Hole diameter (D_H).

$$D_H = D_P + 2 * E \quad (3.5)$$

$D_P = Pin\ Diameter$

$E = Eccentricity$

Pin Diameter (D_P) can be chosen depending on the design requirements. For this design, the Pin Diameter (D_P) is set to 2 mm and Pin-Hole Diameter (D_H) is computed to be 6 mm. A bearing with an inner diameter of 6 mm was selected such that it serves as a Pin-Hole and also helps make the design back drivable by reducing friction between the pin and the rotor.

After the Pin-Hole Diameter (D_H) is computed, the Mounting Circle Diameter (D_{Mount}) must be defined so the center of the Pin-Hole can be placed on it. Multiple Pin-Holes can be created based on the requirements. For this design, there are a total of 4 Pin-Holes, and the Mounting Circle Diameter (D_{Mount}) is set to 31 mm.

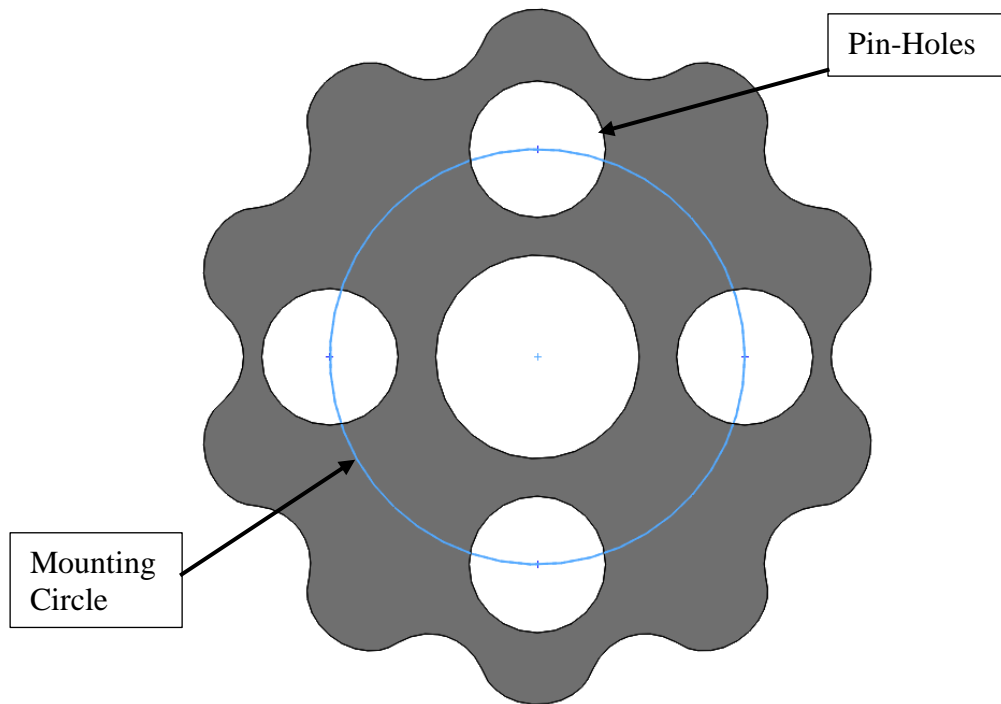


Figure 3.3 Representation of the pin-holes and the mounting circle.

The height of the pin can be selected based on the joint thickness or desired design compactness. For this design, the pin height is set to 14 mm.



Figure 3.4 Representation of the pin with 2 mm diameter.

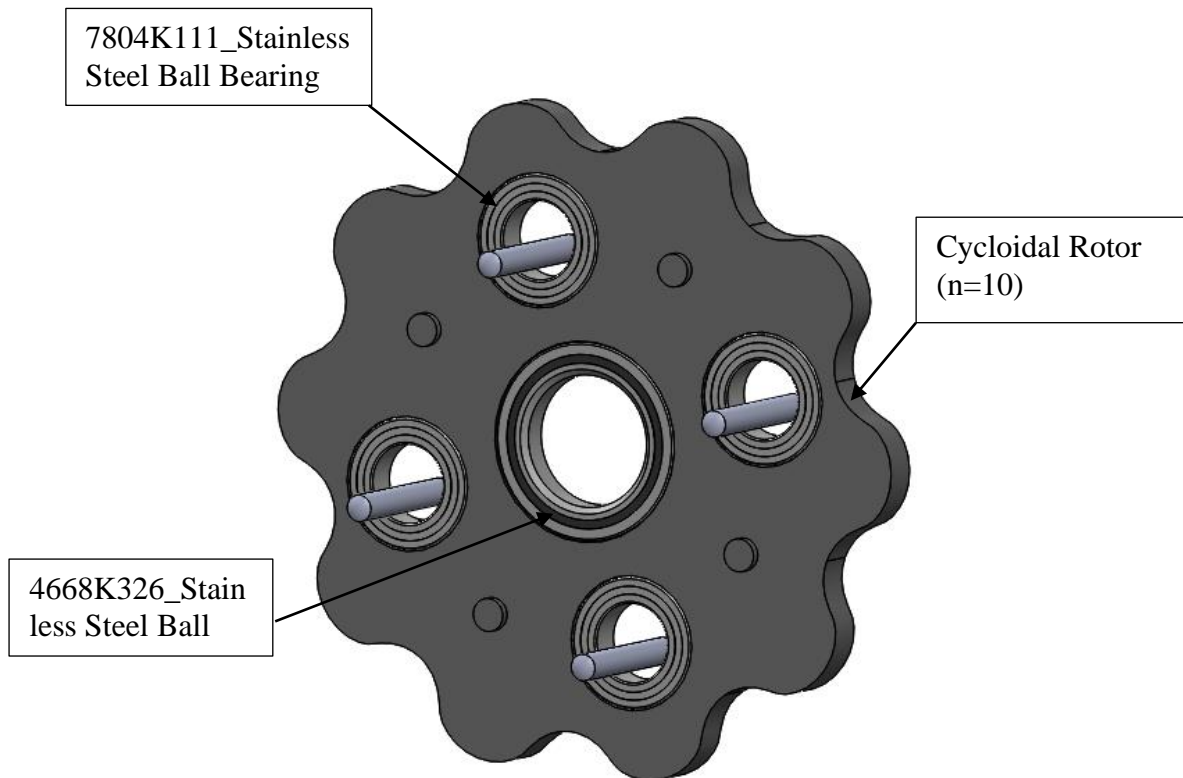


Figure 3.5 Interaction of rotor assembly with fixed pins.

Components involved in the Rotor assembly.

Table 3.1 List of Components of the Cycloidal Rotor Assembly

	Components	Quantity
1	Cycloidal Rotor	1
2	7804K111_Stainless Steel Ball Bearing	4
3	4668K326_Stainless Steel Ball Bearing	1

Figure 3.4 represents the cycloidal rotor assembly consisting of the cycloidal rotor ($n=10$) and two types of bearings as labeled in the table above. The primary reason for introducing the 4668K326 stainless steel bearings is to minimize a significant amount of friction between the cycloidal rotor and the eccentric shaft. The cycloidal rotor rotates in the opposite direction of the input shaft, and while it rotates a significant amount of friction may get generated; therefore, introducing a bearing between them certainly makes the friction negligible.

Also, as the cycloidal rotor rotates, it interacts with the fixed pins. In the absence of bearing, the high friction prevents the rotor from smoothly tangentially rotating around the fixed pins; thus, the system may degrade. However, introducing 7804K11 stainless steel bearing significantly reduces the friction between the components, resulting in smooth tangential rotation.

3.4 Eccentric Shaft

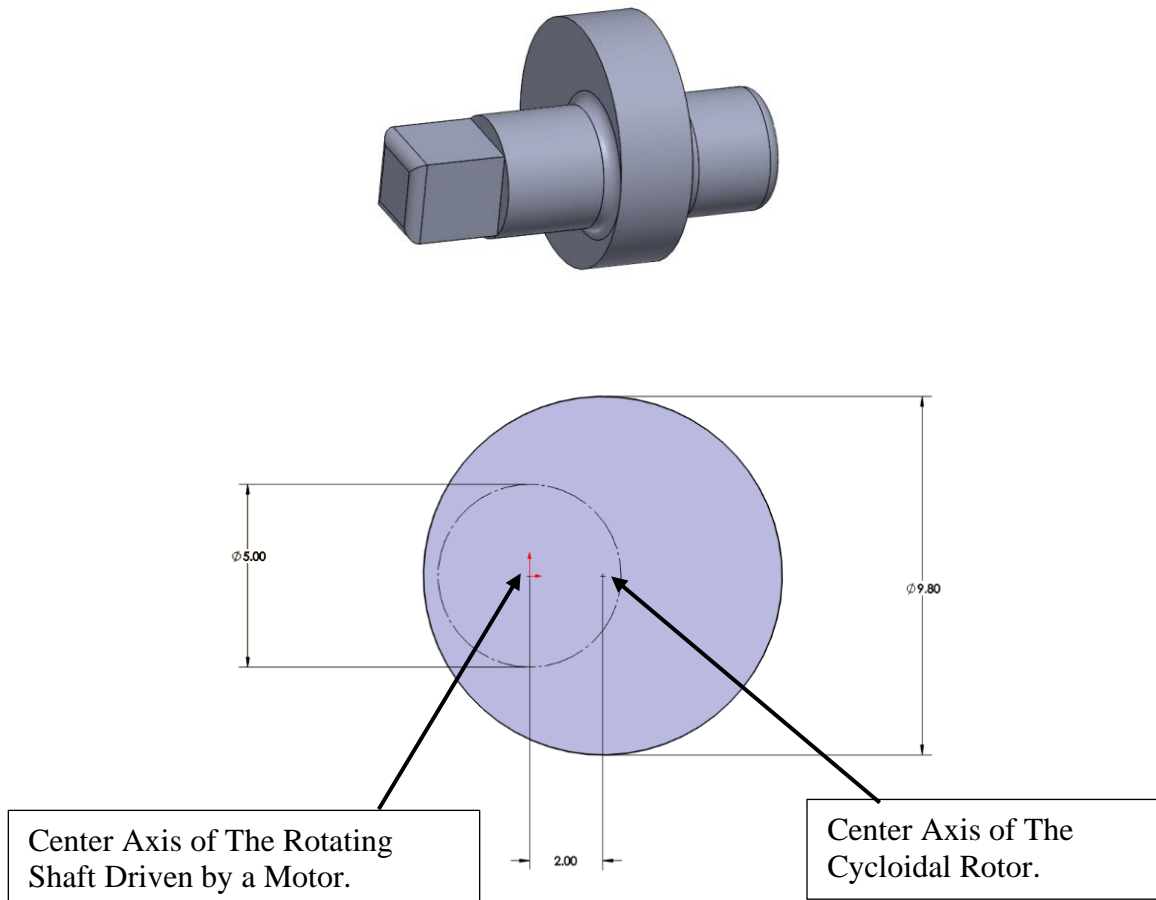


Figure 3.6 Representation of center axis of the rotating shaft driven by the motor and the center axis of the cycloidal rotor.

The eccentric shaft is designed based on the eccentricity computed in chapter 3, and the rotor thickness of 3 mm. The shaft eccentricity is the offset between the center axis of the rotating shaft driven by a motor and the center axis of the cycloidal rotor mounted onto the shaft at a specific offset.

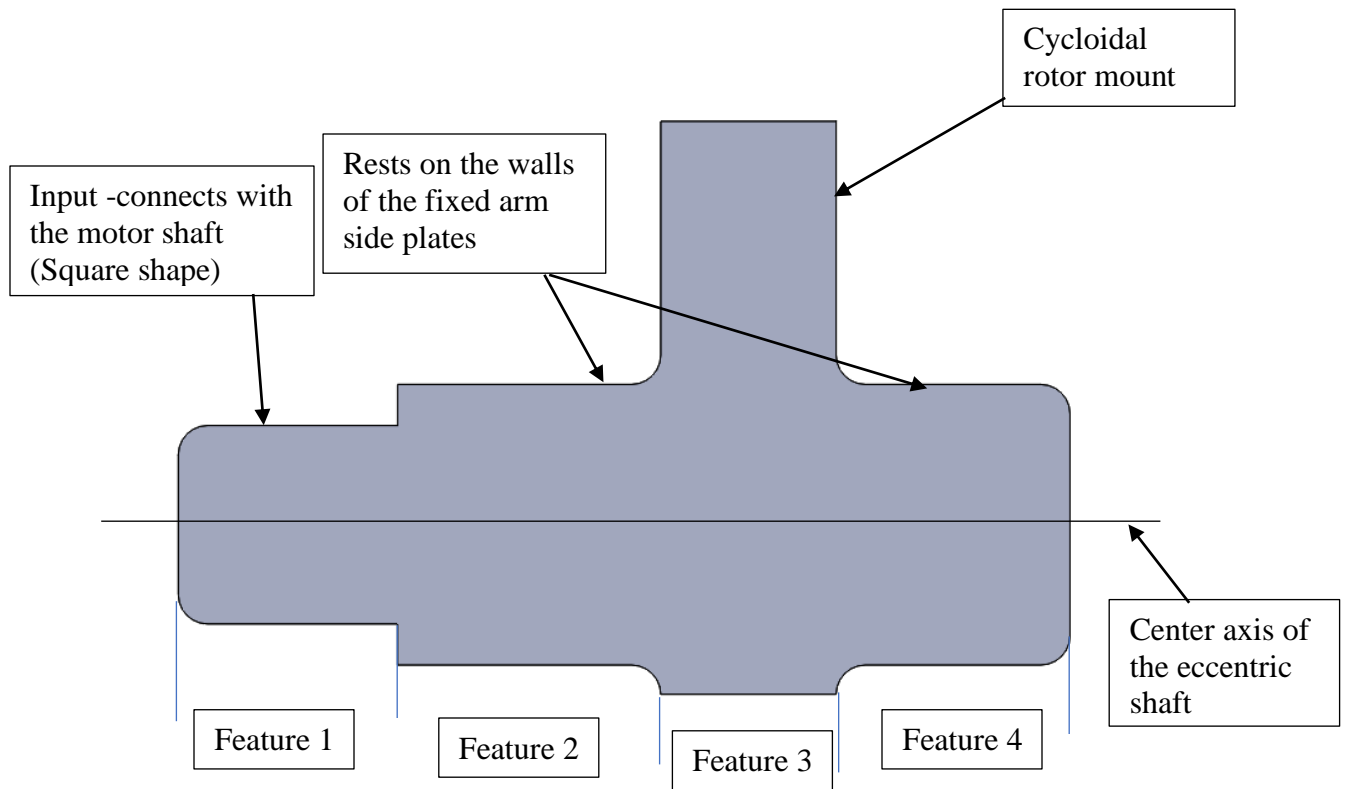


Figure 3.7 Cross-section of the eccentric shaft.

The center axis of the eccentric shaft aligns with the center axis of the roller gear. Feature 1, as shown in figure 4.2, serves as the primary interface between the cycloidal gearbox and the motor. Feature 1 is designed using a square shape to ensure it stays intact with the motor shaft. The square shape provides ample surface area in contact to ensure the eccentric shaft does not slip. Having other shapes such as hexagon will have more chances of slippage if not properly fabricated. Feature 2 and feature 4 can be viewed as simple cylindrical shapes resting on the walls of the fixed arm side plates. Bearings have been mounted on feature 2 and feature 4 to facilitate smooth rotation of the eccentric shaft while resting on the fixed arm plate walls. Feature 3 is the cycloidal rotor mount and its center is at an offset of 2 mm from the center of the eccentric shaft. The cycloidal rotor assembly includes a bearing in the center hole that significantly eliminates the friction between the eccentric shaft and the cycloidal rotor.

3.5 Motor Shaft

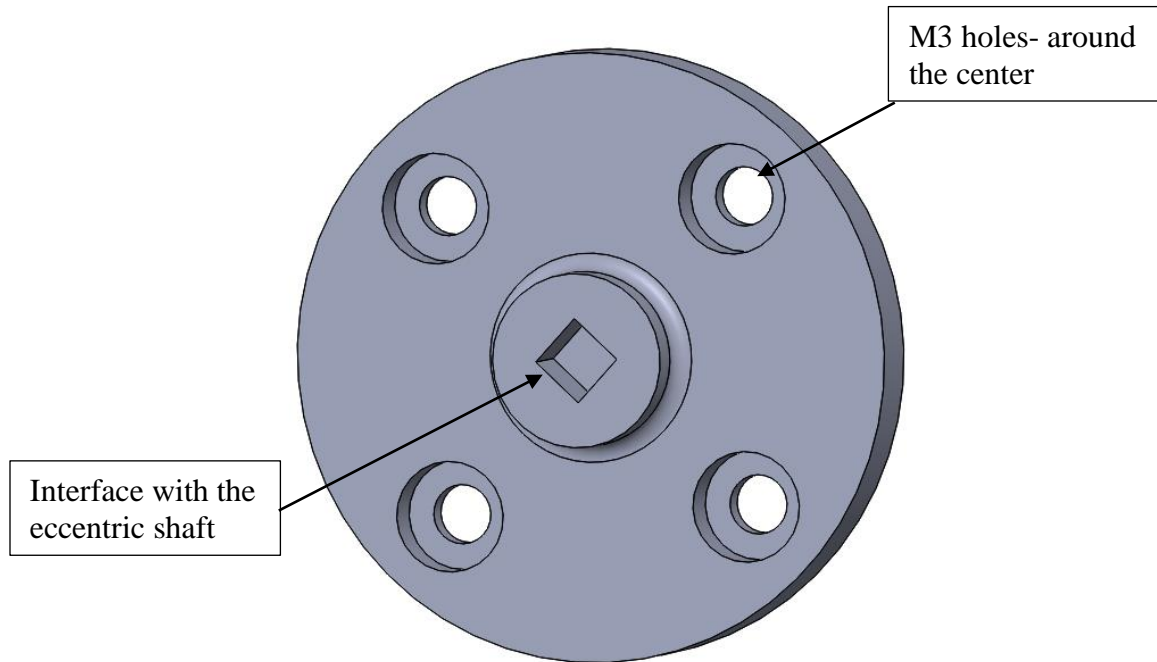


Figure 3.8 Representation of the motor shaft that will transfer torque from the motor to the eccentric shaft.

The motor shaft is mainly designed based on the specification of the BLDC motor. It is attached to the output side of the BLDC motor with four M3 screws. A square shape interface has been designed in the center to securely connect with the eccentric shaft. This ensures no slippage and successfully transfers motion from the motor to the eccentric shaft, ultimately rotating the output ring gear.

CHAPTER 4

DESIGN OF THE FIXED ARM ASSEMBLY

AND REPRESENTATION OF THE FINAL ASSEMBLY

4.1 Design of the Fixed Arm Side Plates

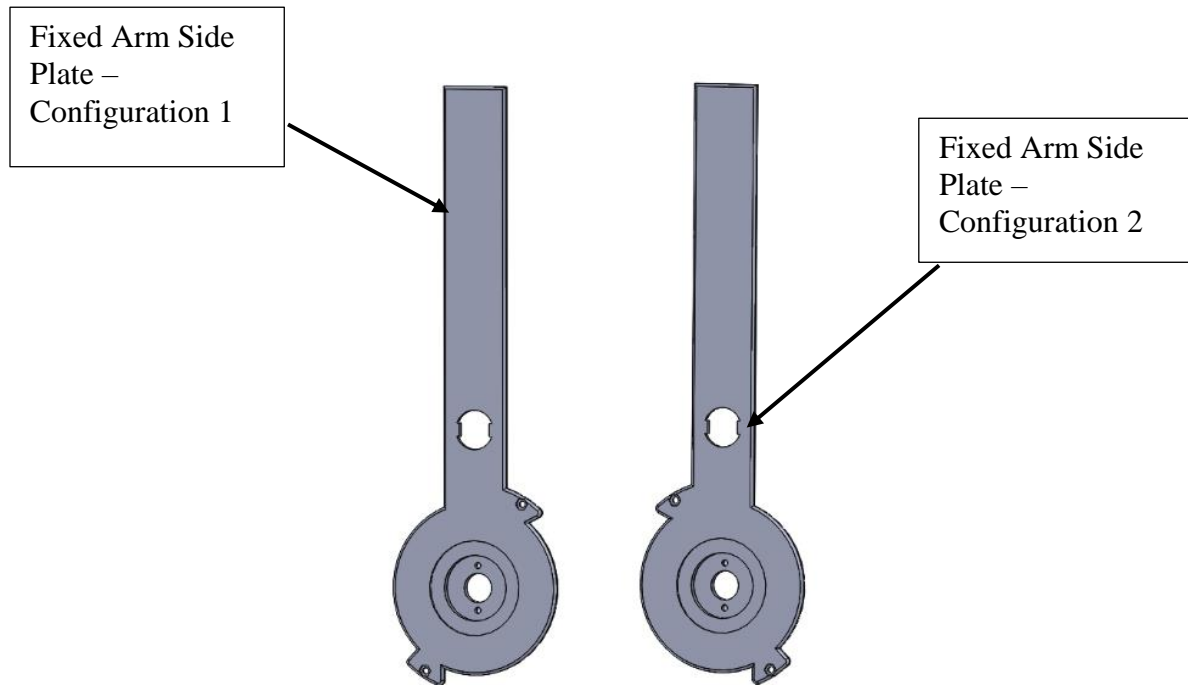


Figure 4.1 Fixed arm side plates.

The fixed arms assembly consists of two different fixed arm side plates. The side plates are designed based on the Mounting Circle Diameter (D_{Mount}) on which the pins are fixed (figure 3.2). The design includes rotation lock features restricting the rotation of the moving arm from 0 degrees to 135 degrees. The rotation lock features are vital in preventing over-rotation of the rotating arm, ultimately reducing the chances of physical injuries. The fixed arm side plates design allows users to mount the motor on either side, allowing them to use the joint for the left and right limb.

4.2 Design of the Motor Mount & Sensor Holding Bracket

The motor mount (Figure 4.2) is designed for securely mounting the motor to the fixed arm side plates. The mount is compatible with both fixed arm side plates, which means it can be mounted on either side of the joint. The design includes notches that engage with notches on the side plates to prevent any unnecessary rotational displacement caused by the torque exerted by the motor. The motor mount is designed based on the specifications of the BLDC motor to ensure a safe and robust interface with the motor. The sensor holding bracket was designed based on the design specification of the AS5147- magnetic rotary position sensor board. The bracket is designed such that the rotary position sensor board can be securely attached to the mount for controlling the motor speed and position.

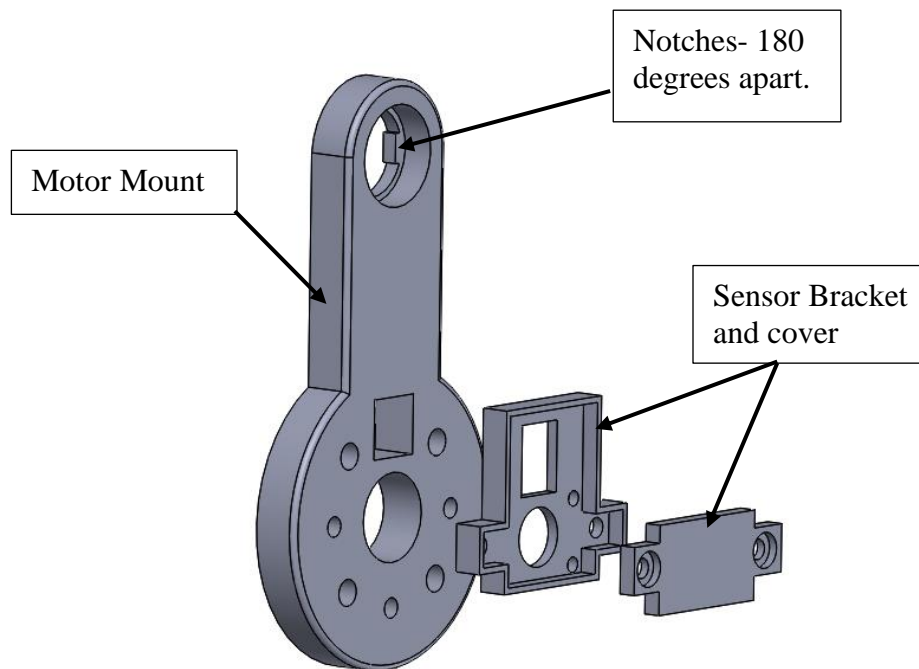


Figure 4.2 Motor mount & sensor holding bracket assembly.

4.3 Design of the Fixed Arm Assembly

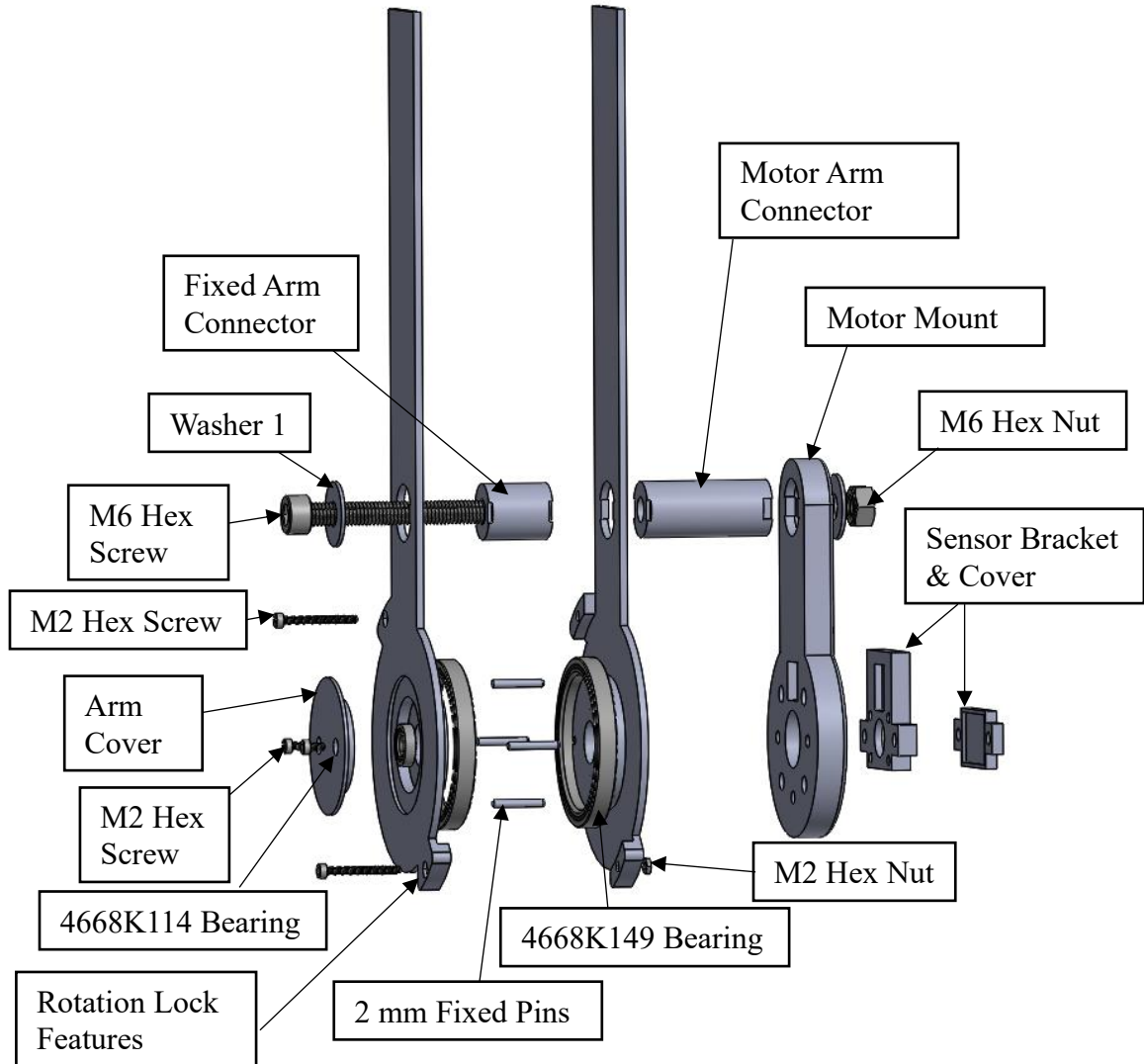


Figure 4.3 Exploded view of the fixed arm assembly.

Two 44 x 35 x 5 mm bearings are introduced to allow smooth rotation of the rotating arm assembly. Also, the arm cover was designed to hide the rotating eccentric shaft. The fixed arm connector is part of the fixed arm side plates but was designed as a separate

component to make the fabrication of the design cost friendly. A similar approach was taken with the design of the motor mount; the motor arm connector is an integral part of the motor mount but is designed as an individual component to save manufacturing costs. The motor mount is securely connected to the fixed arm side plates by a single M6 bolt and nut. The fixed arm side plates are securely intact by two M2 bolts and nuts.

Components involved in the fixed arm assembly:

Table 4.1 List of Components Involved in the Fixed Arm Assembly

	Components	Quantity
1	Arm Cover	1
2	Hex Screw, M2 x 0.4 mm Thread, 4 mm Long	2
3	Hex Screw, M2 x 0.4 mm Thread, 20 mm Long	2
4	Steel Thin Hex Nut, M2 x 0.4 mm Thread	2
5	4668K114_Stainless Steel Bearing	2
6	Washer 1	2
7	Fixed Arm Connector	1
8	Motor Arm Connector	1
9	Motor Mount	1
10	Fixed Arm Side Plate- Configuration 1	1
11	Fixed Arm Side Plate – Configuration 2	1
12	4668K149_Stainless Steel Bearing	2
13	Head Screw, M6 x 1 mm Thread, 60 mm Long	1
14	Steel Hex Nut, M6 x 1 mm Thread	1
15	Dowel Pin, 2 mm Diameter, 14 mm Long	4
16	Sensor Bracket and Cover	1

4.4 Complete Assembly

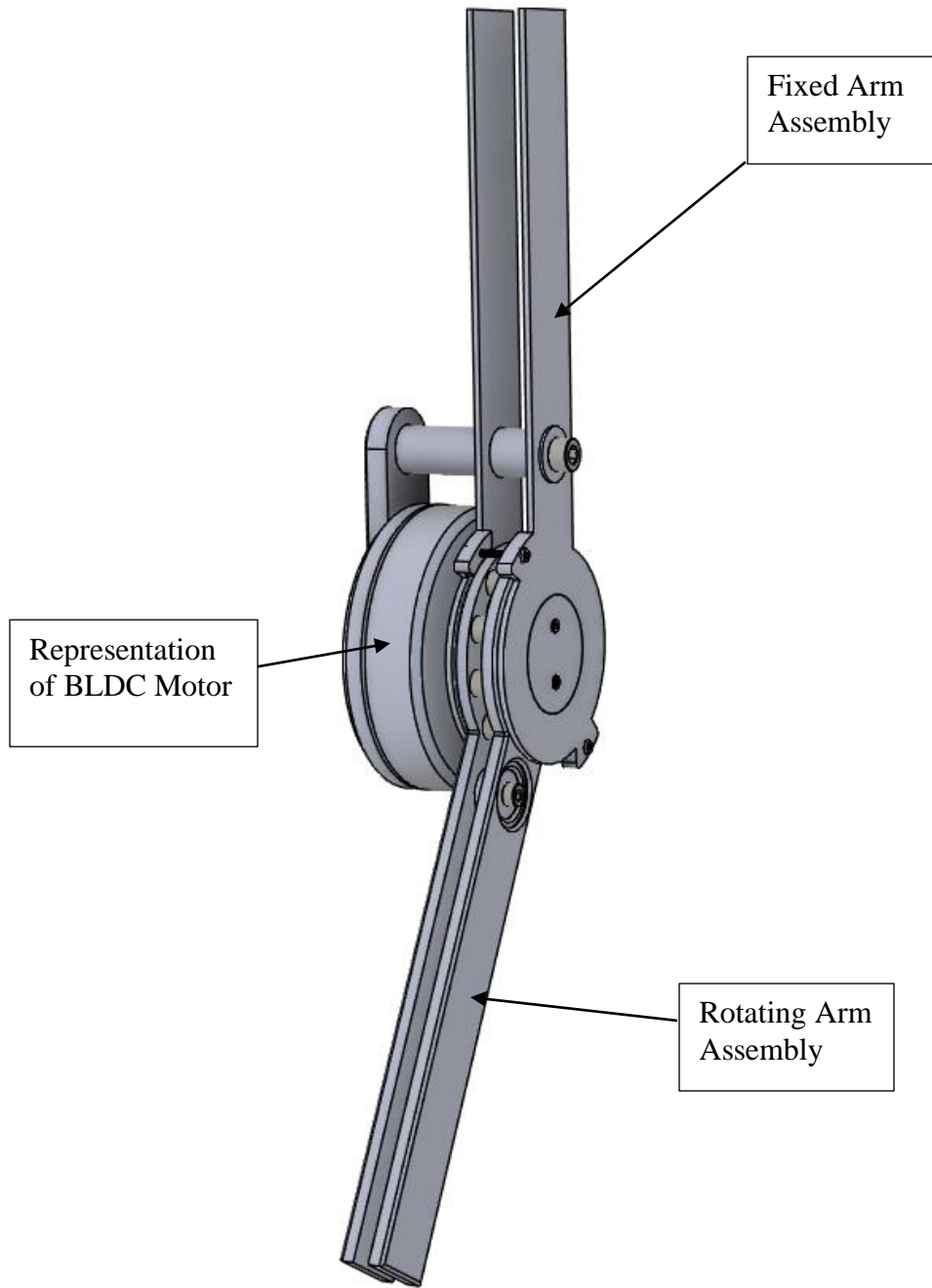


Figure 4.4 Complete assembly.

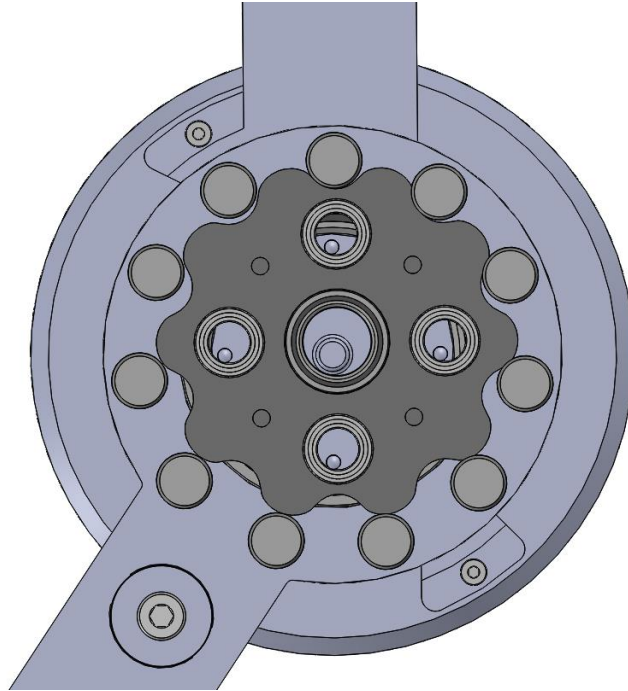
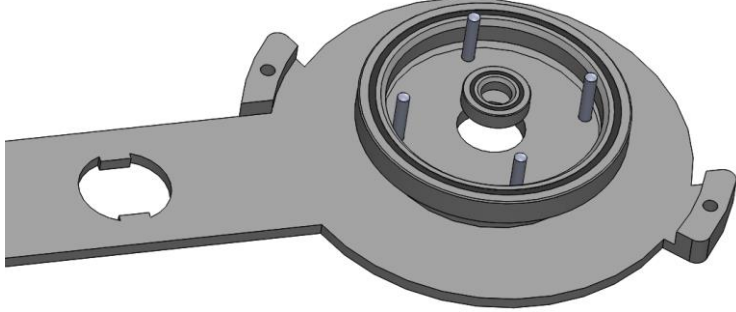
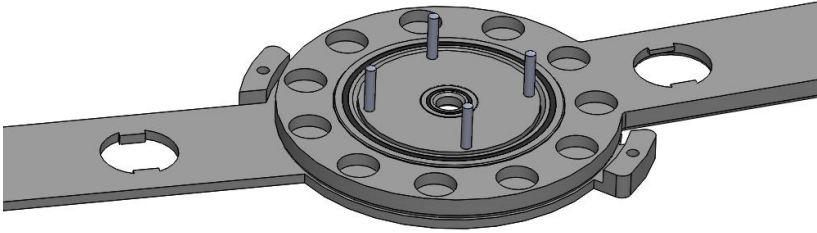
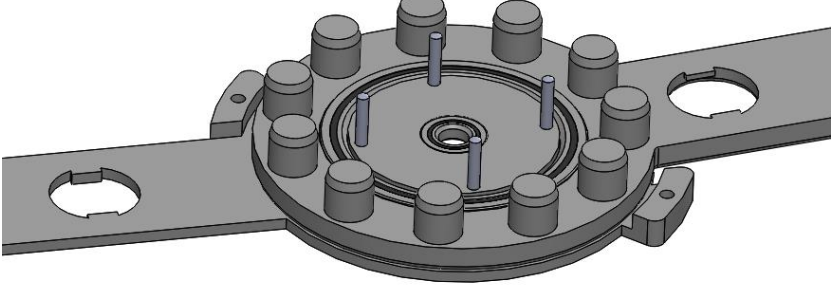


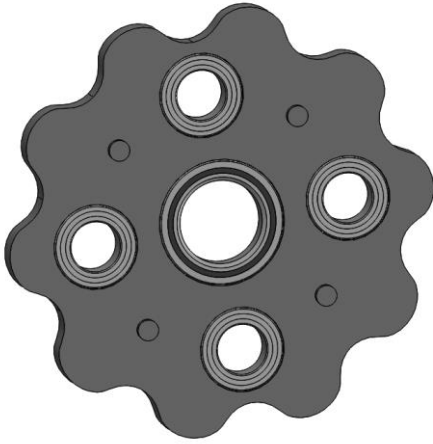
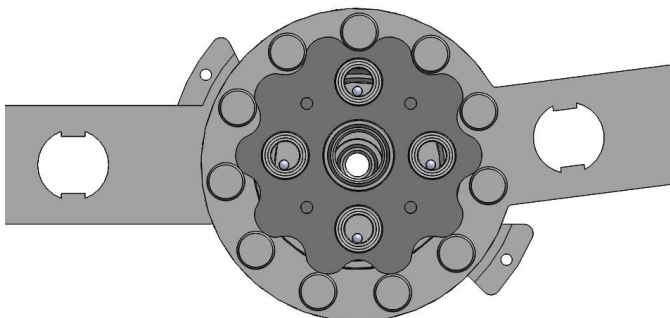
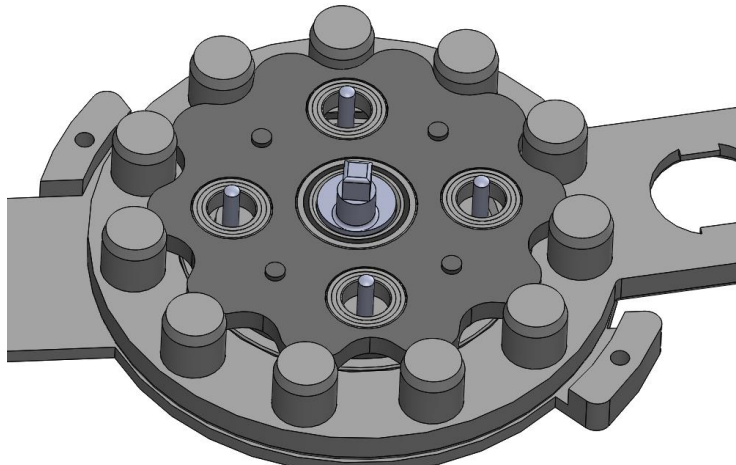
Figure 4.5 Internal mechanisms of the joint.

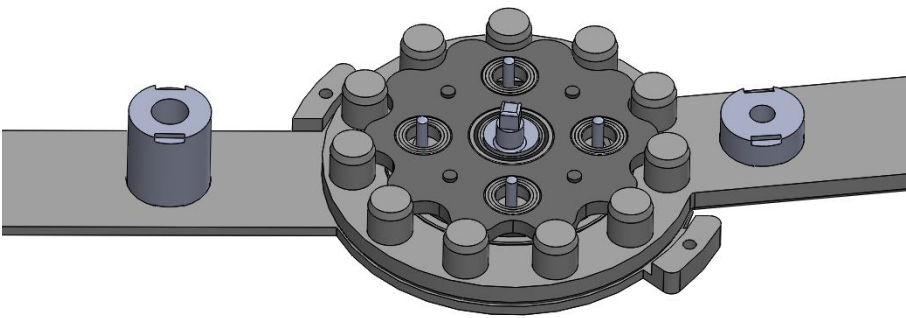
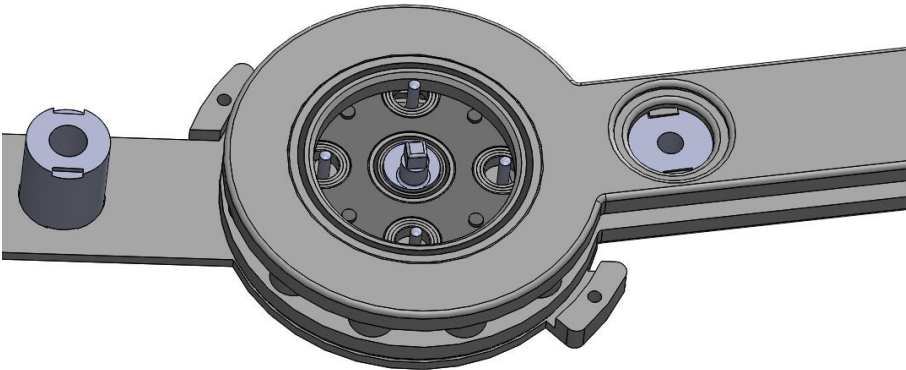
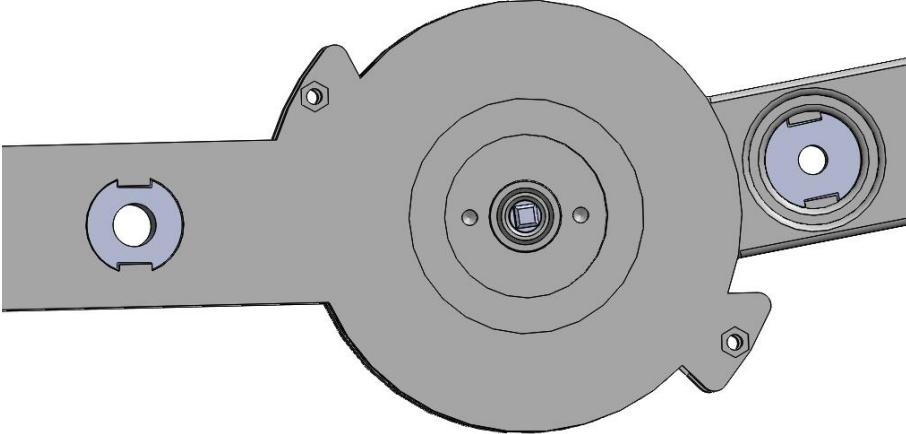
The operating principle of the proposed joint is as followed:

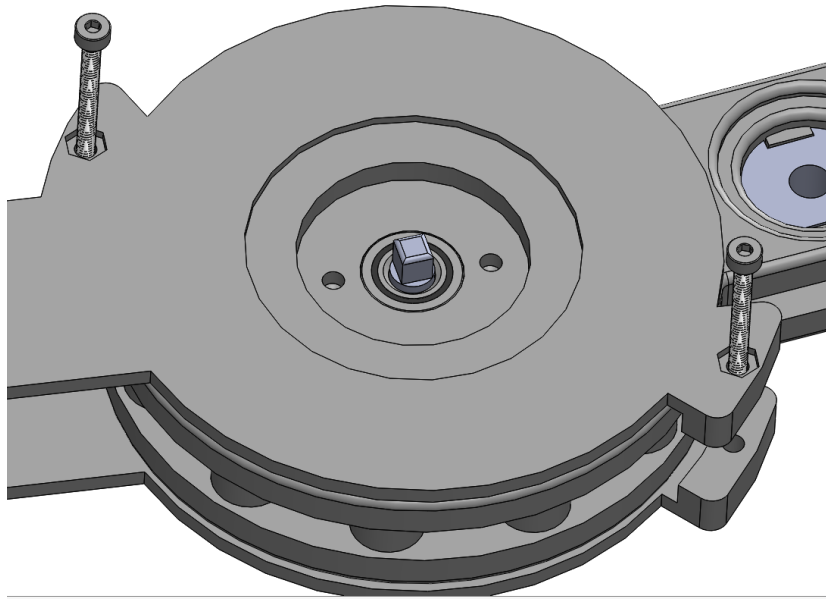
The eccentric shaft is connected to the motor shaft and is driven by the BLDC motor. As the eccentric shaft rotates, it forces the cycloidal rotor to rotate in the opposite direction. As the cycloidal rotor rotates, it interacts with the rollers fixed on the rotating arm side plates, ultimately forcing the rotating arm assembly to rotate in the same direction as the eccentric shaft. As mentioned in section 1.3, the proposed design is based on the rotating ring gear epicycloid drive. The rotating arm assembly can be viewed as the rotating ring gear in the proposed design. The proposed drive has a 10 to 1 transmission ratio; this means there are 11 rollers and 10 teeth on the cycloidal rotor.

Table 4.2 Step by Step Assembly Instructions

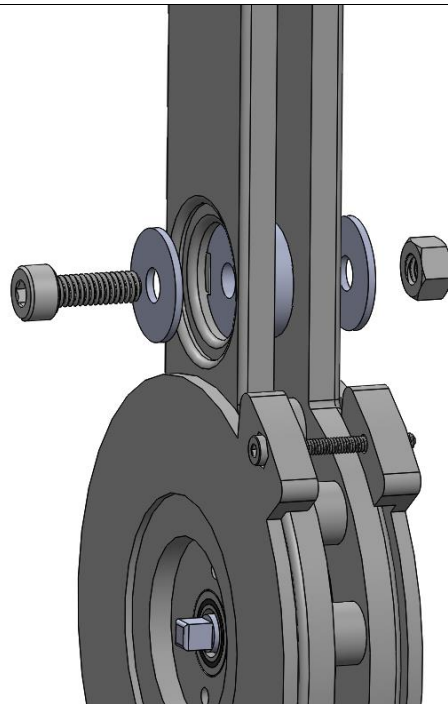
	<p><i>Step 1.</i> Insert 2 mm dowel pins (total 4) into a fixed arm side plate (any configuration).</p> <p><i>Step 2.</i> Place 44x35x5 mm bearing (4668K149) and 5x11x3 mm bearing (4668K114) as shown in the image.</p>
	<p><i>Step 3.</i> Place the rotating arm side plate (circular slots facing up as shown in the image).</p> <p><i>Note:</i> Make sure you have placed the rotating arm plate between the rotation lock features and not outside.</p>
	<p><i>Step 4.</i> Insert Rollers into the circular slots.</p>

	<p><i>Step 5.</i> Prepare the rotor assembly as shown in the image.</p> <p>Components required:</p> <ol style="list-style-type: none"> 1. Cycloidal Rotor 2. 6x10x3 mm (7804K111) bearings (4 total) 3. 10x15x3 mm (4668K3260) bearing
	<p><i>Step 5.</i> Place the rotor assembly as shown in the image.</p>
	<p><i>Step 6.</i> Place the eccentric shaft as shown in the image. The square end of the shaft gets connected with the motor shaft, so depending on the side you choose to mount the motor on, the square end should be facing on that side.</p>

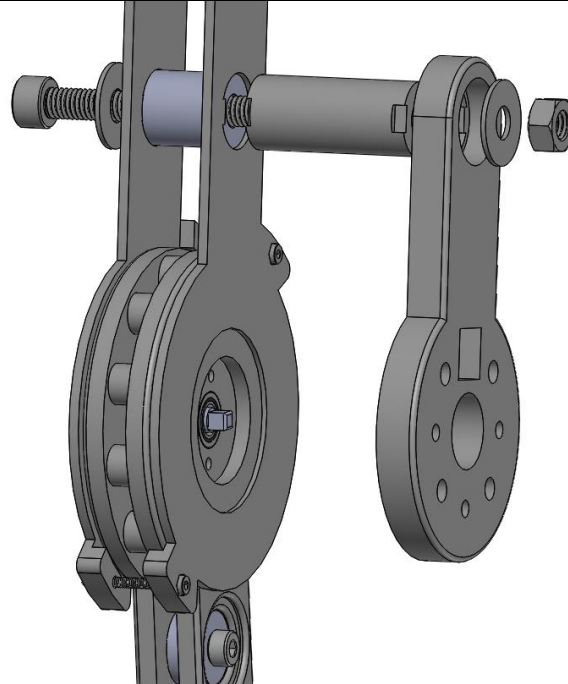
	<p><i>Step 7.</i> Place the fixed arm connector (left) and the rotating arm connector (right) in their respective slots.</p>
	<p><i>Step 8.</i> Place the rotating arm side plate and 44x35x5 mm bearing as shown in the image.</p>
	<p><i>Step 9.</i> Place the fixed arm assembly side plate (not the same configuration as taken in Step 1) and 5x11x3 mm bearing as shown in the image.</p>



Step 10. Insert two Hex Screw, M2 x 0.4 mm Thread, 20 mm Long and secure them using M2 hex nut on the other side.



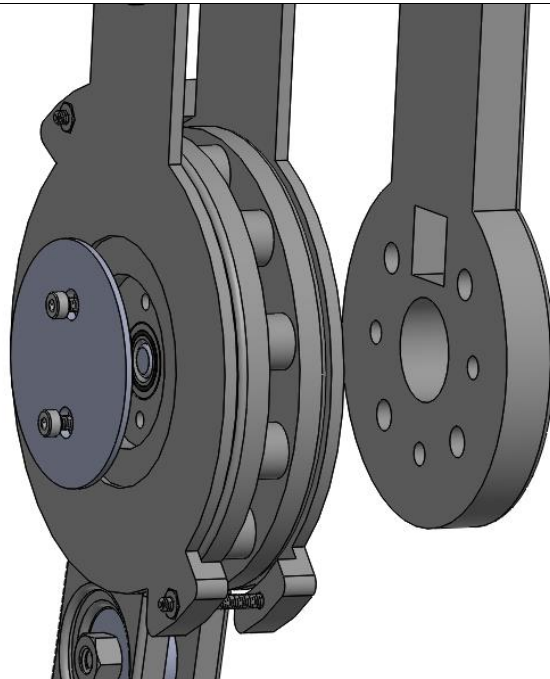
Step 11. Secure the rotating arm assembly by M4 hex screw and M4 hex nut as shown in the image. You will also need two washers 2 to keep the assembly intact.



Step 12. Assemble the motor mount and the motor arm connector with the fixed arm as shown in the image.

Components required:

1. Motor mount
2. Motor arm Connector
3. Washer 1 (one on each side)
4. M6 hex screw
5. M6 hex nut



Step 13. Assemble the Arm cover as shown in the image below by using M2 Screw.

This concludes the assembly of the joint.

Note: BLDC Motor can be assembled with the joint using the respective screw size. The motor shaft and sensor holding bracket can be attached to the BLDC motor using M3 screws.

4.5 Backdrivability Test

Backdrivability test can be classified into two categories: static and dynamic. The static backdrive torque is defined as the minimum torque required to overcome the static friction of the joint's internal mechanisms to initiate the motion of the output shaft by applying torque to the output shaft. For the proposed design, a static backdrivability torque test was conducted using the Baseline push-pull mechanical force gauge (SN: 056671-4-0067).

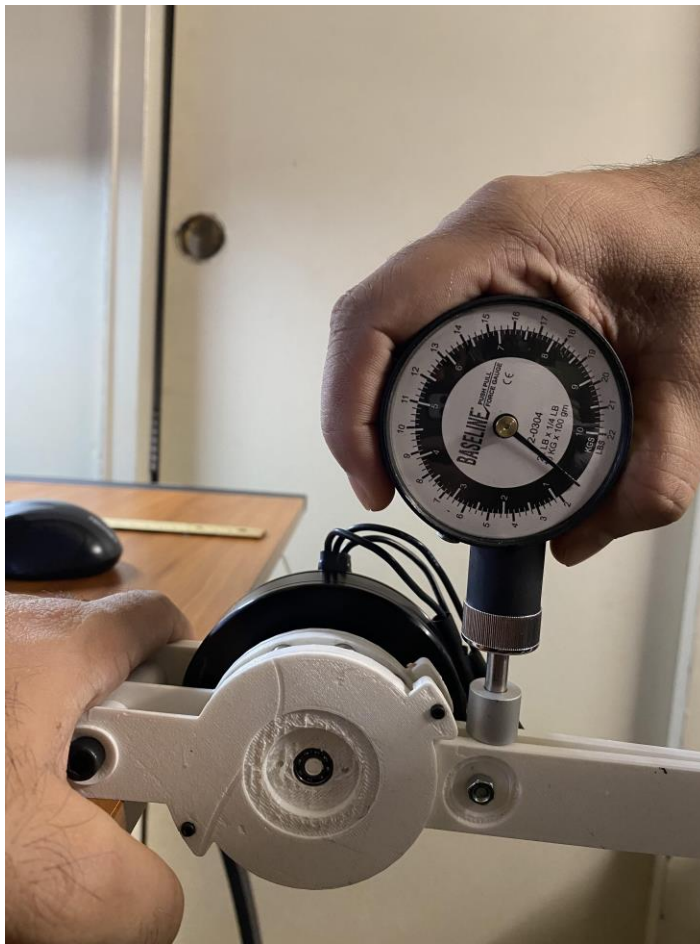


Figure 4.6 Backdrivability test set up.

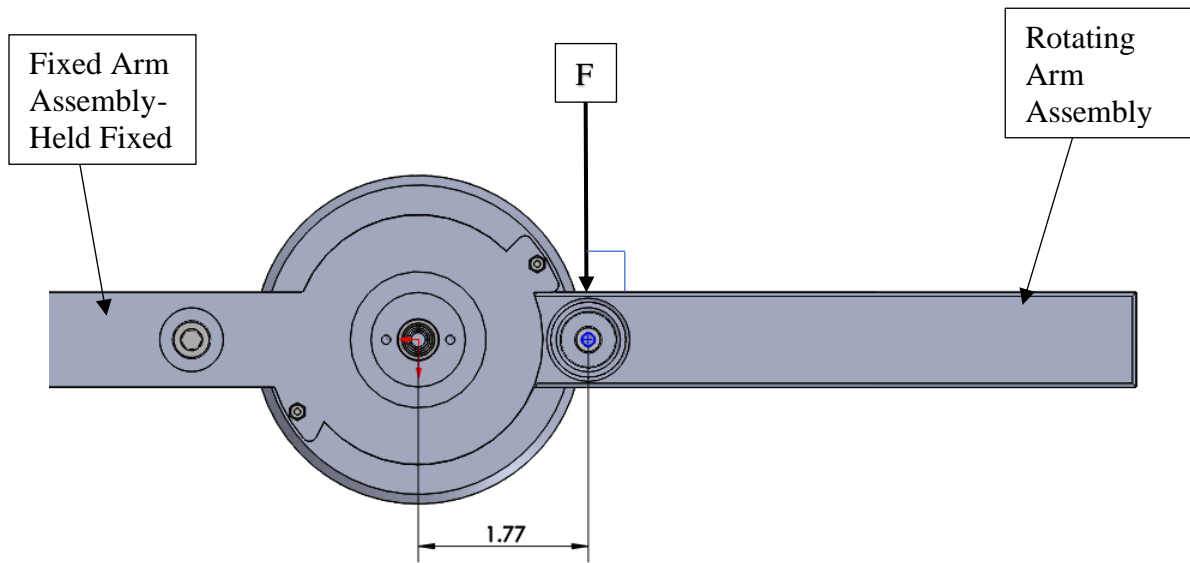


Figure 4.7 Backdrivability test set up diagram.

The joint was placed on a tabletop, and the fixed arm assembly was pressed against a stable workbench by second personnel to eliminate the unwanted up-down motion of the fixed arm. The force gauge was used to apply a perpendicular force downward on the rotating arm, as shown in figure 4.7. The gauge reader was used to measure the force at the time when the rotating arm started rotating. Equation 4.1 [31] was used to compute the torque required to backdrive the joint, with the motor being an integral part of the joint.

$$\tau = r * F * \sin\theta \quad (4.1)$$

$$\tau = 1.77 \text{ Inch} * 6 \text{ lbs} * \sin 90^\circ$$

$$\tau = 0.885 \text{ ft} - \text{lb} \approx \mathbf{1.20 \text{ Nm}}$$

Where r is the horizontal distance from the center axis of the eccentric shaft to the location of the force applied. The r value is set to 1.77 inches. The F is the perpendicular force applied to the rotating arm assembly (the output arm) at a specific distance from the center axis of the eccentric shaft to initiate the motion of the output arm. The force value was recorded to be 6 lbs. And θ is the angle in degrees at which the force is applied to the rotating arm. θ is set to 90 degrees for calculating the torque since the force is applied at 90 degrees or is normal to the output arm.

This is the most simple test set up to obtain the static torque based on applying a perpendicular force to the output arm using a force gauge. However, the same test can be conducted using a better test set up if done in a lab or in a facility that has equipment like Instron machines as they are known for their precision.

CHAPTER 5

CONCLUSION AND FUTURE WORK

5.1 Conclusion

A highly backdrivable and compact joint was designed and prototyped. The joint design includes various important features such as rotation lock features that help prevent hyperextension, the motor mount that offers the benefit of using the joint for the left and right limb. Also, the sensor holding bracket and cover were designed to securely mount the AS5147- magnetic rotary position sensor board for controlling the motor speed and position. In addition, highly backdrivable (1.20 Nm torque required to backdrive) cycloidal transmission was designed with a thin cycloidal disk, amplifying the torque output of the chosen brushless dc motor. The integrity of the design was validated based on the successful testing of the 3D printed prototype. The design will be fabricated using 1018 Steel and 6061 Aluminum to increase the robustness in comparison to the 3D printed plastic materials. Detailed manufacturing drawings have been included as part of Appendix A. I look forward to see the proposed joint design being used for future rehabilitation exoskeleton designs.

5.2 Future Work

In the future, further improvements can be made to the proposed design to obtain higher output torque by increasing the transmission ratio. Equation 2.1 can be used to compute a new transmission ratio.

Also, to increase the robustness of the design, a second cycloidal rotor can be introduced. Introducing the second cycloidal rotor will offer more contact area between the

rollers and the rotors teeth, as a result the stress will be distributed across the increased contact region and will help prevent design failure due to fatigue stresses or if an extreme amount of backdriving torque is suddenly experienced. To introduce an additional cycloidal rotor, the following steps can be taken.

1. Redesign the eccentric shaft such that the second rotor can be mounted. Figure 5.1 includes the sketch that shows how to add the additional rotor mount. The centers of the rotor mounts are located 2 mm away from the center of the shaft in both directions.

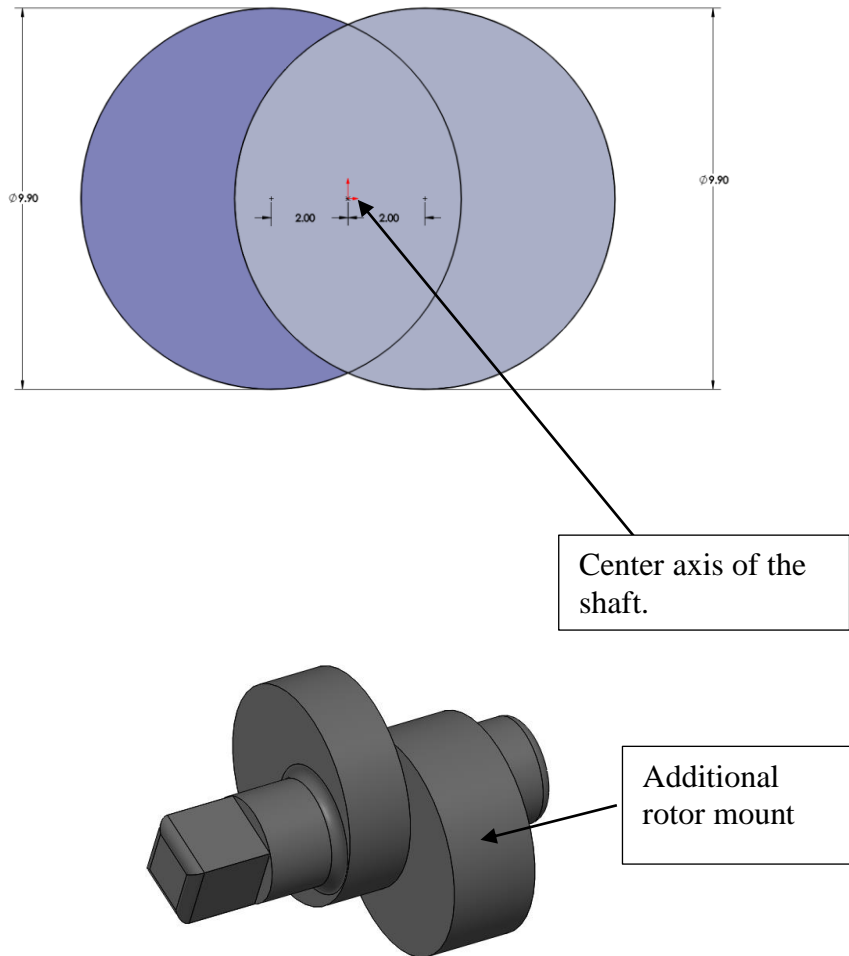


Figure 5.1 Sketch of the double rotor eccentric shaft.

2. The length of the following housing components must be adjusted to accommodate the addition of the second cycloidal rotor.
 - a. 2 mm Dowel pins fixed to the fixed arm assembly.
 - b. 8 mm Rollers attached to the rotating arm assembly.
 - c. The fixed arm connector and the rotating arm connector.

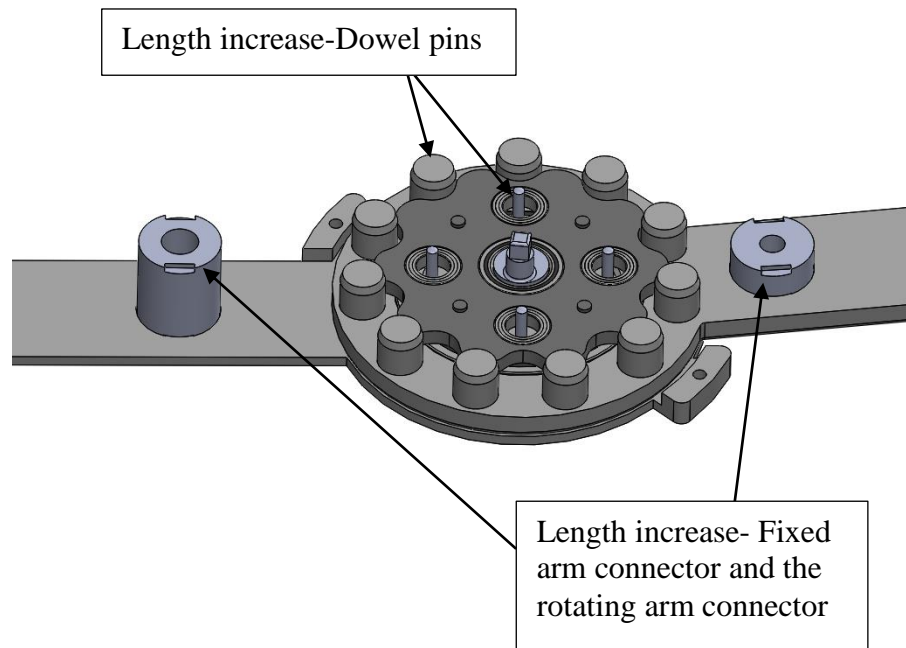


Figure 5.2 Increase in length required for the pointed components.

In addition, the current roller bearings can be replaced by needle roller bearings to make the design more compact and decrease friction in the mechanism. From the design durability view, the needle roller bearing will allow an increase in shaft diameter due to its compactness, and as a result the design will experience less stress. Also, needle roller bearings can be cost-effective since they can be fabricated in house without much fabrication resources.

APPENDIX A
MANUFACTURING DRAWINGS

Figure A.1 to A.29 show manufacturing drawings of the designed components.

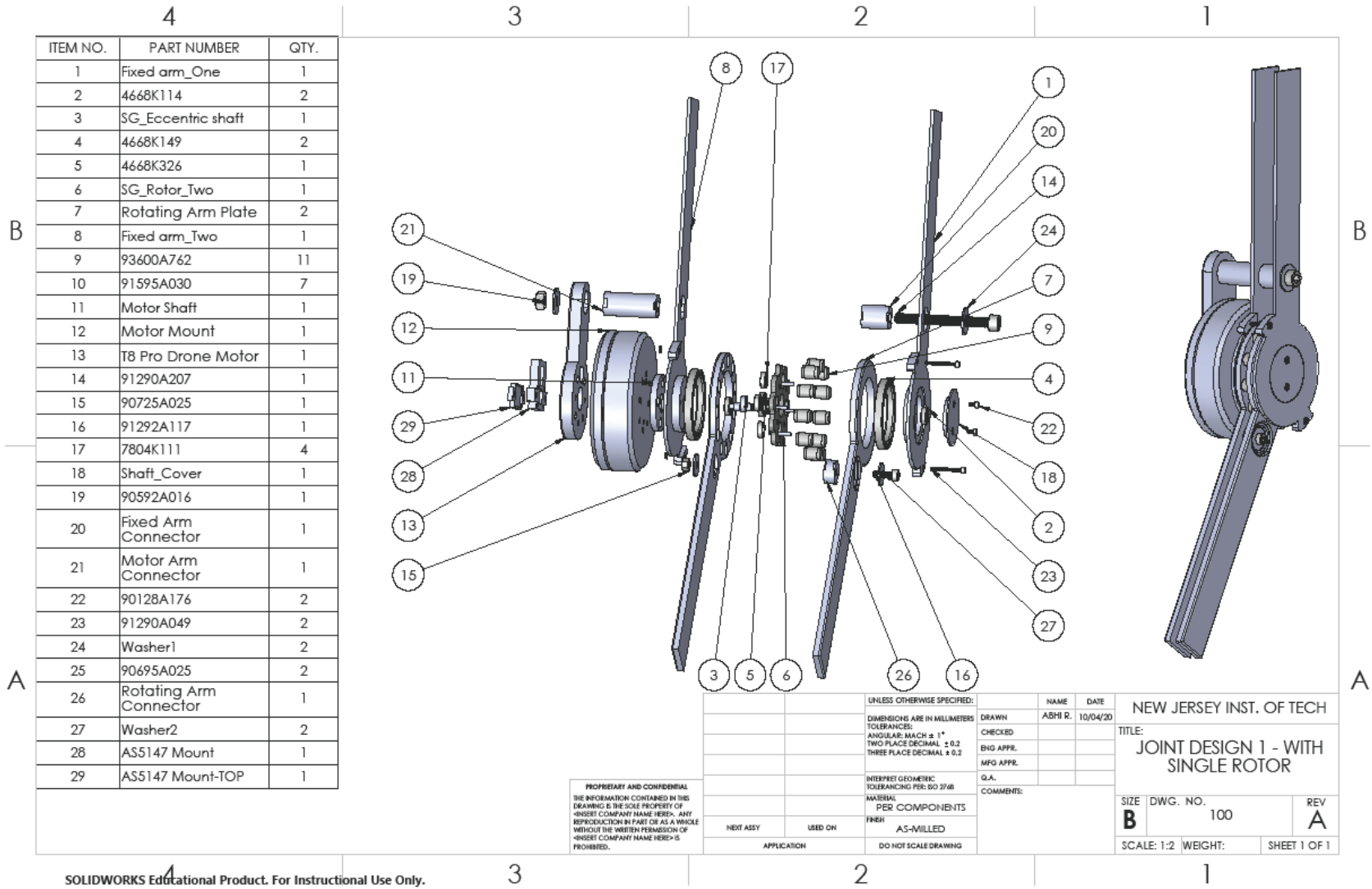


Figure A.1 Exploded view of the joint design.

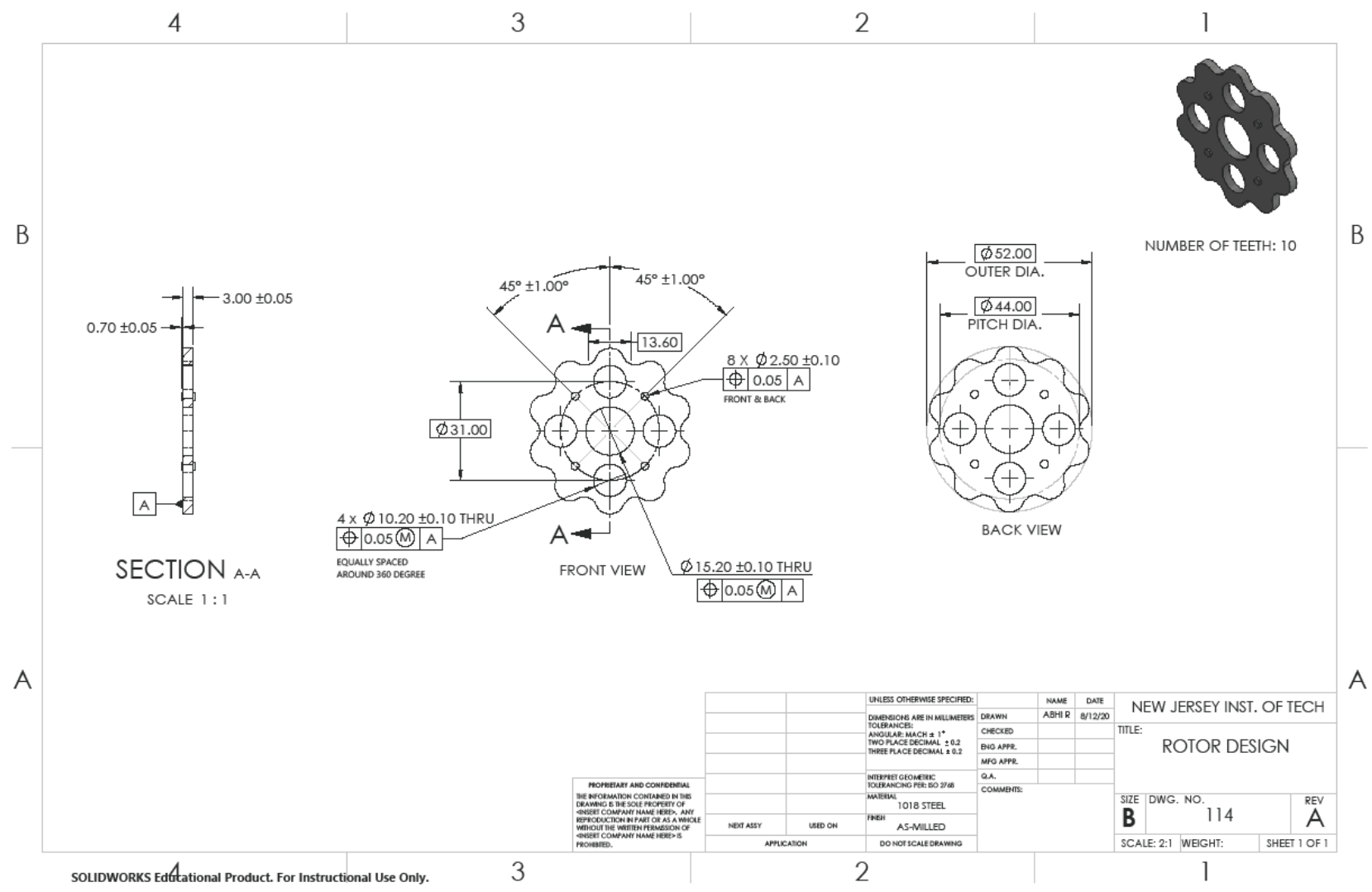


Figure A.2 Cycloidal rotor design.

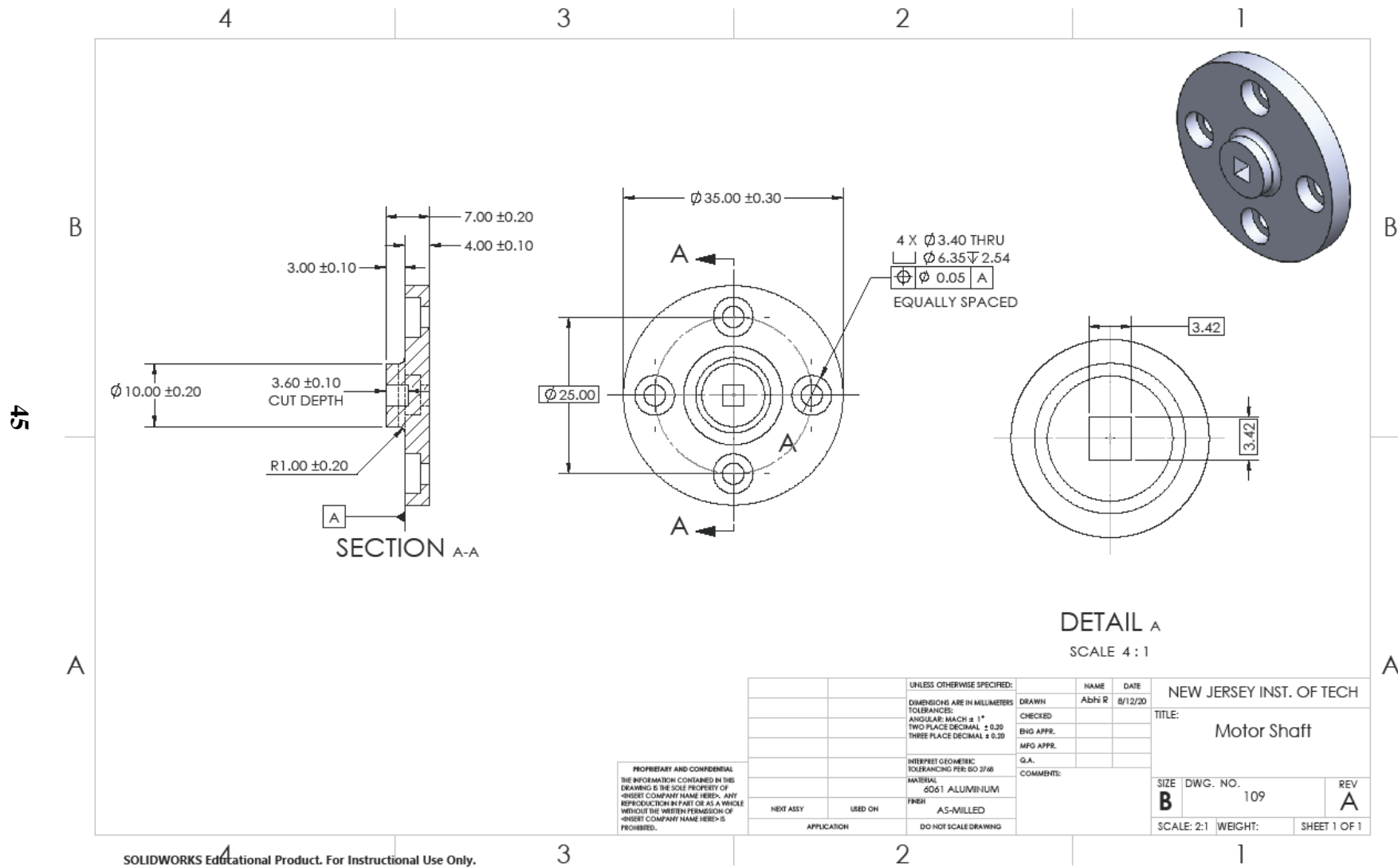


Figure A.3 Motor shaft.

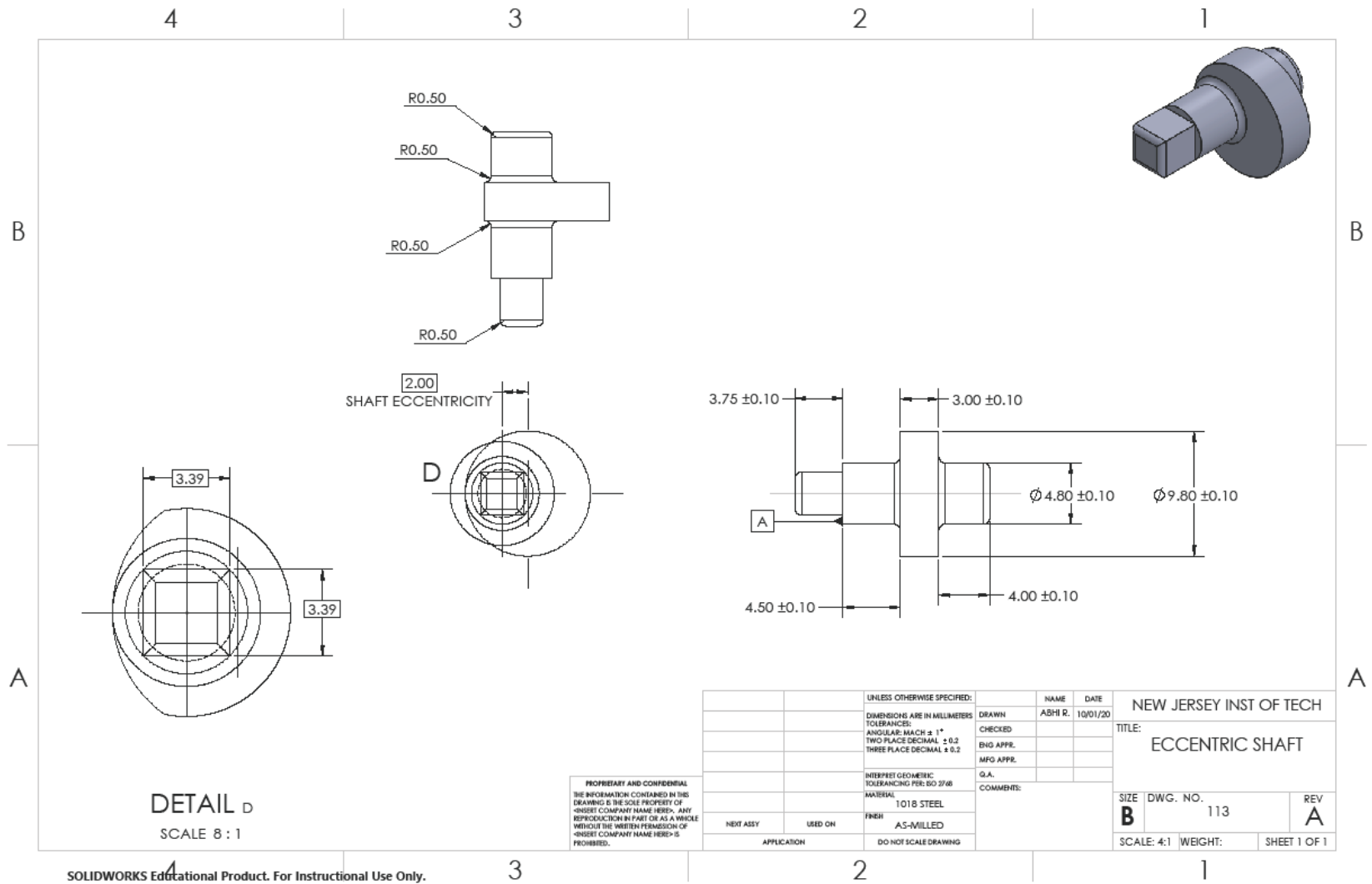


Figure A.4 Eccentric shaft.

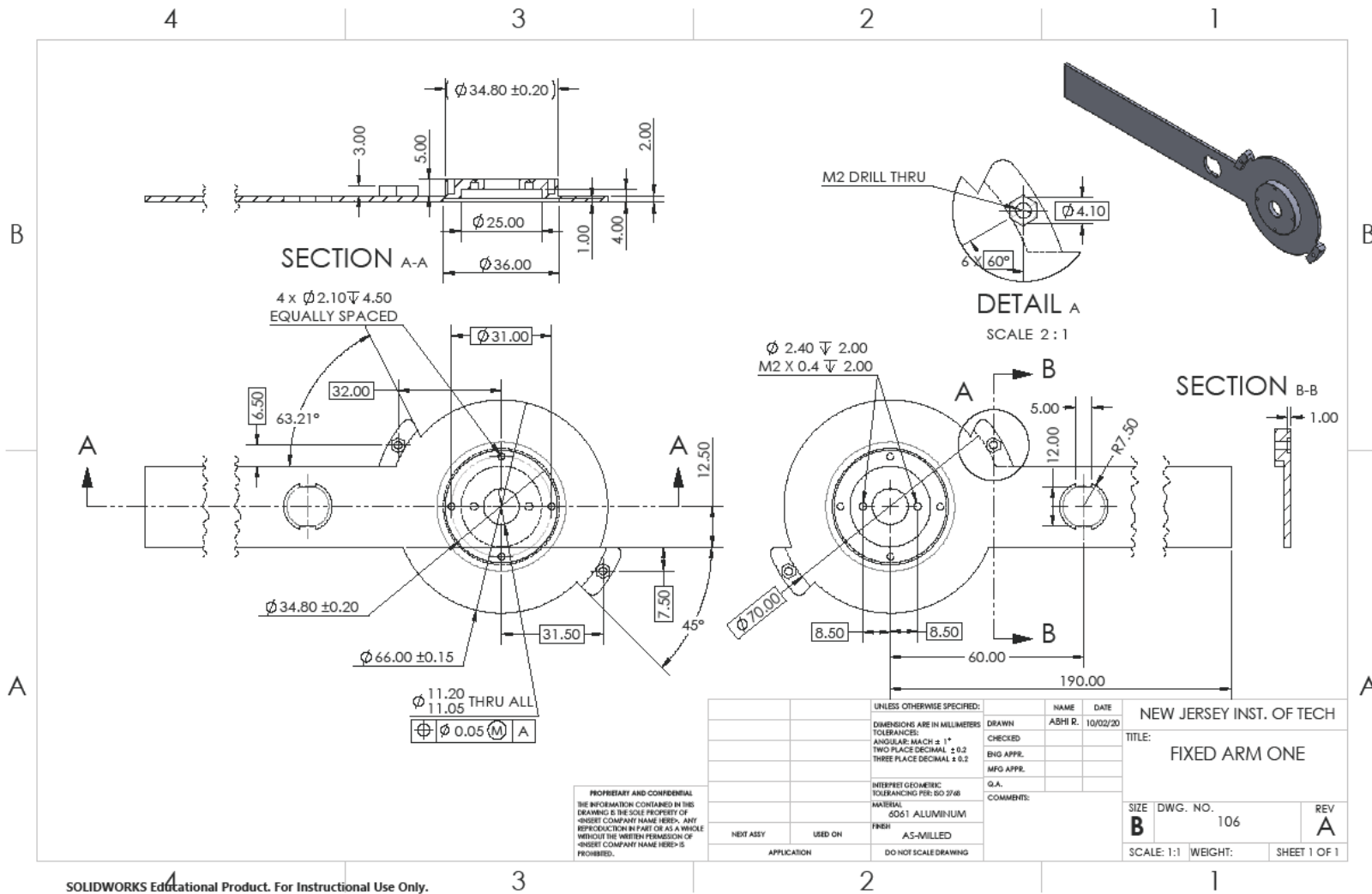


Figure A.5 Fixed arm side plate configuration 1.

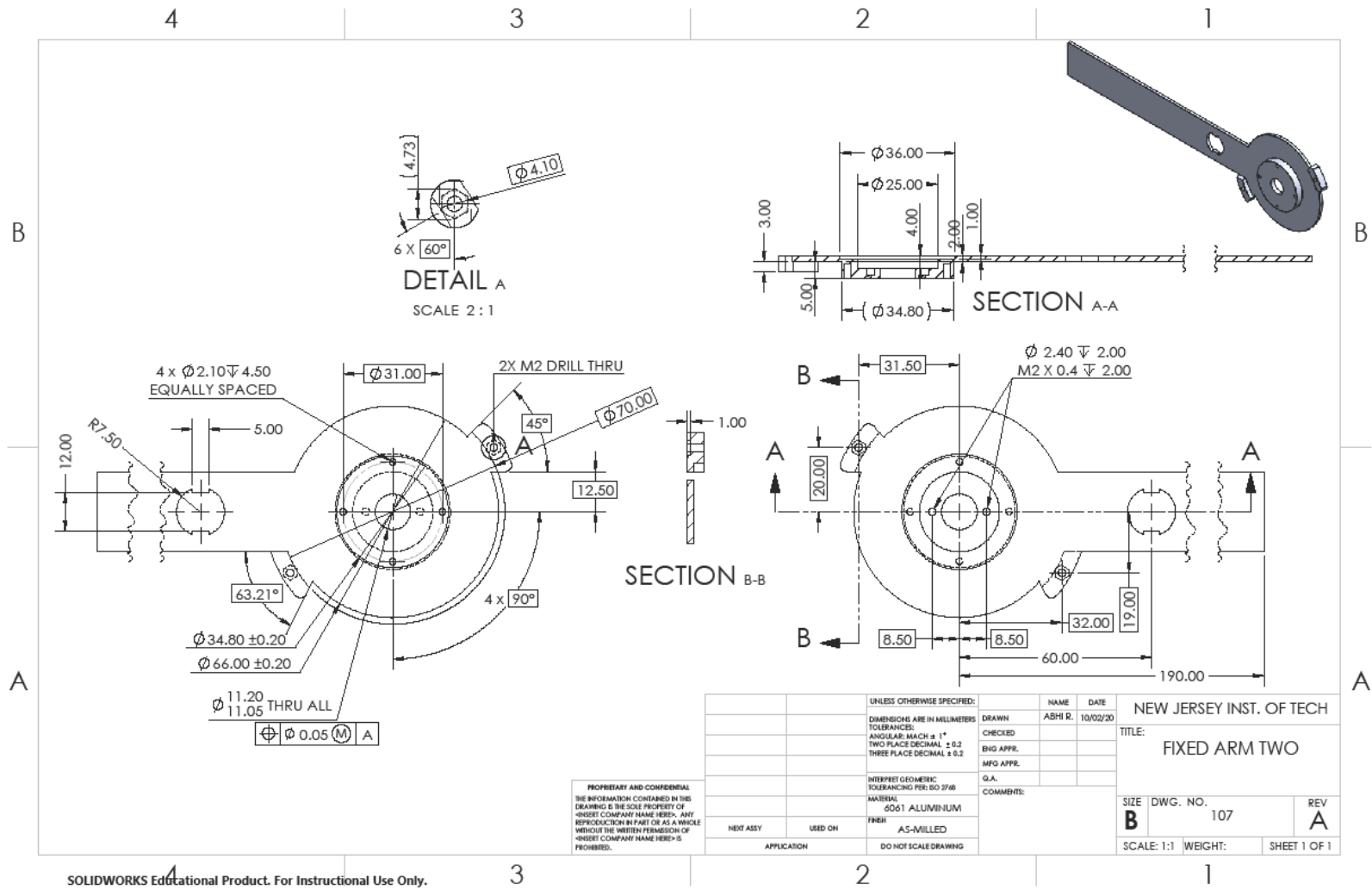


Figure A.6 Fixed arm side plate configuration 2.

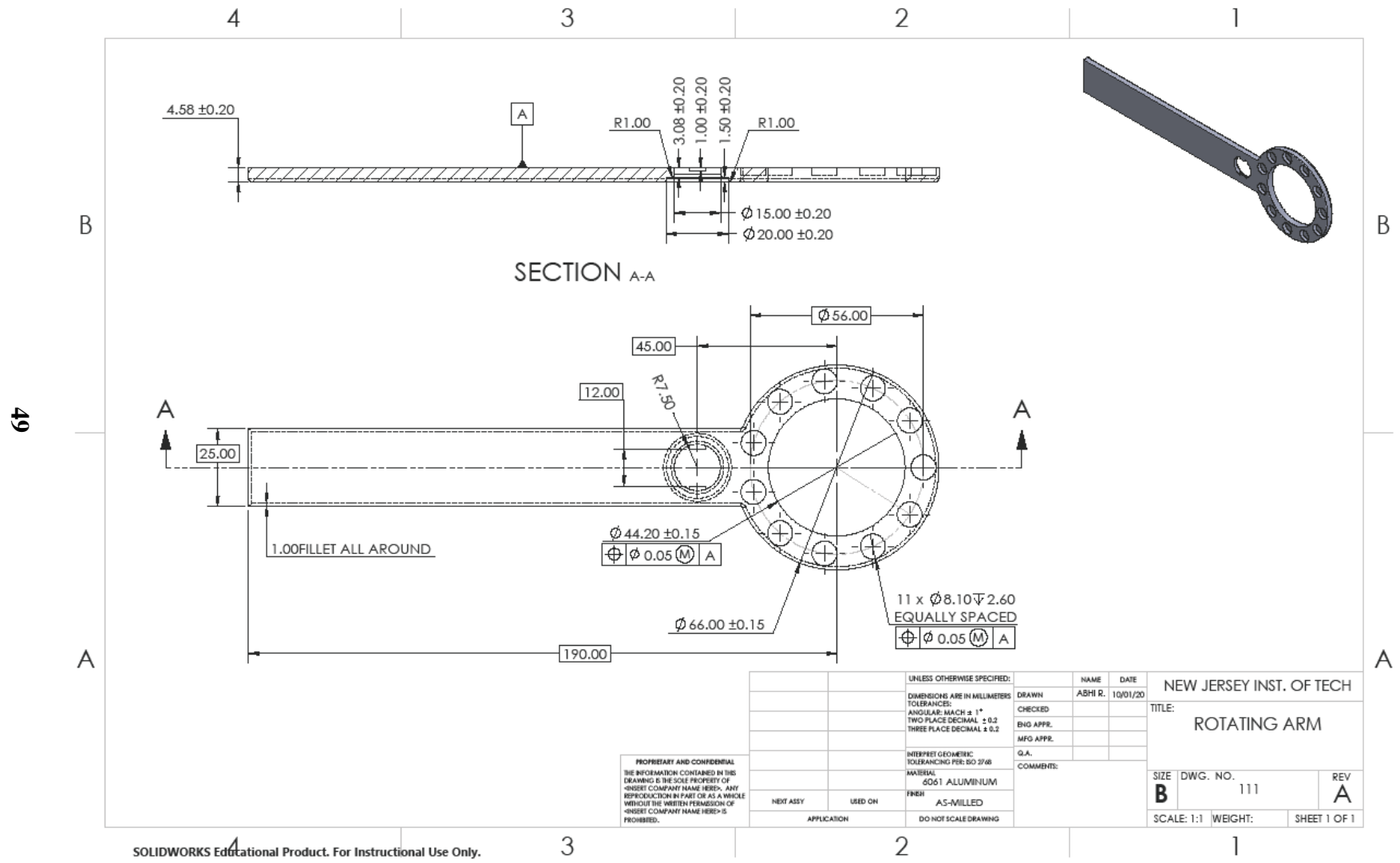


Figure A.7 Rotating arm side plate.

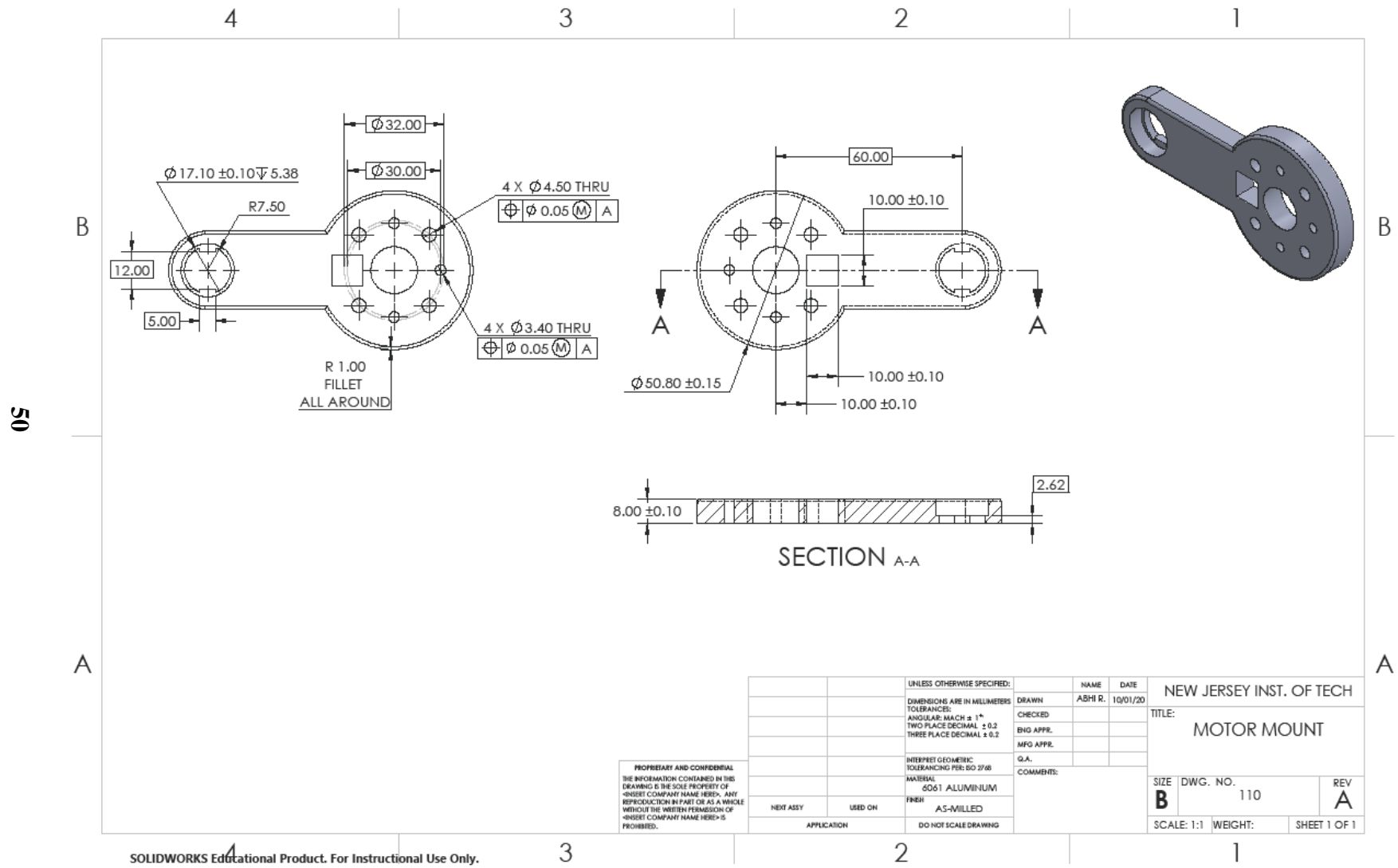


Figure A.8 Motor mount.

SOLIDWORKS Educational Product. For Instructional Use Only.

PROPRIETARY AND CONFIDENTIAL
 THE INFORMATION CONTAINED IN THIS
 DRAWING IS THE SOLE PROPERTY OF
 <INSERT COMPANY NAME HERE>. ANY
 REPRODUCTION IN PART OR AS A WHOLE
 WITHOUT THE WRITTEN PERMISSION OF
 <INSERT COMPANY NAME HERE> IS
 PROHIBITED.

		UNLESS OTHERWISE SPECIFIED:	NAME	DATE	NEW JERSEY INST. OF TECH TITLE: MOTOR MOUNT
		DIMENSIONS ARE IN MILLIMETERS TOLERANCES: ANGULAR: MACH $\pm 1^\circ$ TWO PLACE DECIMAL ± 0.2 THREE PLACE DECIMAL ± 0.2	DRAWN ABHI R.	10/01/20	
		INTERPRET GEOMETRIC TOLERANCING PER: ISO 2768	CHECKED		
		MATERIAL: 6061 ALUMINUM FINISH AS-MILLED	ENG APPR. MFG APPR.		
NEXT ASSY	USED ON	APPLICATION	Q.A.	COMMENTS:	SIZE DWG. NO. B 110
		DO NOT SCALE DRAWING			REV A
					SCALE: 1:1 WEIGHT: SHEET 1 OF 1

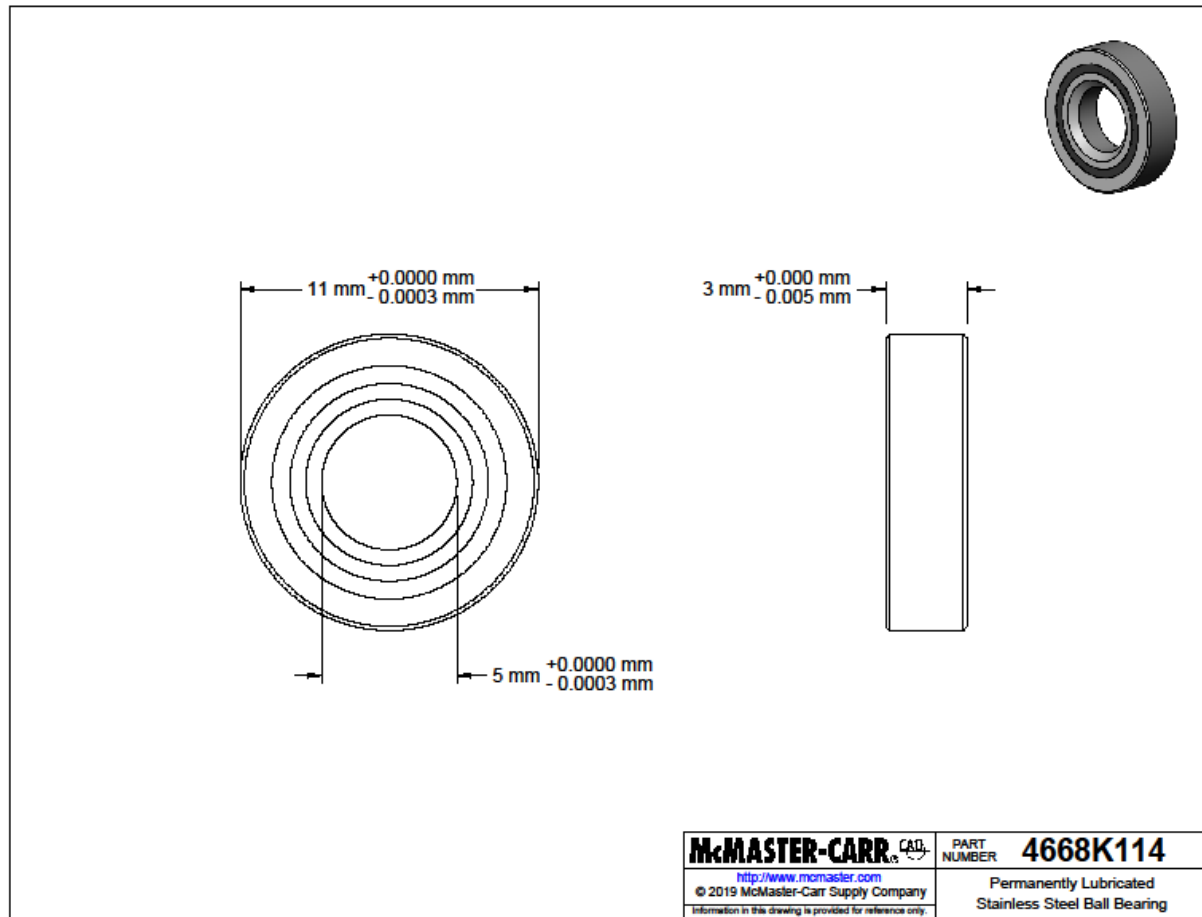


Figure A.9 Bearing-4668K114.

Permanently Lubricated Stainless Steel Ball Bearing Open, Trade Number 685H, for 5 mm Shaft Diameter. (2019). McMASTER-CARR.

<https://www.mcmaster.com/4668K114/>

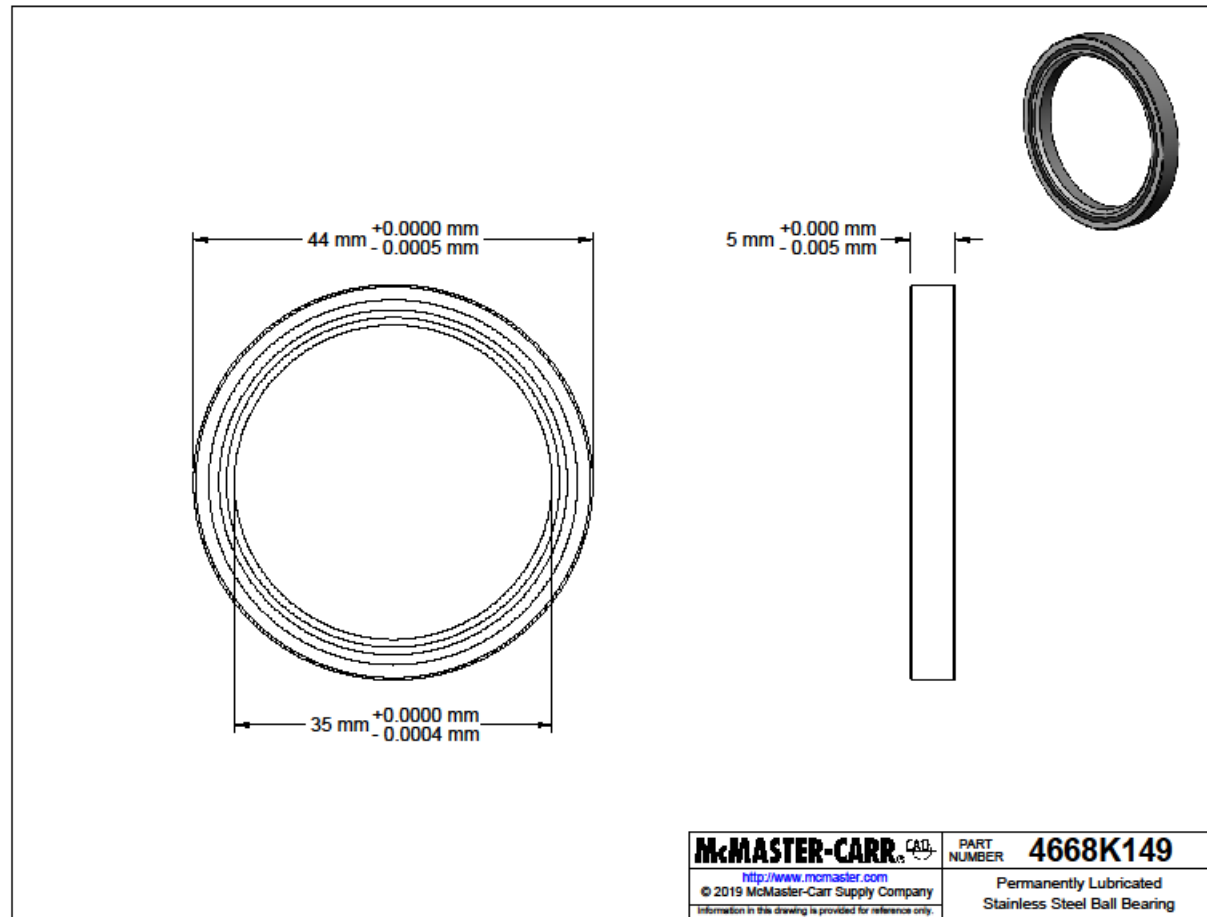


Figure A.10 Bearing-4668K149.

Permanently Lubricated Stainless Steel Ball Bearing Open, Trade Number 6707H, for 35 mm Shaft Diameter. (2019). McMaster-CARR.
<https://www.mcmaster.com/4668K149/>

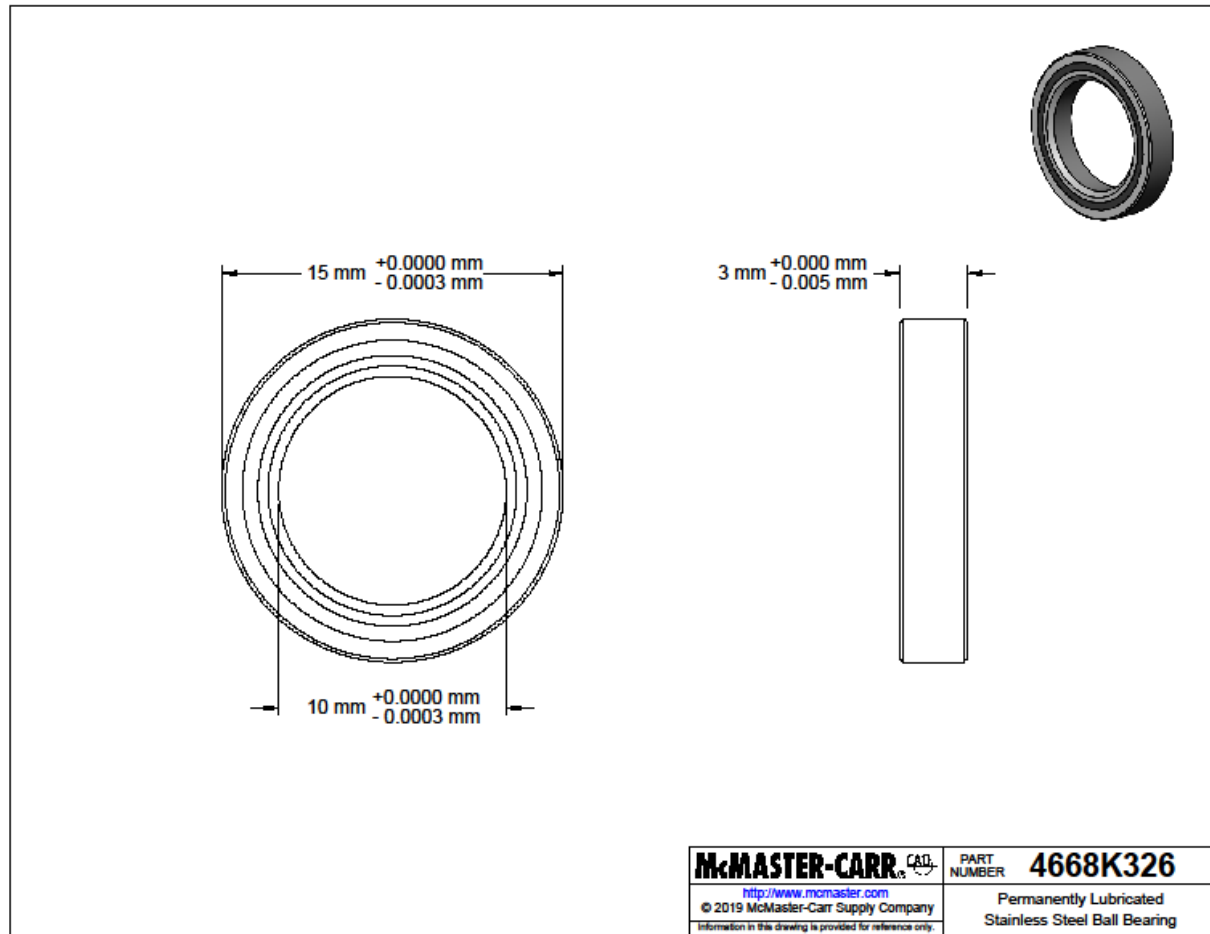


Figure A.11 Bearing-4668K326.

Permanently Lubricated Stainless Steel Ball Bearing Open, Trade Number 6700H, for 10 mm Shaft Diameter. (2019). McMASTER-CARR.

<https://www.mcmaster.com/4668k326>

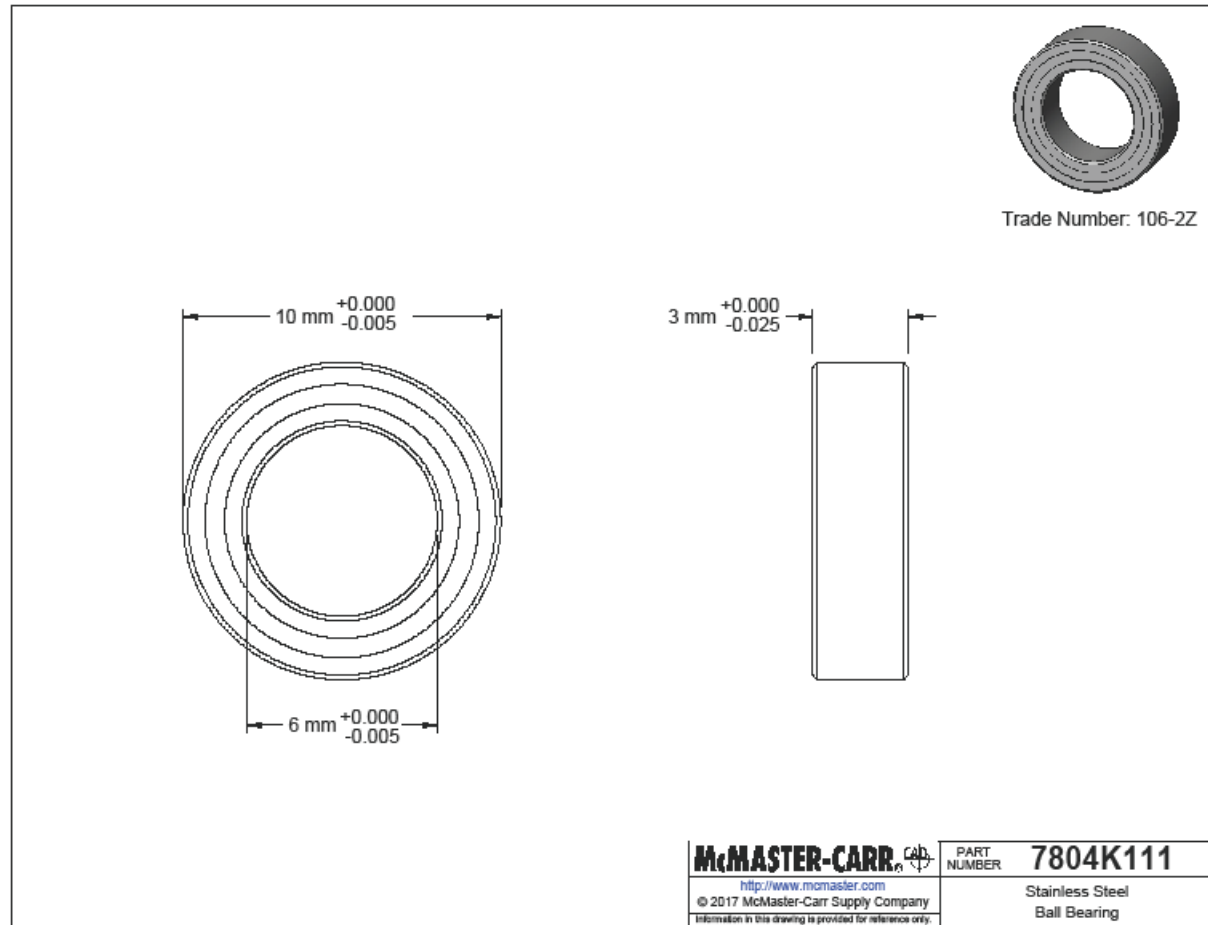


Figure A.12 Bearing-7804K111.

Stainless Steel Ball Bearing Shielded, Trade No. 106-2Z, for 6 mm Shaft Diameter. (2017). McMaster-CARR. <https://www.mcmaster.com/7804K111/>

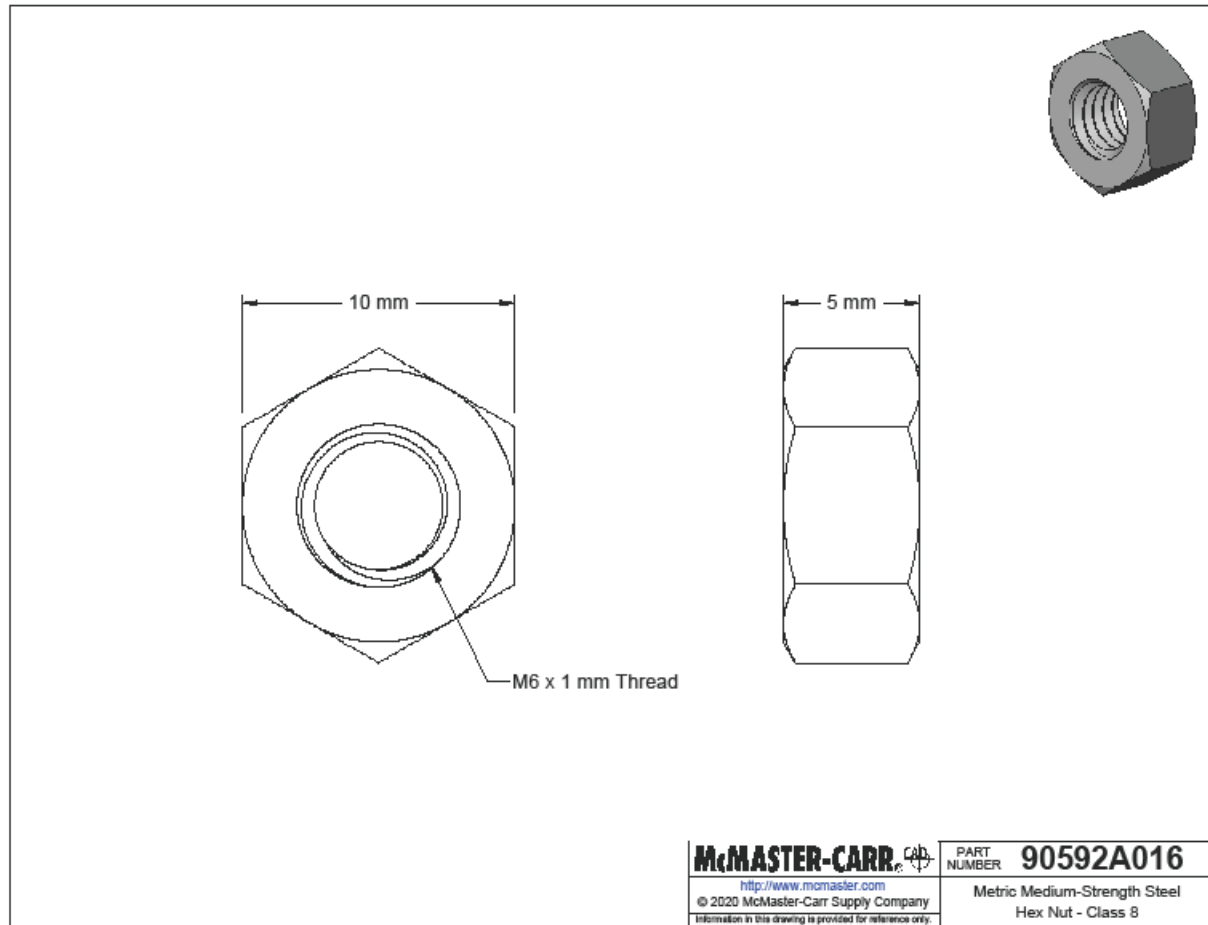


Figure A.13 Hex nut-90592A016.

Steel Hex Nut Medium-Strength, Class 8, M6 x 1 mm Thread. (2020). McMaster-CARR. <https://www.mcmaster.com/90592A016/>

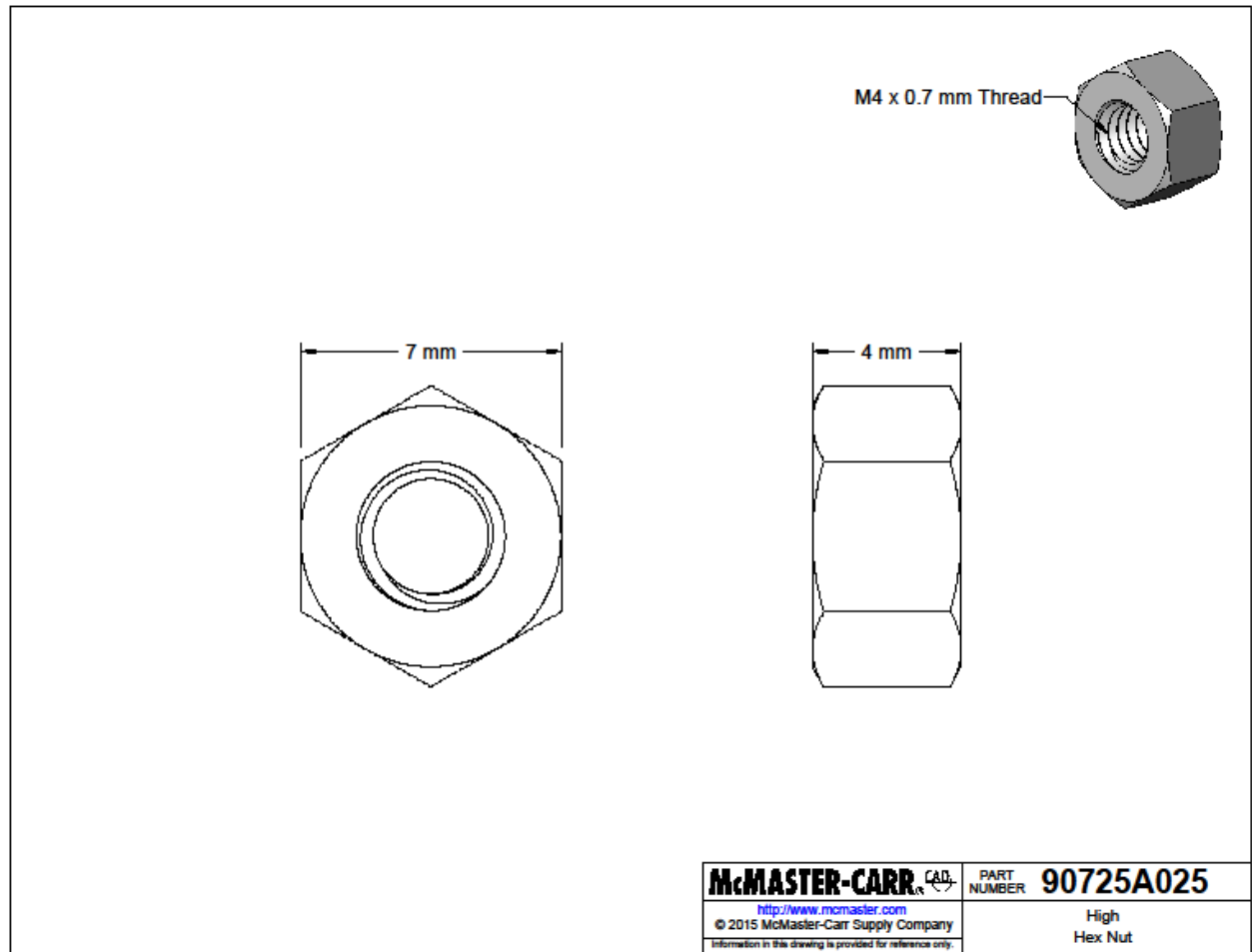


Figure A.14 Hex nut-90725A025.

Zinc-Plated Steel High Hex Nut Class 6, M4 x 0.7 mm Thread. (2015). McMASTER-CARR. <https://www.mcmaster.com/90725A025/>

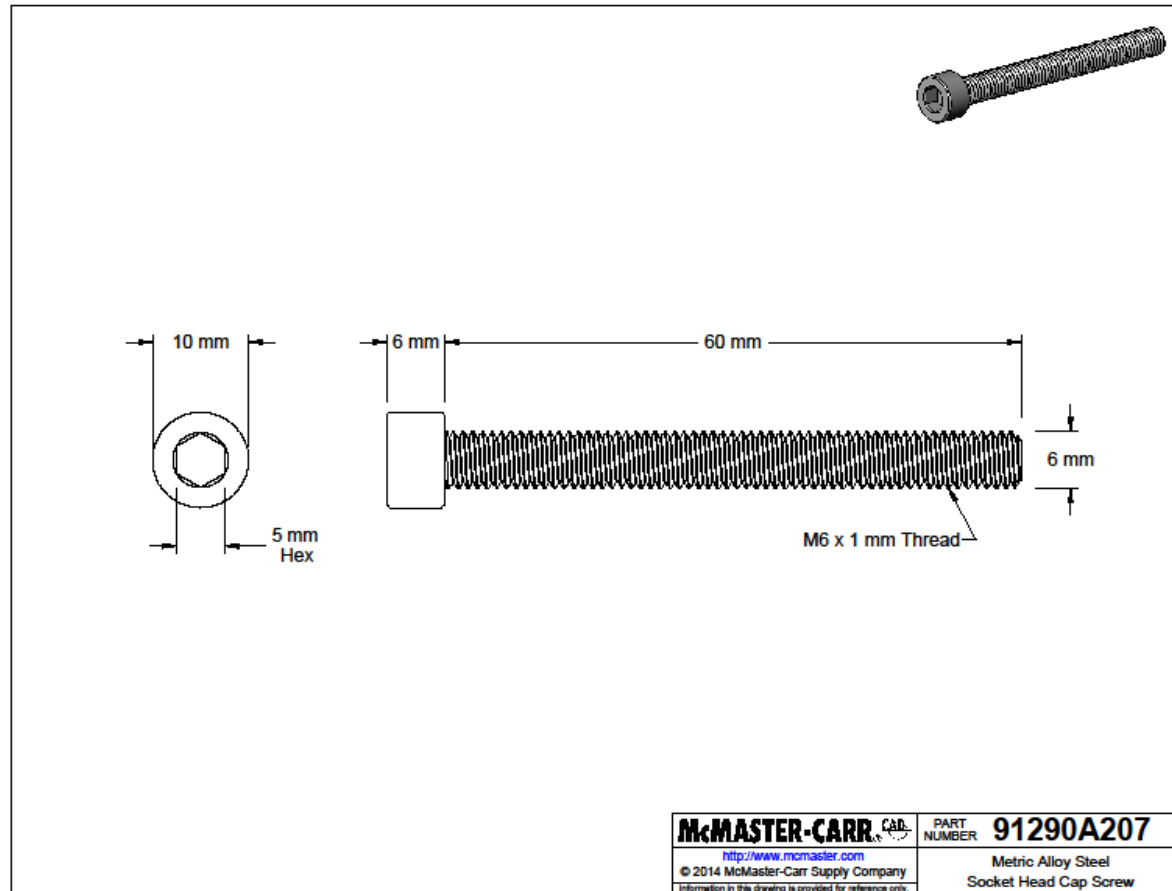


Figure A.15 Head cap screw-91290A207.

Black-Oxide Alloy Steel Socket Head Screw M6 x 1 mm Thread, 60 mm Long, Fully Threaded. (2014). McMaster-CARR.

<https://www.mcmaster.com/91290A207/>

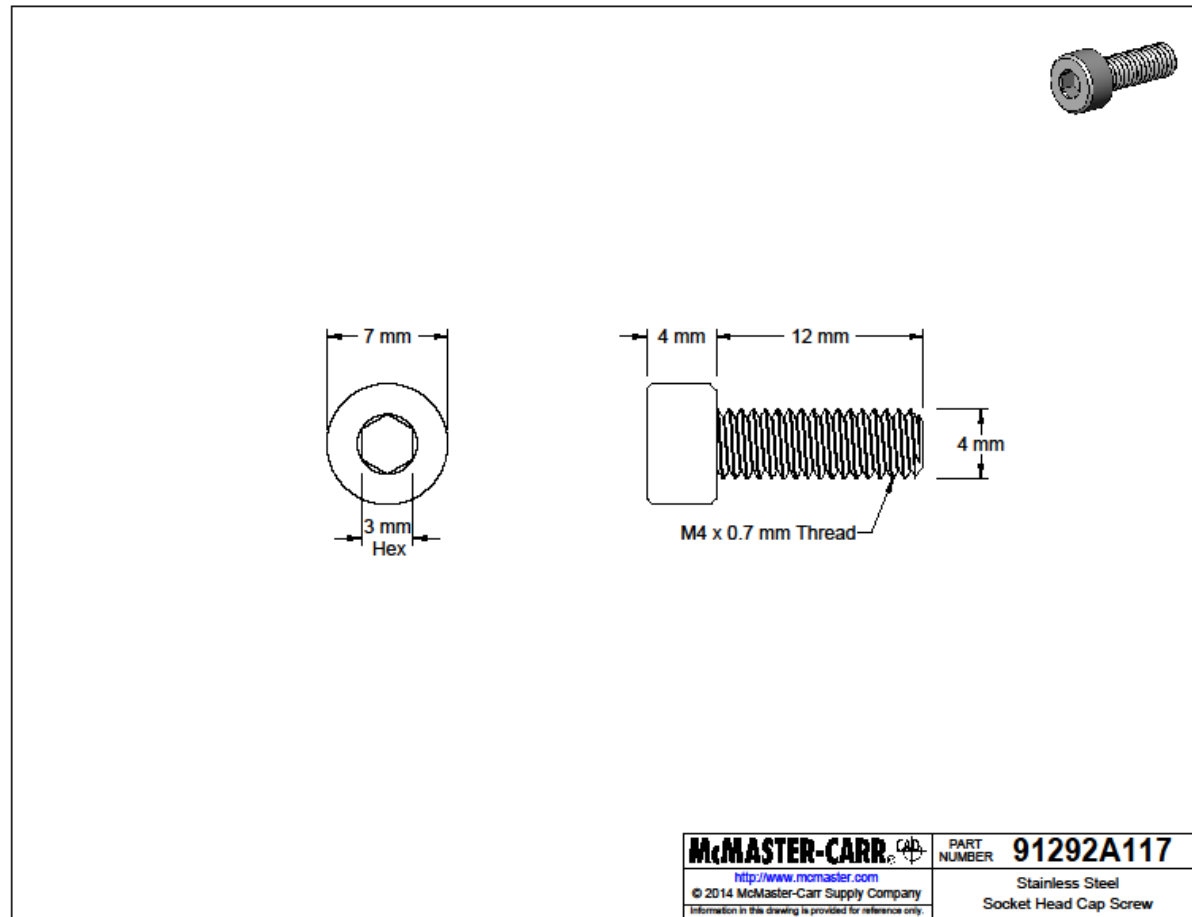


Figure A.16 Head cap screw-91292A117.

18-8 Stainless Steel Socket Head Screw M4 x 0.7 mm Thread, 12 mm Long. (2014). McMaster-CARR. <https://www.mcmaster.com/91292A117/>

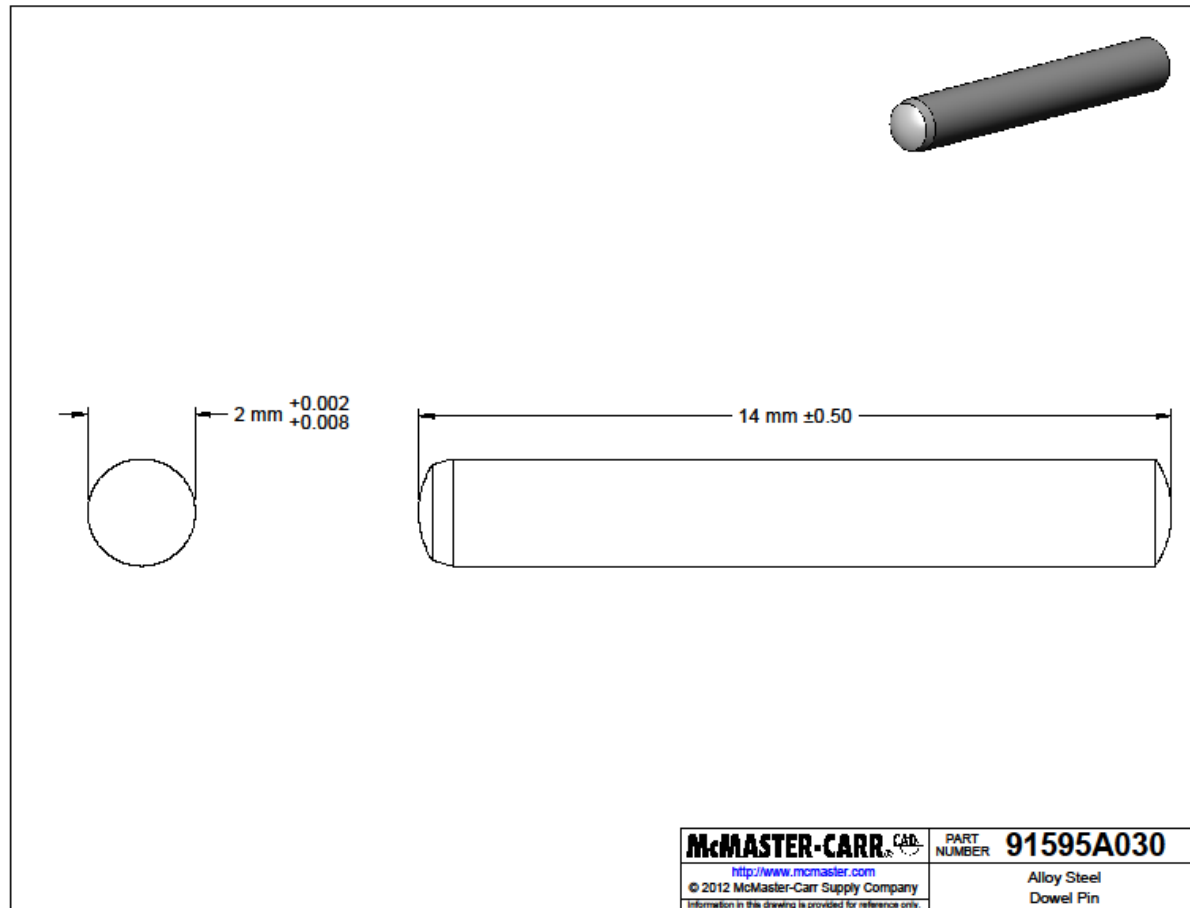


Figure A.17 Dowel pin-91595A030.

Dowel Pin 52100 Alloy Steel, 2 mm Diameter, 14 mm Long. (2012). McMaster-CARR. <https://www.mcmaster.com/91595A030/>

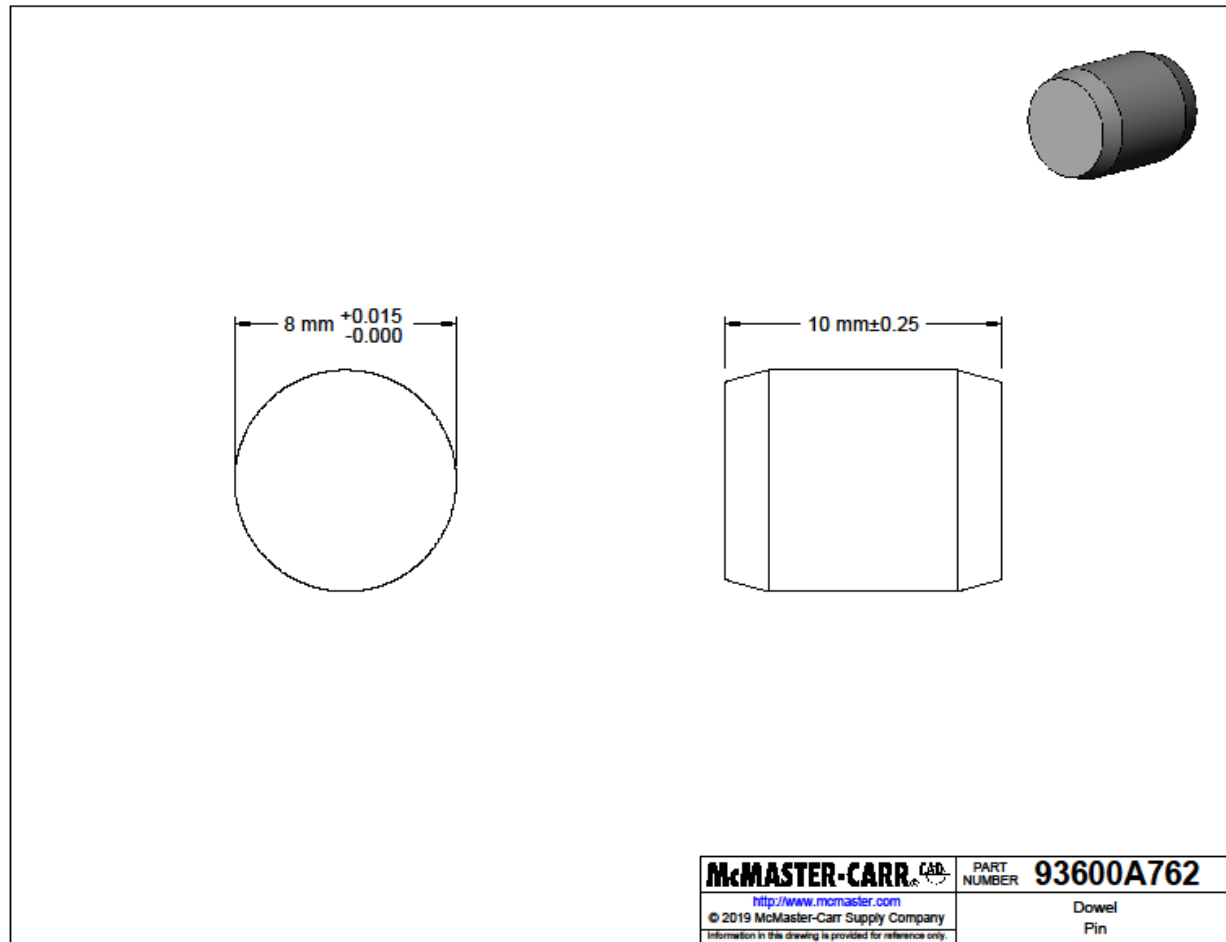


Figure A.18 Dowel pin- 93600A762.

316 Stainless Steel Dowel Pin 8 mm Diameter, 10 mm Long. (2019). McMaster-CARR. <https://www.mcmaster.com/93600A762/>

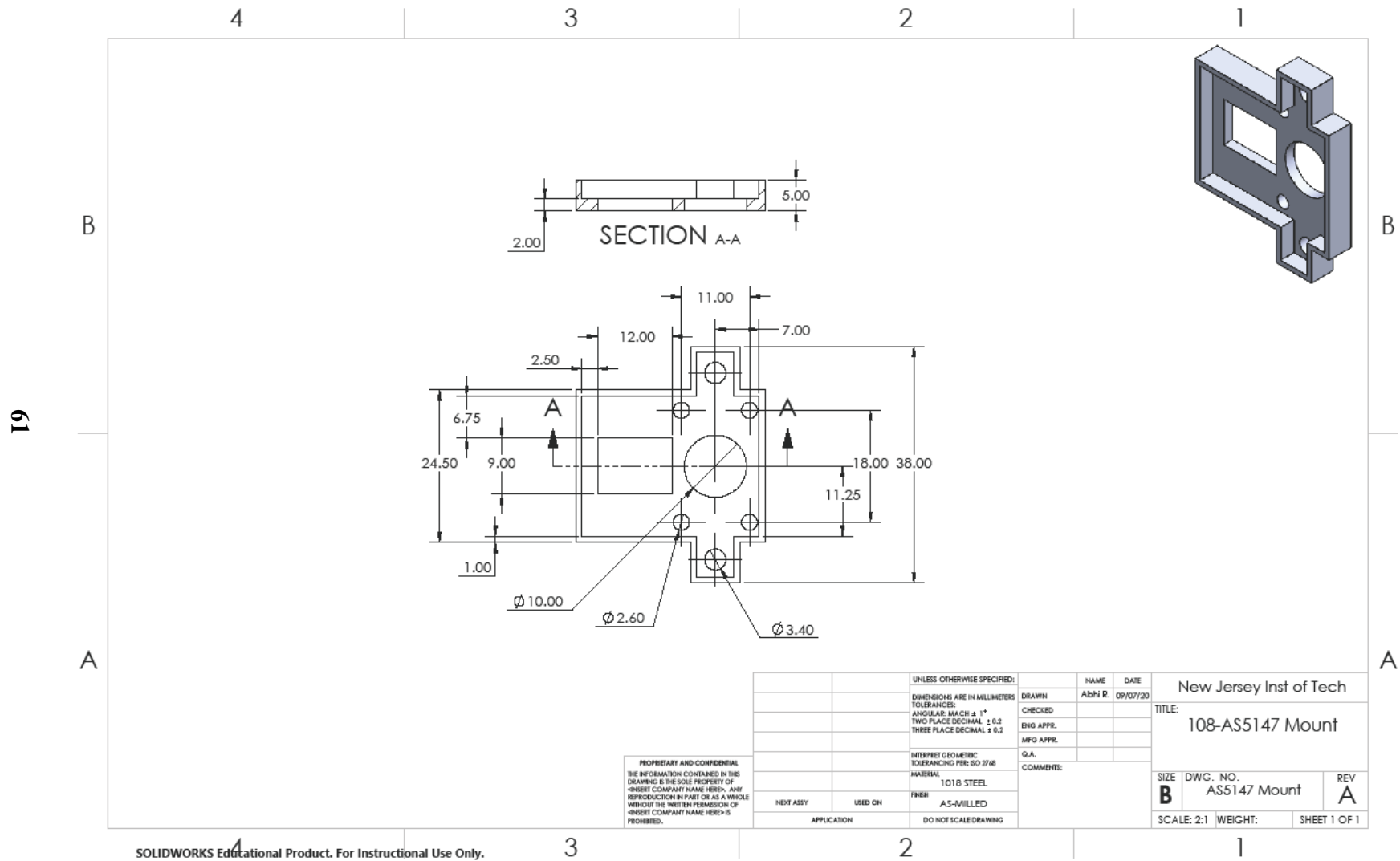


Figure A.19 AS5147 mount bracket.

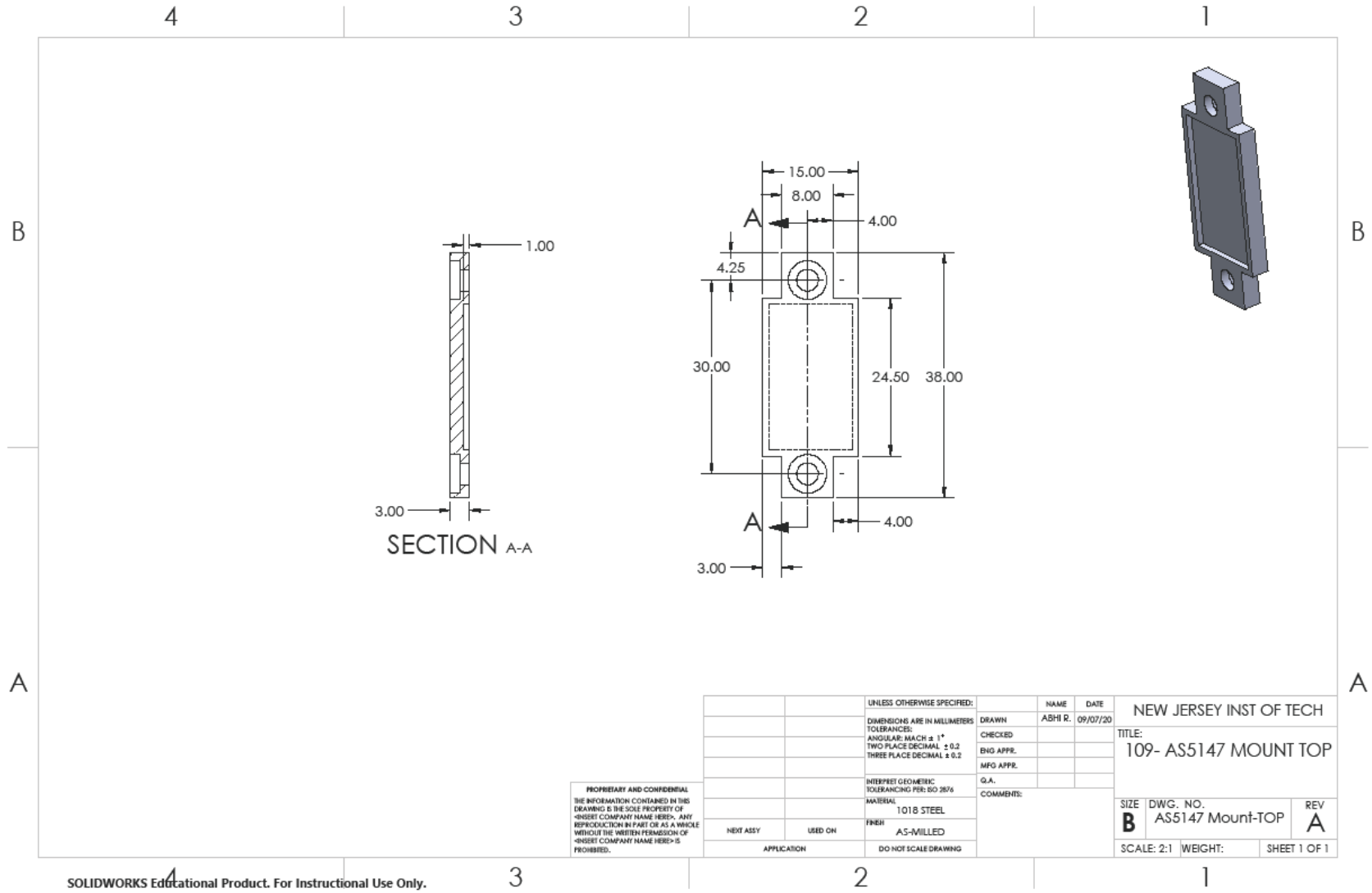


Figure A.20 AS5147 mount bracket top.

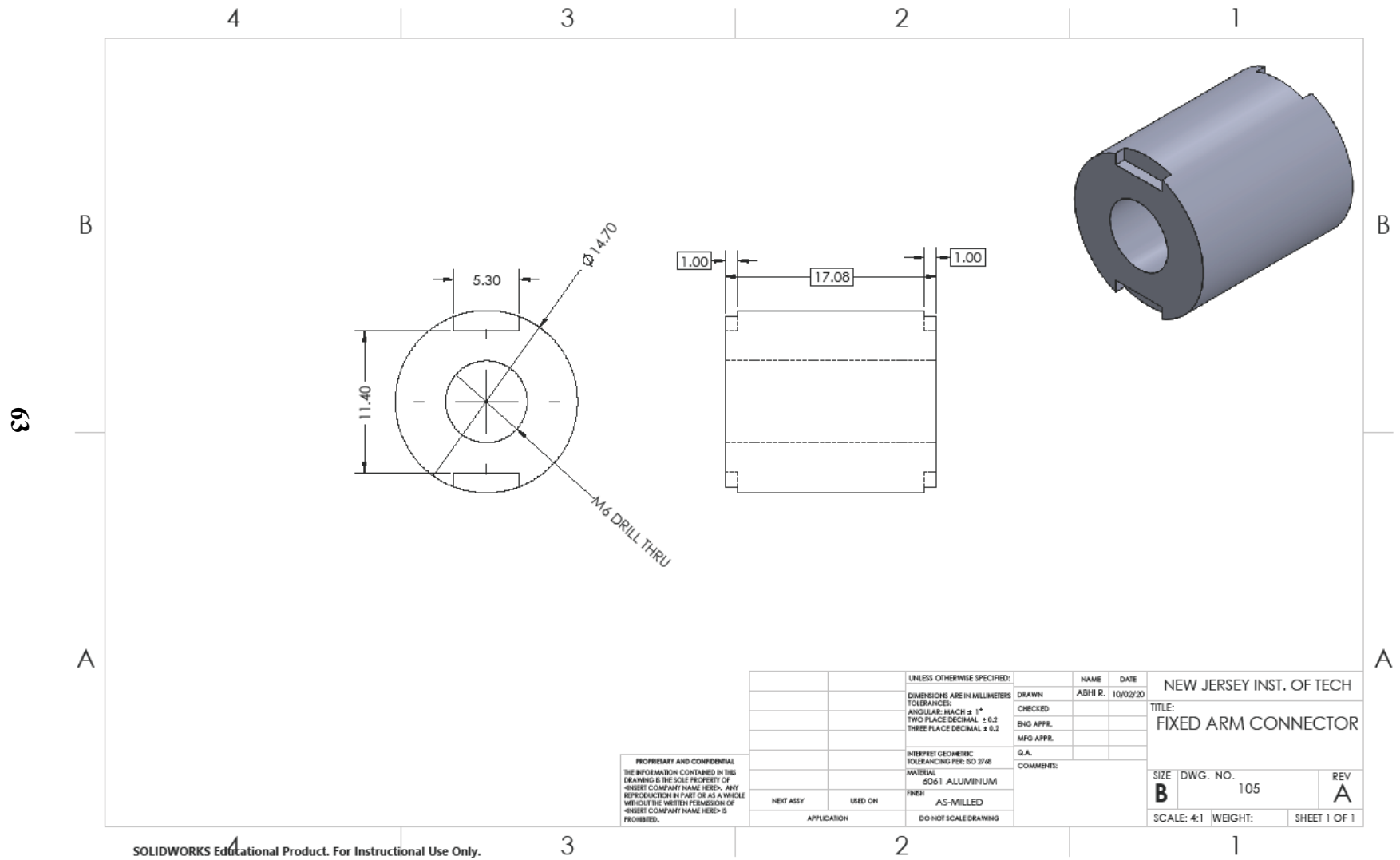


Figure A.21 Fixed arm connector.

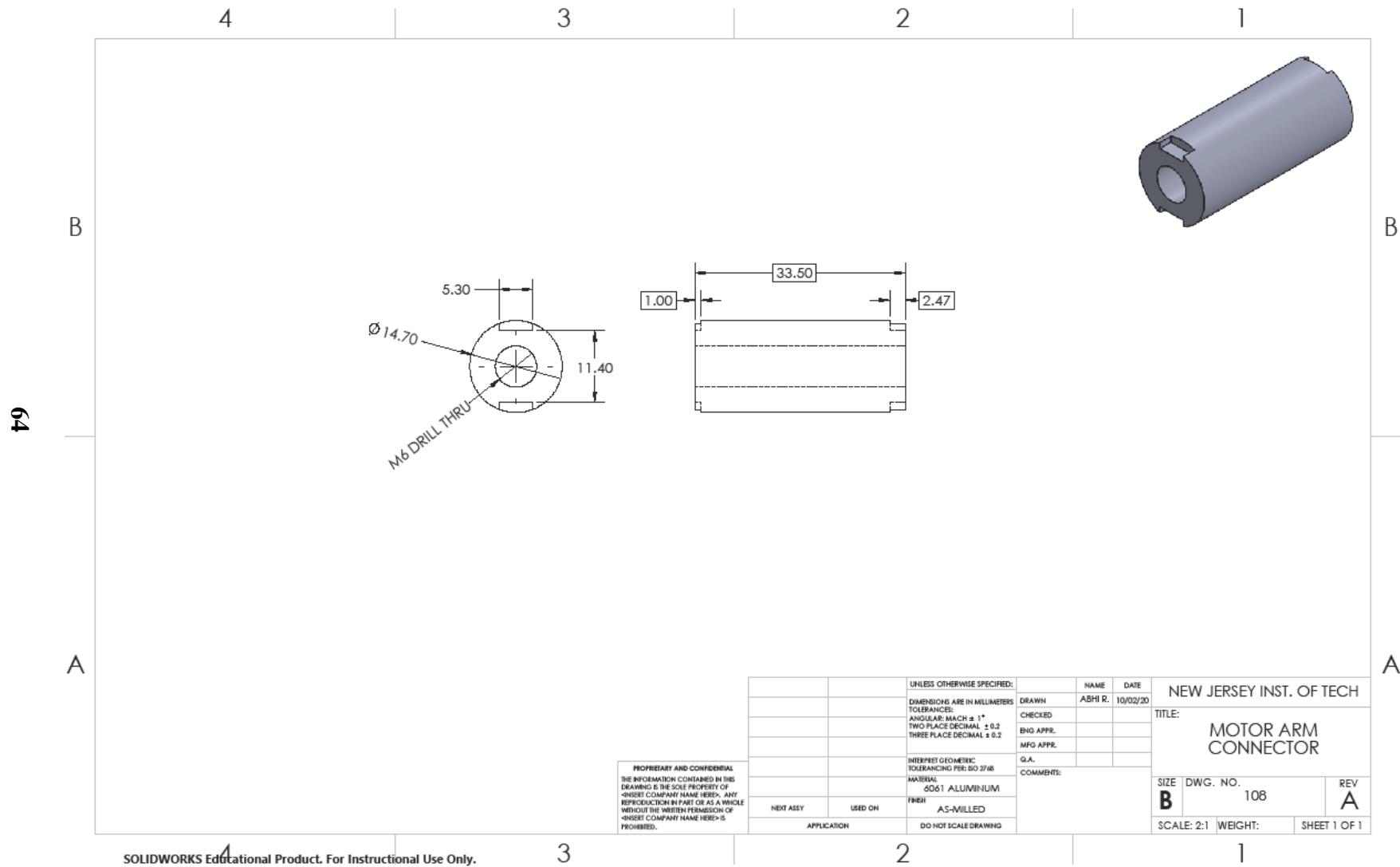


Figure A.22 Motor arm connector.

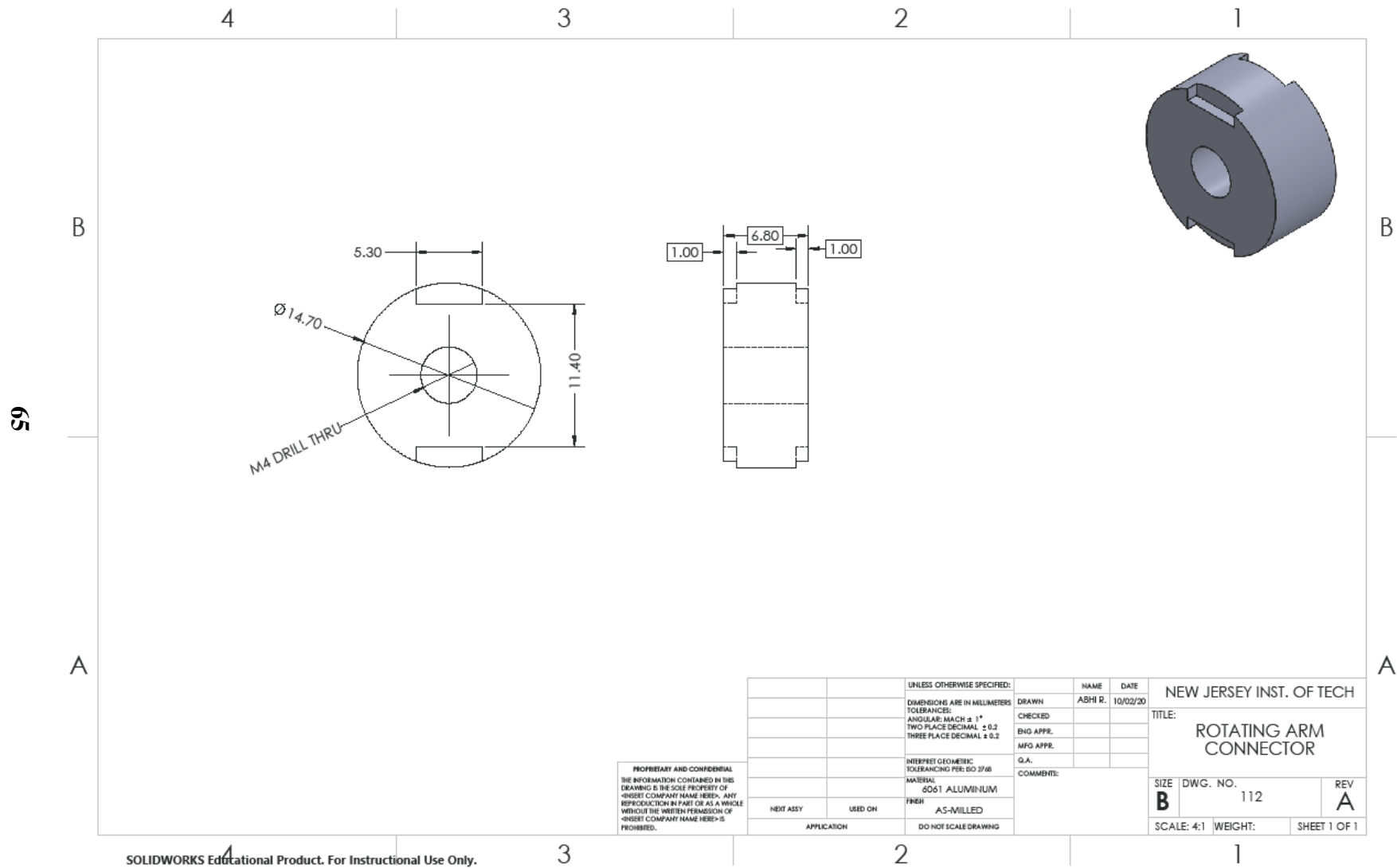


Figure A.23 Rotating arm connector.

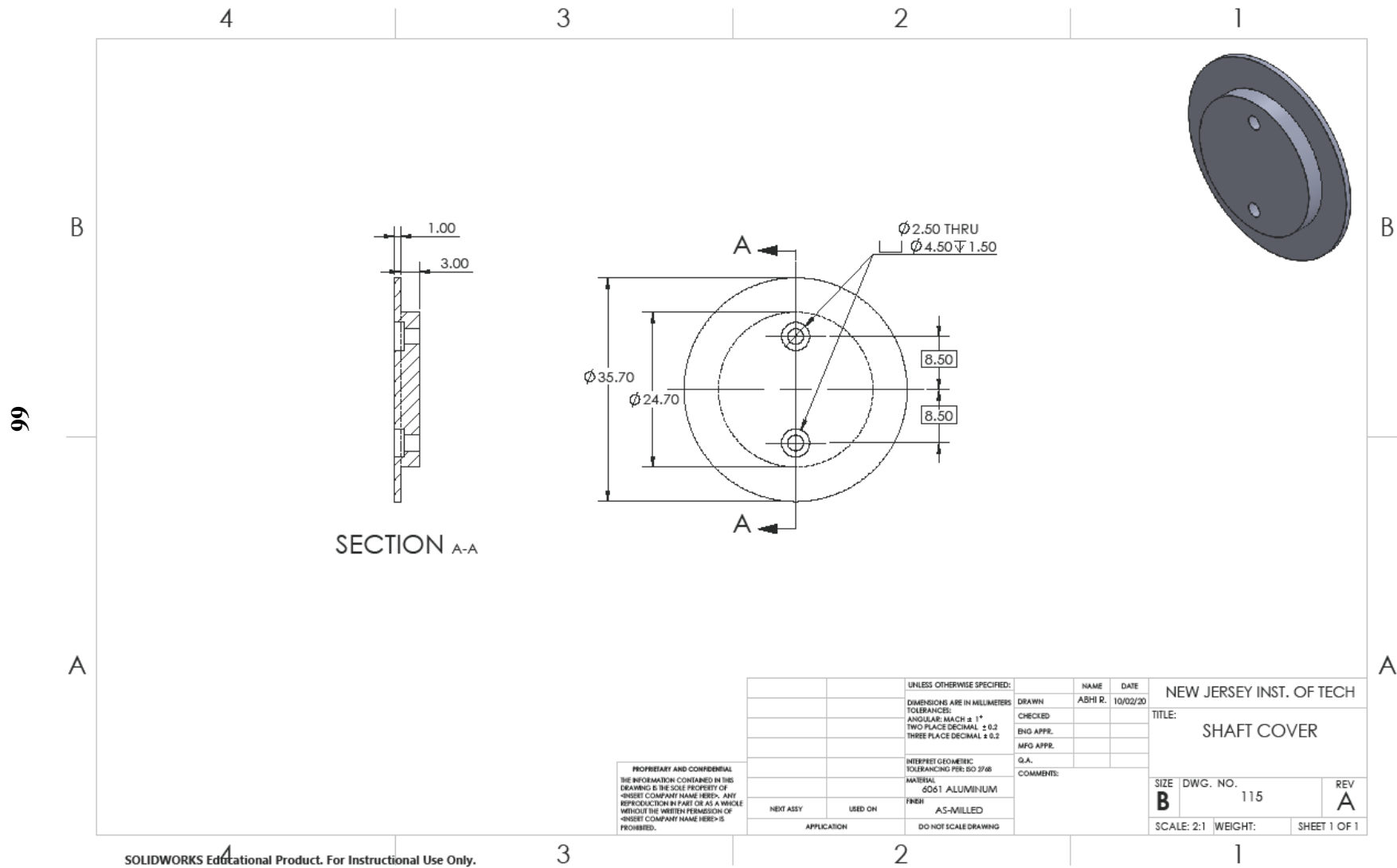


Figure A.24 Shaft cover.

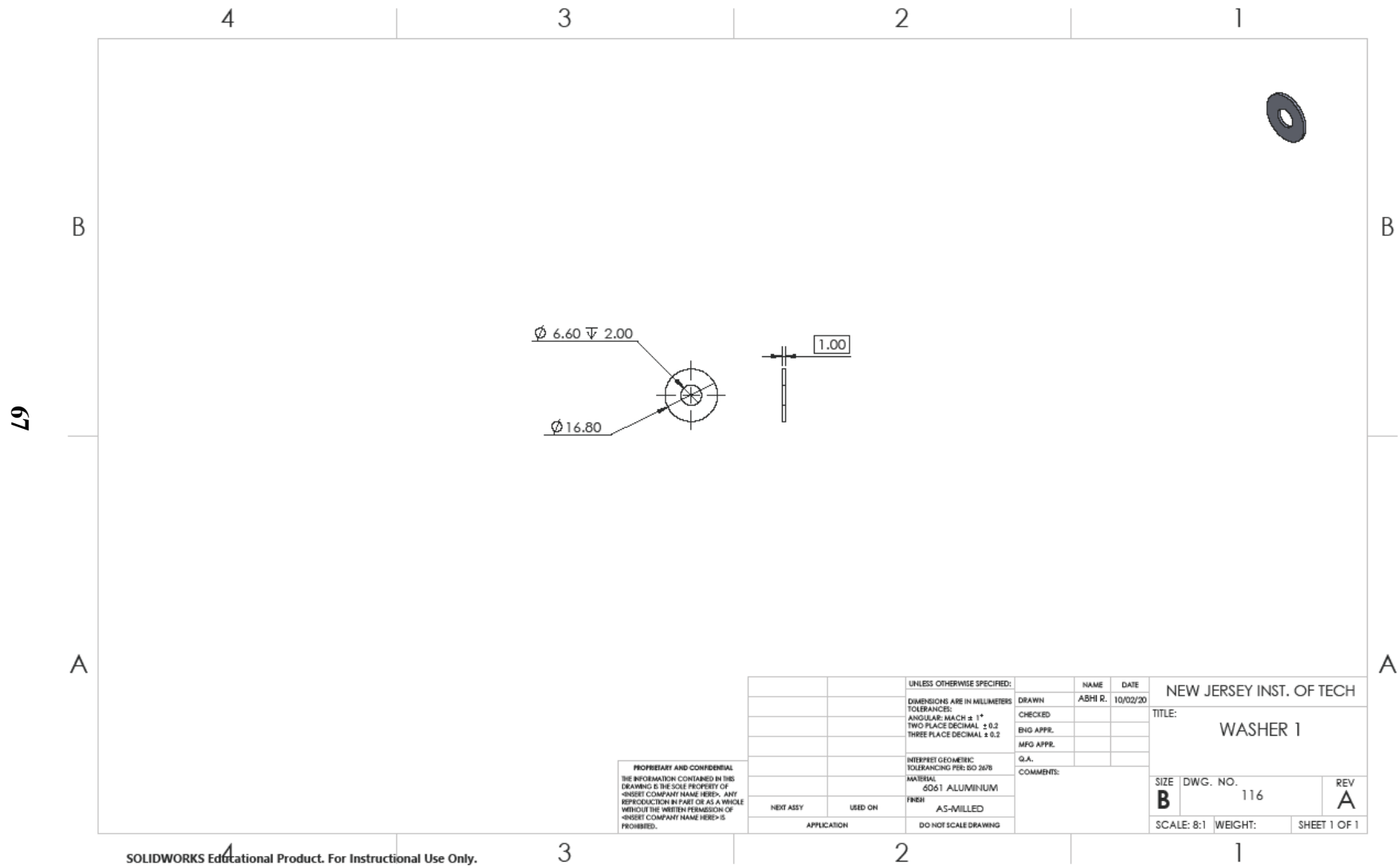


Figure A.25 Washer 1.

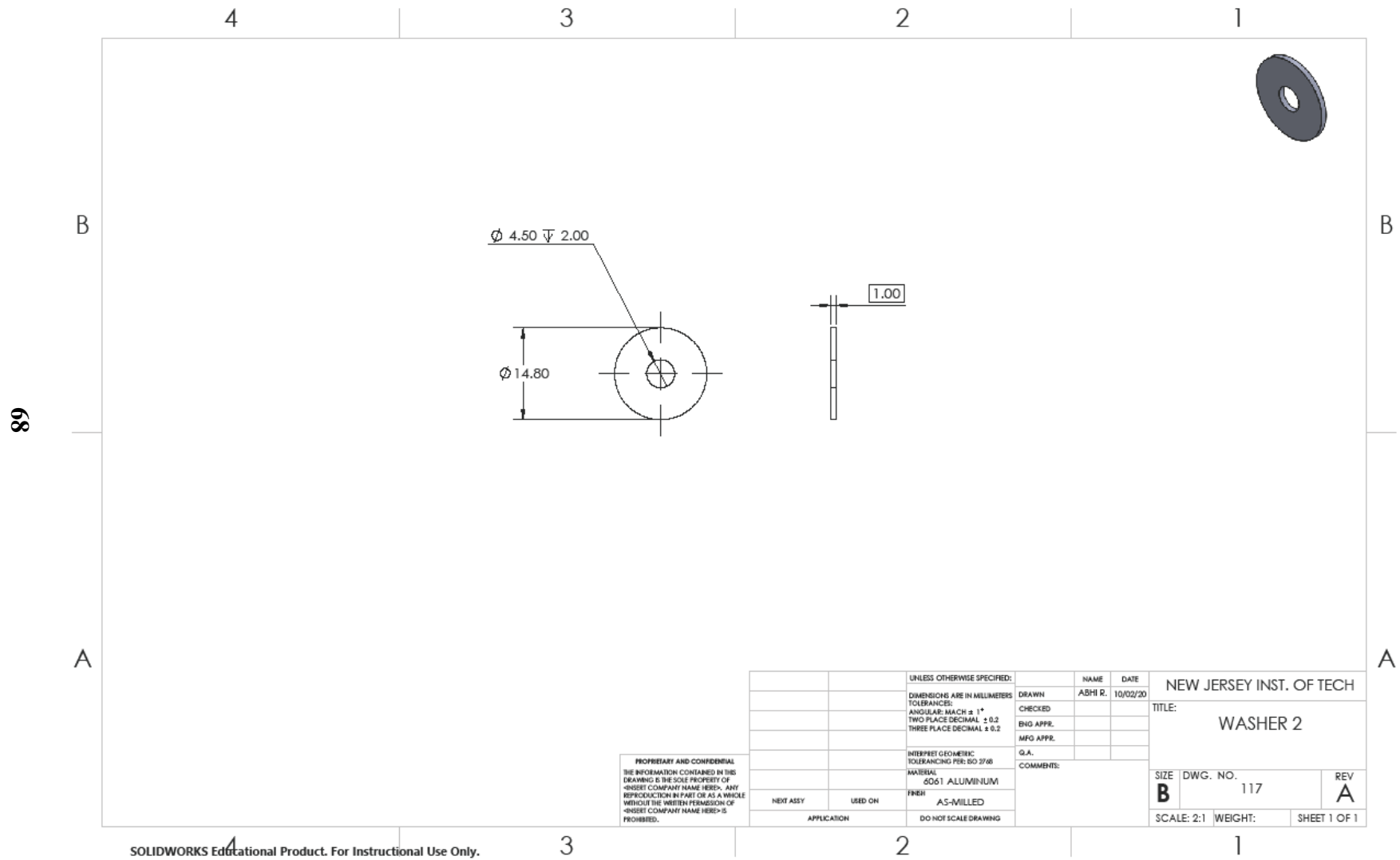


Figure A.26 Washer 2.

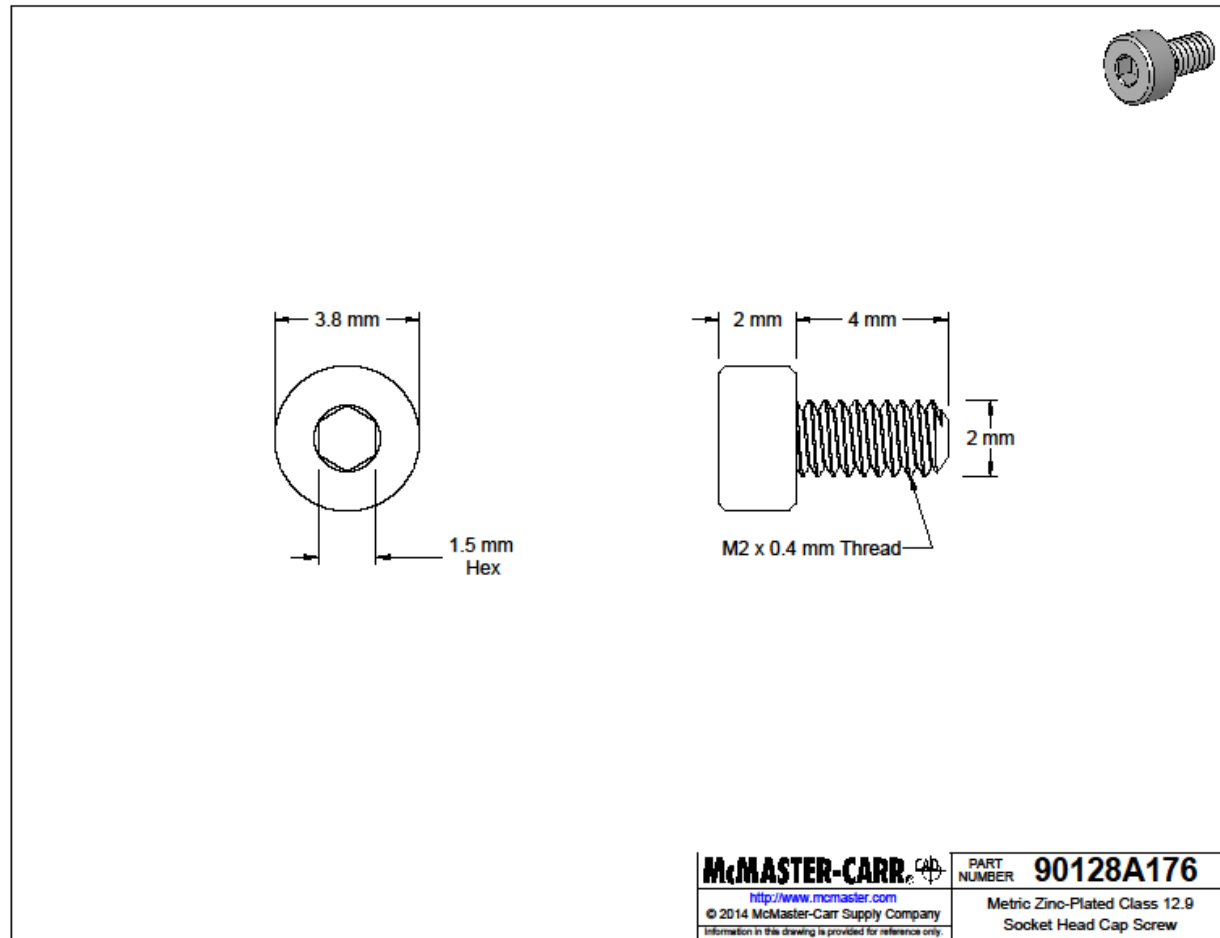


Figure A.27 Socket head cap screw-90125A176.

Zinc-Plated Alloy Steel Socket Head Screw M2 x 0.4 mm Thread, 4 mm Long. (2014). McMaster-CARR. <https://www.mcmaster.com/90128A176/>

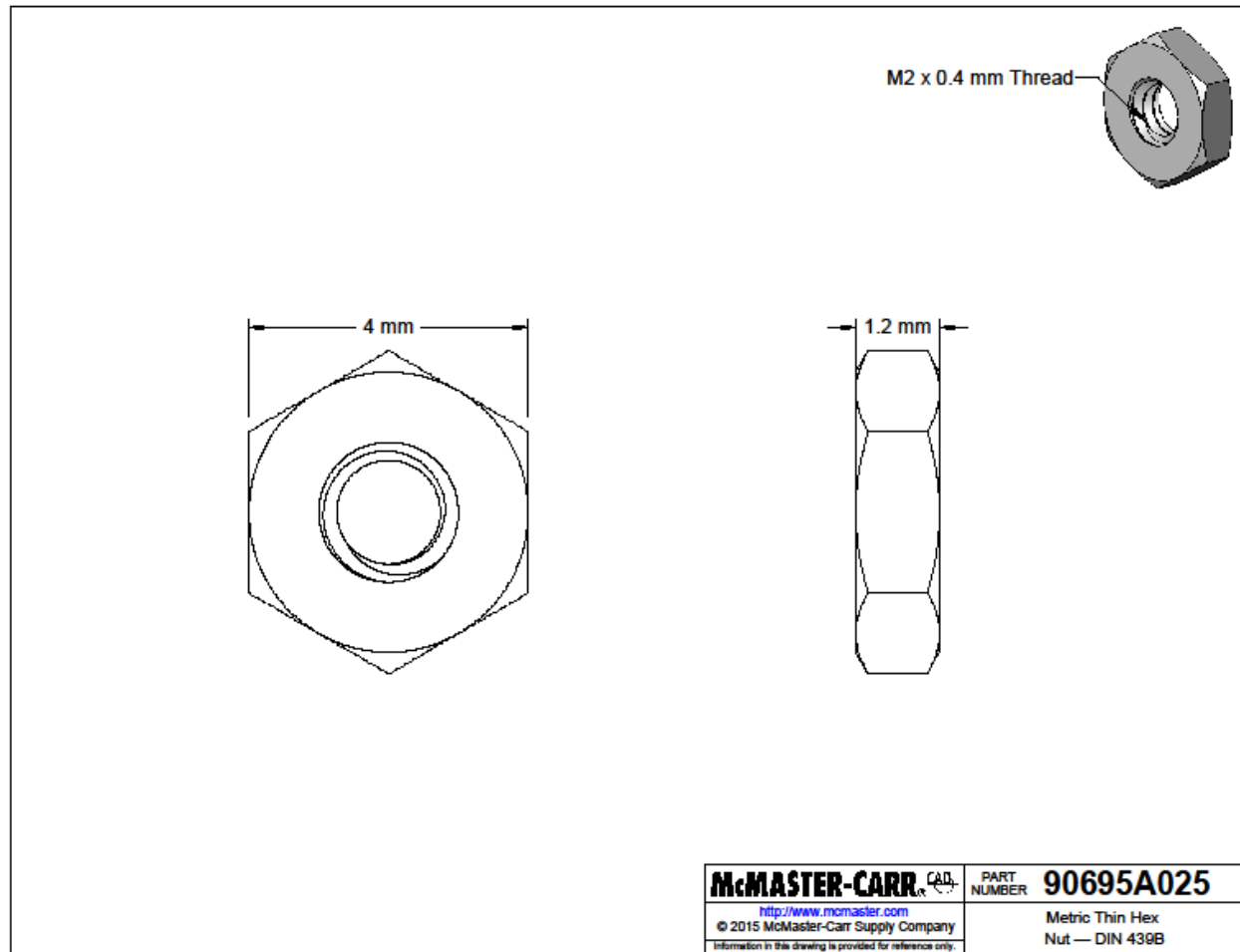


Figure A.28 Nut-90695A025.

Medium-Strength Steel Thin Hex Nut Class 04, Zinc-Plated, M2 x 0.4 mm Thread. (2015). McMASTER-CARR. <https://www.mcmaster.com/90695A025/>

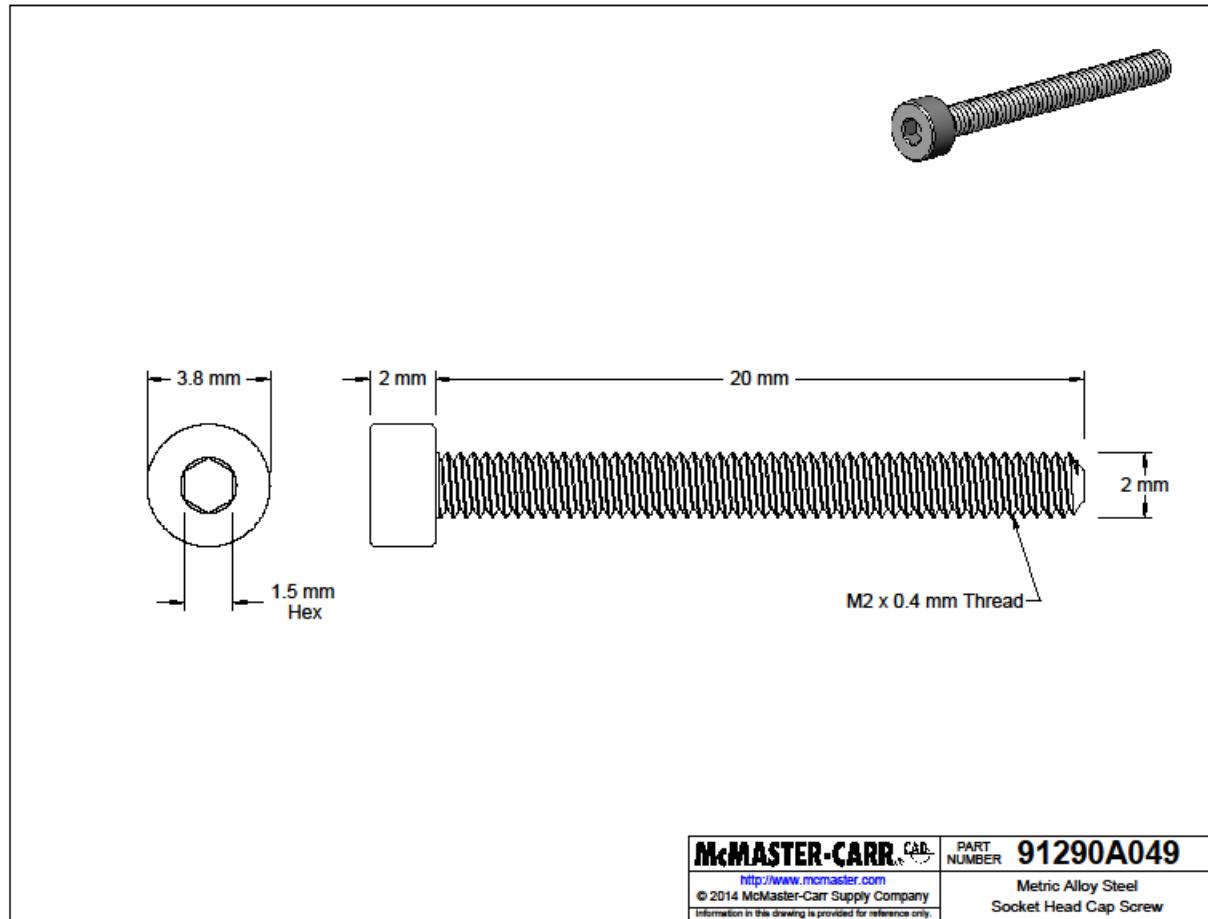


Figure A.29 Socket head cap screw-91290A049.

Black-Oxide Alloy Steel Socket Head Screw M2 x 0.4 mm Thread, 20 mm Long. (2014). McMaster-CARR. <https://www.mcmaster.com/91290A049/>

APPENDIX B

BASELINE PUSH-PULL FORCE GAUGE

Appendix B includes an image of the Baseline push-pull force gauge used to apply and measure the perpendicular force to the rotating (output) arm assembly.



Figure B.1 BASELINE Push-Pull Guage.

REFERENCES

- [1] Spotts, M. F., Shoup, T. E., & Hornberger, L. E. (2003). *Design of Machine Elements (8th Edition)* (8th ed.). Pearson. Chapter 10, page 550
- [2] Mawildoer. (2019, July 25). cycloidal drive generator. GitHub.
https://github.com/mawildoer/cycloidal_generator
- [3] Gould, P. (2019, May 15). Anti-Backlash 3D Printed Cycloidal BLDC Actuator.
<https://hackaday.io/project/165592-anti-backlash-3d-printed-cycloidal-blDC-actuator>
- [4] Tec-Science. (2020, August 16). How does a cycloidal drive work? <https://www.tec-science.com/mechanical-power-transmission/cycloidal-drive-speed-reducer-gear/how-does-a-cycloidal-gear-drive-work/>
- [5] Tec-Science. (2019, January 14). Construction of the Cycloidal disc <https://www.tec-science.com/mechanical-power-transmission/cycloidal-drive-speed-reducer-gear/construction-of-the-cycloidal-disc/>
- [6] Nachimowicz, J., & Rafałowski, S. (2016). Modelling the Meshing of Cycloidal Gears. *Acta Mechanica et Automatica*, 10(2), 137–140.
<https://doi.org/10.1515/ama-2016-0022>
- [7] Zhu, H., Nesler, C., Divekar, N., Ahmad, M. T., & Gregg, R. D. (2019). Design and Validation of a Partial-Assist Knee Orthosis with Compact, Backdrivable Actuation. *2019 IEEE 16th International Conference on Rehabilitation Robotics (ICORR)*, 917–924. <https://doi.org/10.1109/icorr.2019.8779479>
- [8] Sensinger, J. W., & Lipsey, J. H. (2012). Cycloid vs. harmonic drives for use in high ratio, single stage robotic transmissions. *2012 IEEE International Conference on Robotics and Automation*, 4130–4135. <https://doi.org/10.1109/icra.2012.6224739>
- [9] Timing Belt Advantages & Disadvantages. Retrieved October 03, 2020, from <https://www.pfeiferindustries.com/timing-belt-advantages-and-disadvantages>
- [10] Rocon, E., & Pons, J. L. (2011). *Exoskeletons in Rehabilitation Robotics: Tremor Suppression (Springer Tracts in Advanced Robotics (69))* (2011th ed.). Springer. Page 5.
- [11] Wang, J., Li, X., Huang, T.-H., Yu, S., Li, Y., Chen, T., Carriero, A., Oh-Park, M., & Su, H. (2018). Comfort-Centered Design of a Lightweight and Backdrivable Knee Exoskeleton. *IEEE Robotics and Automation Letters*, 3(4), 4265–4272.
<https://doi.org/10.1109/lra.2018.2864352>

- [12] Eib, Andrew (2018). Design of a Backdrivable Upper-Limb Exoskeleton for Use in Rehabilitation Therapy of Stroke Patients. Master's thesis, Texas A & M University. from <http://hdl.handle.net/1969.1/173937>
- [13] Lv, G., Zhu, H., & Gregg, R. D. (2018). On the Design and Control of Highly Backdrivable Lower-Limb Exoskeletons: A Discussion of Past and Ongoing Work. *IEEE Control Systems*, 38(6), 88–113. <https://doi.org/10.1109/mcs.2018.2866605>
- [14] Tuttle, T. (1992, May). *Understanding and Modeling the Behavior of a Harmonic Drive Gear Transmission* (Technical Report 1365). Artificial Intelligence Laboratory, Massachusetts Institute of Technology.
- [15] J. W. Sensinger and J. H. Lipsey, Cycloid vs. harmonic drives for use in high ratio, single stage robotic transmissions, *2012 IEEE International Conference on Robotics and Automation*, Saint Paul, MN, 2012, pp. 4130-4135, doi: 10.1109/ICRA.2012.6224739
- [16] Shin, J.-H., & Kwon, S.-M. (2006). On the lobe profile design in a cycloid reducer using instant velocity center. *Mechanism and Machine Theory*, 41(5), 596–616. <https://doi.org/10.1016/j.mechmachtheory.2005.08.001>
- [17] Liu, R. (2017, July). High Torque Density Cycloid Electric Machines for Robotic Application. Oregon State University. From https://ir.library.oregonstate.edu/concern/graduate_thesis_or_dissertations/wm117t864
- [18] *Permanently Lubricated Stainless Steel Ball Bearing Open, Trade Number 685H, for 5 mm Shaft Diameter*. (2019). McMaster-CARR. <https://www.mcmaster.com/4668K114/>
- [19] *Permanently Lubricated Stainless Steel Ball Bearing Open, Trade Number 6707H, for 35 mm Shaft Diameter*. (2019). McMaster-CARR. <https://www.mcmaster.com/4668K149/>
- [20] *Stainless Steel Ball Bearing Shielded, Trade No. 106-2Z, for 6 mm Shaft Diameter*. (2017). McMaster-CARR. <https://www.mcmaster.com/7804K111/>
- [21] *Permanently Lubricated Stainless Steel Ball Bearing Open, Trade Number 6700H, for 10 mm Shaft Diameter*. (2019). McMaster-CARR. <https://www.mcmaster.com/4668k326>
- [22] *316 Stainless Steel Dowel Pin 8 mm Diameter, 10 mm Long*. (2019). McMaster-CARR. <https://www.mcmaster.com/93600A762/>
- [23] *Dowel Pin 52100 Alloy Steel, 2 mm Diameter, 14 mm Long*. (2012). McMaster-CARR. <https://www.mcmaster.com/91595A030/>

- [24] *18-8 Stainless Steel Socket Head Screw M4 x 0.7 mm Thread, 12 mm Long.* (2014). McMASTER-CARR. <https://www.mcmaster.com/91292A117/>
- [25] *Black-Oxide Alloy Steel Socket Head Screw M6 x 1 mm Thread, 60 mm Long, Fully Threaded.* (2014). McMASTER-CARR. <https://www.mcmaster.com/91290A207/>
- [26] *Steel Hex Nut Medium-Strength, Class 8, M6 x 1 mm Thread.* (2020). McMASTER-CARR. <https://www.mcmaster.com/90592A016/>
- [27] *Zinc-Plated Steel High Hex Nut Class 6, M4 x 0.7 mm Thread.* (2015). McMASTER-CARR. <https://www.mcmaster.com/90725A025/>
- [28] *Zinc-Plated Alloy Steel Socket Head Screw M2 x 0.4 mm Thread, 4 mm Long.* (2014). McMASTER-CARR. <https://www.mcmaster.com/90128A176/>
- [29] *Medium-Strength Steel Thin Hex Nut Class 04, Zinc-Plated, M2 x 0.4 mm Thread.* (2015). McMASTER-CARR. <https://www.mcmaster.com/90695A025/>
- [30] *Black-Oxide Alloy Steel Socket Head Screw M2 x 0.4 mm Thread, 20 mm Long.* (2014). McMASTER-CARR. <https://www.mcmaster.com/91290A049/>
- [31] Haponiuk, B. (2020, August 6). *Torque Calculator.* Omni Torque Calculator. <https://www.omnicalculator.com/physics/torque#torque-equation>